

University of Southampton Research Repository
ePrints Soton

Copyright © and Moral Rights for this thesis are retained by the author and/or other copyright owners. A copy can be downloaded for personal non-commercial research or study, without prior permission or charge. This thesis cannot be reproduced or quoted extensively from without first obtaining permission in writing from the copyright holder/s. The content must not be changed in any way or sold commercially in any format or medium without the formal permission of the copyright holders.

When referring to this work, full bibliographic details including the author, title, awarding institution and date of the thesis must be given e.g.

AUTHOR (year of submission) "Full thesis title", University of Southampton, name of the University School or Department, PhD Thesis, pagination

UNIVERSITY OF SOUTHAMPTON
FACULTY OF ENGINEERING, SCIENCE AND MATHEMATICS
National Oceanography Centre, Southampton
School of Ocean and Earth Science

Iron Speciation Study In the High Latitude North Atlantic Ocean

by

Khairul Nizam Mohamed

Thesis for the degree of Doctor of Philosophy

November 2011

ABSTRACT

The speciation of iron (Fe) was studied in the high latitude North Atlantic Ocean - a seasonally Fe limited region. The presence of organic Fe(III) binding ligands and siderophores as specific Fe chelators were investigated in order to improve our understanding of their role in the biogeochemical cycle of Fe in this region.

The presence of organic ligands (L_T) in the high latitude North Atlantic Ocean maintains Fe in the soluble phase and enhances the residence time of Fe in the oceanic water column by preventing its precipitation. Analysis of Fe speciation by competitive ligand exchange-adsorptive cathodic stripping voltammetry (CLE-AdCSV) showed that 99.5% - 99.9% of total dissolved Fe (dFe) was bound to Fe(III) binding ligands in this region. The ratio of $[L_T]/[dFe]$ was used to highlight the variations in ligand distribution. High and variable $[L_T]/[dFe]$ ratios (1.6-5.8) were observed in surface waters as a result of the low dFe concentrations (~0.1 nM) and possible ligands production by heterotrophic bacteria. The $[L_T]/[dFe]$ ratio decreased with depth to a more constant value (1.2-2.6) in deeper waters (300-1000 m) due to a steady state between dFe and L_T which is reflecting a balance between Fe removal by scavenging and Fe supply by remineralisation of biogenic particles with stabilisation through ligands. Moreover, the $\log K'_{FeL}$ in the surface waters in this study compared well with those reported for siderophore type ligands.

Dissolved siderophores - specific low molecular weight (600 - 1000 Da) Fe binding ligands were also determined in this region. Three hydroxamate-type siderophores (ferrioxamine B, ferrioxamine G and ferrioxamine E) were detected in the dissolved phase in the high latitude North Atlantic. Total dissolved siderophore concentrations ranged between $0-135 \times 10^{-18}$ M and the distributions of the siderophores varied both spatially and temporally. The low total dissolved siderophore concentrations in the seawater in the region indicated that these siderophores will not greatly influence Fe biogeochemistry in this high latitude region. Furthermore, the low concentrations may be related to the low seawater temperature (9-12°C) which can restrict siderophore production by heterotrophic bacteria. Siderophores production was also investigated in seawater samples amended with combinations of Fe, glucose, ammonium or nitrate and phosphate. Siderophore production either decreased or remained unchanged in the presence of added Fe and nitrate. Diversity and concentration of siderophores were highest in incubations with added glucose, ammonia and phosphate, confirming that readily available nutrient sources are likely to be important to siderophore production by heterotrophic bacteria in the ocean.

Contents

ABSTRACT	i
Contents	iii
List of figures	vii
List of tables	xi
List of accompanying materials	xiii
DECLARATION OF AUTHORSHIP	xv
Acknowledgements	xvii
CHAPTER 1 - Introduction	1
1.1 Introduction.....	1
1.2 Iron limiting conditions.....	3
1.3 Iron speciation	5
1.3.1 Organic Fe(III) binding ligands	5
1.4 Specific Fe(III) chelators: Siderophores.....	7
1.5 Future speciation study in the high latitude North Atlantic Ocean.....	10
1.6 Objectives of study.....	12
1.7 Thesis structure.....	13
References	14
CHAPTER 2 - Methodology	21
2.1 Cleaning Processes.....	21
2.1.1 Low density polyethylene bottles (Nalgene)	21
2.1.2 Teflon fluorinated ethylene polypropylene (FEP) (Nalgene)	21
2.1.3 Polyethylene heavy duty carboy (Nalgene)	21
2.2 Sampling	21
2.3 Determination of total dissolved iron (dFe) concentration	23
2.4 Determination of natural organic Fe(III) binding ligands.....	25
2.4.1 Chemical preparation.....	28
2.4.1.1 2-(2-Thiazolylazo)-p-cresol (TAC) stock solution.....	28
2.4.1.2 Borate buffer (H_3BO_3)	28
2.4.1.3 Iron(III) stock solution	28
2.4.2 Sample preparation	28
2.4.3 Voltammetric procedure	29

2.4.4 Calculation of organic Fe(III) binding ligands	30
2.5 Determination of dissolved siderophores.....	32
2.5.1 Preparation of reagents	33
2.5.1.1 Ammonium carbonate	33
2.5.1.2 Extraction Solvent	34
2.5.1.3 Mobile phase solvent	34
2.5.1.4 Gallium working standard	34
2.5.1.5 Iron (III) chloride	34
2.5.1.6 DFOB standard	34
2.5.1.7 FOB working standard	34
2.5.1.8 Ga-FOB working standard.....	35
2.5.1.9 Nitric acid	35
2.5.2 Solid phase extraction (SPE)	35
2.5.3 Quantification of dissolved siderophores	36
2.5.4 Identification of dissolved siderophores	39
2.6 Nutrient enrichment experiments	40
2.6.1 Chemical preparation	41
2.6.1.1 Glucose solution.....	41
2.6.1.2 Ammonium chloride solution.....	41
2.6.1.3 Sodium nitrate solution.....	41
2.6.1.4 Di-sodium hydrogen orthophosphate solution.....	41
2.6.1.5 Paraformaldehyde	41
2.6.2 Nutrient cleaning	41
2.6.3 Incubation conditions.....	42
2.6.4 Determination of siderophores produced in nutrient enrichment experiments	43
2.6.5 Flow cytometry analysis.....	44
References	45
CHAPTER 3 - Dissolved Fe(III) speciation in the high latitude North Atlantic Ocean.....	49
3.1 Introduction.....	49
3.2 Material and methods	51
3.2.1 Sampling	51
3.2.2 Determination of dissolved Fe	51

3.2.3 Determination of organic Fe(III)-binding ligands.....	51
3.2.4 Calculation of Fe speciation.....	52
3.3 Results and discussion.....	53
3.3.1 Study area.....	53
3.3.2 Dissolved Fe (dFe) distribution	58
3.3.3 Organic Fe(III)-binding ligands	63
3.3.4 Fe speciation.....	66
3.4 Conclusion	68
References	70
CHAPTER 4 - Determination of dissolved hydroxamate siderophores in the high latitude North Atlantic Ocean	75
4.1 Introduction	75
4.2 Methodology.....	77
4.3 Results and discussion.....	79
4.3.1 Concentration of dissolved siderophores.....	79
4.3.2 Identification of dissolved siderophores.....	82
4.3.3 Distribution of dissolved hydroxamate siderophores in the high latitude North Atlantic Ocean	87
4.3.4 Production of dissolved hydroxamate siderophores	89
4.4 Conclusion	91
References	93
CHAPTER 5 - Diversity of siderophores in surface waters of the high latitude North Atlantic Ocean	99
5.1 Introduction	99
5.2 Methodology.....	100
5.3 Results and discussion.....	102
5.3.1 Bacterial growth in the nutrient enrichment samples.....	102
5.3.2 Diversity and concentration of siderophore type chelates.....	106
5.3.3 Effect of iron and nitrogen on siderophores production in the high latitude North Atlantic.....	112
5.4 Conclusion	113
References	114
Conclusion and future works	117
References	120

List of figures

Figure 1: Various chemical forms and species of Fe which can exist in dissolved and particulate phase (Bruland & Rue, 2001).	1
Figure 2: Modelling dust fluxes to the world's oceans (Jickells <i>et al.</i> , 2005).	2
Figure 3: World map showing the locations of the ten major Fe addition experiments completed thus far. IronEx-1 (Martin <i>et al.</i> , 1994), IronEx-2 (Coale <i>et al.</i> , 1996), SOIREE (Boyd <i>et al.</i> , 2000), Eisenex (Gervais <i>et al.</i> , 2002), SEEDS I (Tsuda <i>et al.</i> , 2003), SEEDS II (Roy <i>et al.</i> , 2008), SoFeX North (Coale <i>et al.</i> , 2004), SoFeX South (Coale <i>et al.</i> , 2004), SERIES (Boyd <i>et al.</i> , 2004), and Eifex (Hoffmann <i>et al.</i> , 2006).	3
Figure 4: Vertical profile of dissolved Fe concentration in the Iceland Basin. Samples were collected at three stations located in the central Iceland Basin; (station 16236 (59.14°N, 19.31°W), station 16260 (59.19°N, 19.12°W) and station 16282 (59.40°N, 20.61°W) (Nielsdottir <i>et al.</i> , 2009).	5
Figure 5: Schematic representation of the speciation of Fe in natural sea water and the possible uptake pathways of Fe by an algal cell (Gerringa <i>et al.</i> , 2000).	6
Figure 6: The role of siderophores in the Fe cycle in the upper and deep ocean (Tortell <i>et al.</i> , 1999).	8
Figure 7: Examples of siderophores type ligands with enterobactin (catecholate), ferrioxamine B (hydroxamate) and aerobactin (α -hydroxy carboxylic). Three catechol rings wrap around the Fe(III) to afford a right-handed (D) coordination propeller with the highest known binding constant for ferric ion.	9
Figure 8: Structures of the two siderophores identified in Atlantic seawater samples. A less abundant cyclic ferrioxamine E and a more abundant linear ferrioxamine G (Mawji <i>et al.</i> , 2008a).	10
Figure 9: Overview of the study area at high latitude North Atlantic Ocean (reference: http://www.utanrikisraduneyti.is/media/Skyrslur/Icelandic_Continental_Shelf_Executive_Summary.pdf).	22
Figure 10: Titanium CTD frame fitted with 10-20 L trace metal clean Teflon OTE bottles. The OTE bottles which have been taken off from titanium CTD frame and carried to the clean container for seawater sampling.	23
Figure 11: The current (nA) plotted versus the total amount of Fe from St. E2 (10 m depth) (Table 6, Chapter 3). The first few points of the titration indicated that about half of the natural organic complex dissociated due to the competition with the added ligand. The concentration of added ligand and Fe(III) complex is directly related to the peak heights (i_p) of the voltammetric measurements.	26
Figure 12: a) Chemical structure of 2-(2-thiazolylazo)-4-methylphenol or alternatively 2-(2-thiazolylazo)-p-cresol (common name TAC) and b) Proposed coordination of Fe(TAC) ₂ by Croot & Johansson (2000).	27

Figure 13: The voltammeter used for determination of organic Fe(III) binding ligands. Three electrodes electrochemical cell for voltammetric analysis was used; hanging mercury drop electrode (HMDE), reference electrode (KCl) and counter electrode. This instrument was set up on a Class 100 laminar airflow bench at room temperature (25°C).	29
Figure 14: Voltammogram of $\text{Fe}(\text{TAC})_2$ peak under differential pulse mode from seawater sample from St. B4 (10 m depth) (Table 6, Chapter 3). Voltammetric parameters: deposition time 120s; deposition potential -0.5V; start potential -0.42V; end potential -1.0V.	30
Figure 15: Diagram shows a) the filtration and b) extraction procedure for dissolved siderophores pre-concentration from sea water sample. The cellulose nitrate membrane filters were fitted to a polycarbonate 47 mm in-line filter holder (Pall Corporation).	36
Figure 16: Percentage exchange of Ga(III) in FOB complex at the different equilibration time. A 10 μM of Ga(III) standard was equilibrate with 1 nM FOB standard at room temperature before measuring the concentration of GaFOB complex by LC-ICP-MS.	37
Figure 17: Diagram LC-ICP-MS method fitted with MCN-6000 microconcentric nebuliser desolvation system. Sample/working standards were manually injected into the system which fitted with polystyrene-divinylbenze reversed-phase column.....	38
Figure 18: The incubation experiment which carried out in the dark on deck in incubators at ambient seawater temperature.....	43
Figure 19: Sampling stations visited during cruise D321 (August/September 2007) (A1-A5) and cruise D340 (June 2009) (B1-B6). Stations were located in the Iceland Basin (A1, A2, A3, A4, B1, B2 and B3), Hatton-Rockall (B4) and Rockall Trough (A5, B5 and B6). The isobaths represent 1000 and 2000 m depth contours.	53
Figure 20: Potential temperature-salinity plot for CTD data from the Iceland Basin and Rockall Trough regions for the D340 cruise. NEAW: Northeast Atlantic Water; ISOW: Iceland-Scotland Overflow Water; LSW: Labrador Sea Water.	54
Figure 21: Correlation between dFe and nutrients during August/September 2007 (D321) cruise and June 2009 (D340) cruise.	63
Figure 22: Vertical profiles of dissolved Fe (dFe) and ligand (L_7) concentrations for cruises D321 (Stations A1-A5) and D340 (Stations B1-B6).	64
Figure 23: Depth profiles of the $[\text{dFe}]/[\text{L}_7]$ ratio for cruises D321 (Stations A1-A5) and D340 (Stations B1-B6).	67
Figure 24: Map of the high latitude North Atlantic Ocean, blue and red filled circle represents the stations during D350 and D354 sampling, respectively, for dissolved siderophores determined during this study.	79
Figure 25: Structure of ferrioxamine B (FOB), ferrioxamine G (FOG) and ferrioxamine E (FOE) determined during this study in the high latitude North Atlantic Ocean.	80

Figure 26: An example of a ^{69}Ga chromatogram from the LC-ICP-MS analysis. This chromatogram shows the peaks for GaFOB, GaFOG and GaFOE in the samples collected at St. 11 and St. 13 during RRS <i>Discovery</i> D354 cruise.....	81
Figure 27: a) Chromatogram and b) mass spectra for a FOB standard solution (16 nM concentration) which obtained by using the LC-ESI-MS method analysis. The retention time for FOB peak was at 7.64 minutes.....	83
Figure 28: Full chromatogram and mass spectra for a Fe(III) complexed siderophores type compound for a) FOB, m/z 614 and b) FOG, m/z 672. The chromatogram spectra were obtained from the seawater sample collected from Station B11 during RRS <i>Discovery</i> 354 (D354).....	84
Figure 29: Full chromatogram and mass spectra for a FOE, m/z 654. The chromatograms were obtained from the seawater sample collected from Station B13 during RRS <i>Discovery</i> 354 (D354). In the FOE mass spectra, the sodium adduct $[\text{M}+\text{Na}]^+$ (m/z 676) was also observed.	85
Figure 30: Structures and MS^2 spectras of a) FOB and b) FOG from Station A9 during RRS <i>Discovery</i> 350 (D350) in the high latitude North Atlantic Ocean. Structure of FOB and FOG are showing the main cleavages (red line) accounting from fragments ion observed.....	86
Figure 31: Determination of FOE complex by corresponding the retention time for the sodium adducts and FOE peaks. The blue and red chromatogram represents the extracted full mass chromatogram of FOE (m/z 653.6-654.6) and sodium adduct (m/z 675.6-676.6), respectively, in the seawater sample from St. B13, showing a peak at a similar retention time~9.8 minutes. The peak at this retention time is identified as FOE (m/z 654) which showed in mass spectra in Figure 29.....	87
Figure 32: Location for enriched seawater experiments during RRS <i>Discovery</i> cruise D350 and D354 in the high latitude North Atlantic Ocean.....	101
Figure 33: Bacterial abundance in the nutrient enriched samples during RRS <i>Discovery</i> cruise D350 in the Iceland Basin (Inc. 1) and Irminger Basin (Inc.2). GNP represents the addition to the samples of glucose (100 μM), NH_4^+ (200 μM) and PO_4^{3-} (20 μM) to the samples. GNP+Fe and GNP++Fe represent addition of Fe at concentration 9 nM and 90 nM, respectively, along with GNP.....	104
Figure 34: Bacterial abundance in the nutrient enriched incubations during RRS <i>Discovery</i> cruise D354 in the high-latitude North Atlantic Ocean. Two different sources of nitrogen (GNP and GNO_3P) were added to the sample along with glucose and phosphate. G represents the addition of glucose (100 μM) alone to the samples.	105
Figure 35: Structure of amphibactin in the high latitude North Atlantic Ocean during this study. For the FOB and FOG structure, please refer to Chapter 4.....	106
Figure 36: Extracted mass spectra for Ga complexed siderophore type compound (Ga-ferrioxamine B (GaFOBH $^+$), m/z 627/629). This siderophore was identified in the high	

latitude North Atlantic Ocean in Inc. 3 which was amended with glucose (100 μ M), NH_4^+ (200 μ M) and PO_4^{3-} (20 μ M) (GNP).....	107
Figure 37: Extracted mass chromatograms for Ga-ferrioxamine G complexed (GaFOGH $^+$) identified in at Rt = 7.99 (m/z 685/687) obtained from Inc. 3 which was amended with glucose (100 μ M), NH_4^+ (200 μ M) and PO_4^{3-} (20 μ M) (GNP).	108
Figure 38: Extracted mass chromatograms for the protonated Ga-amphibactin E complex in the Inc. 3 which was amended with glucose (100 μ M) plus PO_4^{3-} (20 μ M) plus NH_4^+ (200 μ M), at Rt=21.04 min (m/z 924/926).	108
Figure 39: Extracted mass chromatograms for a Ga complexed siderophores identified in an extract from Incubation 3 which was amended with glucose (100 μ M), NH_4^+ (200 μ M) and PO_4^{3-} (20 μ M) (GNP). Peak at Rt = 19.58 min (m/z 896/898) was identified as the protonated Ga complex of the unknown amphibactin, and peak at Rt=20.38 min (m/z 898/900) was identified as the protonated Ga complex of amphibactin D.	109
Figure 40: Mass spectra obtained on CID analysis of amphibactin D (m/z 885), E (m/z 911) and unknown amphibactin (m/z 883) in Inc. 6 which was amended with glucose (100 μ M), NH_4^+ (200 μ M) and PO_4^{3-} (20 μ M) (GNP).	110
Figure 41: An example of a ^{69}Ga chromatogram from the HPLC-ICP-MS analysis. This chromatogram shows the peaks for the Ga-siderophore complexes in the working standard solution (GaFOB 100 nM) and nutrient enriched seawater sample for the GNP treatment (Sample 75, Inc. 7).....	111

List of tables

Table 1: Overview of oceanic regions with reported organic speciation of Fe: concentrations of dissolved Fe (dFe) and the organic ligands for Fe (L_f), conditional stability constants ($\sim 10^{10}$ conversion factor relates $\log K'_{FeL}$ to $\log K'_{Fe(III)-L}$).....	7
Table 2: Overview of the sampling activities during the RRS <i>Discovery</i> cruises. FeL – organic Fe(III) binding ligands samples, incubation experiment – seawater nutrients enrichment experiment for siderophores production.....	24
Table 3: Comparison between iron speciation data obtained from CLE-AdCSV measurements at National Oceanography Centre Southampton (NOCS) and GEOTRACE data.....	32
Table 4: The final concentration for each nutrient which added into the seawater samples (2000 mL) during the enrichment experiment. The incubation experiment was carried out in duplicate.....	42
Table 5: Physical, nutrient and chlorophyll <i>a</i> data from stations occupied during cruises D321 and D340.	55
Table 6: Iron speciation data for the Iceland Basin from stations occupied during cruises D321 and D340. Total dissolved Fe concentration ([dFe]), total binding ligands ($[L_f]$) and stability constant of Fe ligand ($\log K'_{FeL}$) were determined, and free iron binding-ligand ($[L'] = [L_f] - [dFe]$), $\alpha_{Fe\text{ organic}} = [L'] \times K$, $[pFe] = -\log \{dFe / (\alpha_{Fe\text{ organic}} - \alpha_{Fe\text{ inorganic}})\}$ were calculated. sd – standard deviation (1σ).....	59
Table 7: Iron speciation data averaged for parts of the water column for stations A1, A2, A3, A4, B1, B2 and B3 located in the Iceland Basin, station B4 in the Hatton-Rockall region and stations A5, B5 and B6 in the Rockall Trough region.....	62
Table 8: The Pearson product moment correlation for the relationship between dissolved Fe and nutrients for cruises D321 and D340.	62
Table 9: The coordinate for each station during RRS <i>Discovery</i> D350 and D354 cruise in the high latitude North Atlantic Ocean. Seawater sample at each station was filtrated and dissolved siderophores was extracted by SPE technique.....	78
Table 10: Types of dissolved siderophores present in the seawater of high latitude North Atlantic Ocean during RRS <i>Discovery</i> cruise D350 (April-May 2010) and D354 (July/August) cruise. Quantification and identification were carried out by LC-ICP-MS and LC-ESI-MS methods, respectively. Concentration for each siderophore is represented by the values in brackets. <i>n/a</i> is below the detection limit of LC-ICP-MS..	82
Table 11: The enriched seawater sample treatments used during this study. All treatments were done in duplicate and untreated seawater was used as control.	102
Table 12: Concentrations and diversity of siderophore type chelates determined in nutrient enriched seawater in the high latitude North Atlantic Ocean.....	103

List of accompanying materials

ca.	Approximately
CAS	Chrome azurol S
CLE-AdCSV	Competitive ligands exchange-adsorptive cathodic stripping voltammetry
Eifex	European Iron Fertilization Experiment
Eisenex	Eisen or Iron Experiment
Fe(III)/ Fe ³⁺	Ferric ion
Fe(II)/ Fe ²⁺	Ferrous ion
FeCO ₃	Iron (II) carbonate
FeOH ⁺	Iron (II) hydroxide ion
Fe ₂ O ₃	Iron(III) oxide
Fe(OH) ₃	Iron(III) hydroxide
FeOOH	Iron(III) oxide-hydroxid
FEP	Fluorinated ethylene polypropylene
Fig.	Figure
Ga	Gallium
g/mol	Gram per mole
g/m ² /year	Gram per meter square per year
HCl	Hydrochloric acid
HMDE	Hanging mercury drop electrode
HNLC	High nutrient low chlorophyll
IronEx-1	Iron fertilization experiments 1 in the Equatorial Pacific Ocean
IronEx-2	Iron fertilization experiments 2 in the Equatorial Pacific Ocean
KCl	Potassium chloride
LC-ESI-MS	Liquid chromatography-electrospray ionisation-mass spectrometry
LC-ICP-MS	Liquid chromatography-inductively coupled plasma-mass spectrometry
LDPE	Low density polyethylene
Log K'	Conditional stability constant
L _T	Total natural dissolved organic ligands
m/z	Mass to charge ratio
m	Meter
μm	Micro-meter (10 ⁻⁶ meter)
nm	Nano-meter (10 ⁻⁹ meter)
NaCl	Sodium Chloride

Ni	Nickel
NH_4OH	Ammonium hydroxide
OTE	Ocean test equipment
PFe	Particulate Fe
pM	Pico-Molar (10^{-12} Molar)
RO	Reverse osmosis
RRT	Relative retention time
<i>S</i>	Salinity or sensitivity
SA	Salicylaldoxime
Seeds I	Sub-Artic Pacific Iron Experiment for Ecosystem Dynamic Study I
Seeds II	Sub-Artic Pacific Iron Experiment for Ecosystem Dynamic Study II
Series	Sub-Artic Ecosystem Respond to Iron Enhancement Study
SoFeX north	Southern Ocean Iron Experiment in north section
SoFeX south	Southern Ocean Iron Experiment in south section
Soiree	Southern Ocean Iron Release Experiment
St.	Station
TAC /C ₁₀ H ₉ N ₃ OS	2-(2-thiazolylazo)-4- methylphenol
1N2N	1-nitroso-2-naphthol
v/v	volume/volume

DECLARATION OF AUTHORSHIP

I, Khairul Nizam Mohamed

declare that the thesis entitled

Iron speciation study in the high latitude North Atlantic Ocean

and the work presented in the thesis are both my own, and have been generated by me as the result of my own original research. I confirm that:

- this work was done wholly or mainly while in candidature for a research degree at this University;
- where any part of this thesis has previously been submitted for a degree or any other qualification at this University or any other institution, this has been clearly stated;
- where I have consulted the published work of others, this is always clearly attributed;
- where I have quoted from the work of others, the source is always given. With the exception of such quotations, this thesis is entirely my own work;
- I have acknowledged all main sources of help;
- where the thesis is based on work done by myself jointly with others, I have made clear exactly what was done by others and what I have contributed myself;
- none of this work has been published before submission, or [delete as appropriate] parts of this work have been published as: [please list references]

Signed:

Date:.....

Acknowledgements

I am deeply grateful to my supervisor Prof. Eric P. Achterberg for giving me the confidence to explore my research interests and the guidance to avoid getting lost in my exploration. He was a fabulous advisor, sharp, cheery, perceptive and mindful of the things that truly matter. My sincere thanks go to my co-supervisor Dr. Martha Gledhill whose encouragement, guidance and support from the initial to the final level enabled me to develop an understanding of the subject.

In addition, I would like to thank Dr. Sebastian Steigenberger, who was a great support on cruises RRS *Discovery*, and his great helps. I am grateful to all my friends from the National Oceanography Centre, University of Southampton, for being the surrogate family during the many years I stayed there and for their continued moral support thereafter.

Thanks to Faculty of Environmental Study, Universiti Putra Malaysia (UPM) and Ministry of Higher Education Malaysia (MOHE) for providing my scholarship and study leave under the Staff Training Programme.

I would also like to thank my lovely parents for always supporting me and being there for me whenever needed. This thesis would certainly not have existed without them. My thanks also go to my brothers and sister for understanding me and supportive. My lovely wife, Siti Salizma Salleh has been, always, my pillar, my joy and my guiding light, and I thank her. Thanks to my daughters, Qistina and Qisyah for their love, understanding and enthusiasm.

Lastly, I offer my regards and blessings to all of those who supported me in any respect during the completion of this thesis.

CHAPTER 1 - Introduction

1.1 Introduction

Iron (Fe) exists in seawater in different physical and chemical forms, e.g. inorganic soluble ferric (Fe(III)) and ferrous (Fe(II)) ions, organically complexed Fe, colloidal and particulate Fe (Ye *et al.*, 2009). The physical form of Fe is defined by physical size fractions separated on the basis of filtration methods - either with conventional membrane filters or with the use of various ultra-filtration methods (Bruland & Wells, 1995; Bruland & Rue, 2001) (Fig. 1). Iron can for example be divided into three operationally defined classes; dissolved Fe (dFe: <0.2-0.45 µm), total dissolvable Fe (TdFe: represents Fe in unfiltered seawater left acidified to pH ca. 1.7 for ca. 6 months), and particulate Fe (PFe: >0.2 µm). A significant fraction of the Fe previously classified as dissolved Fe is now considered to be present in the colloidal size range (0.02-0.4 µm) (Wu *et al.*, 2001).

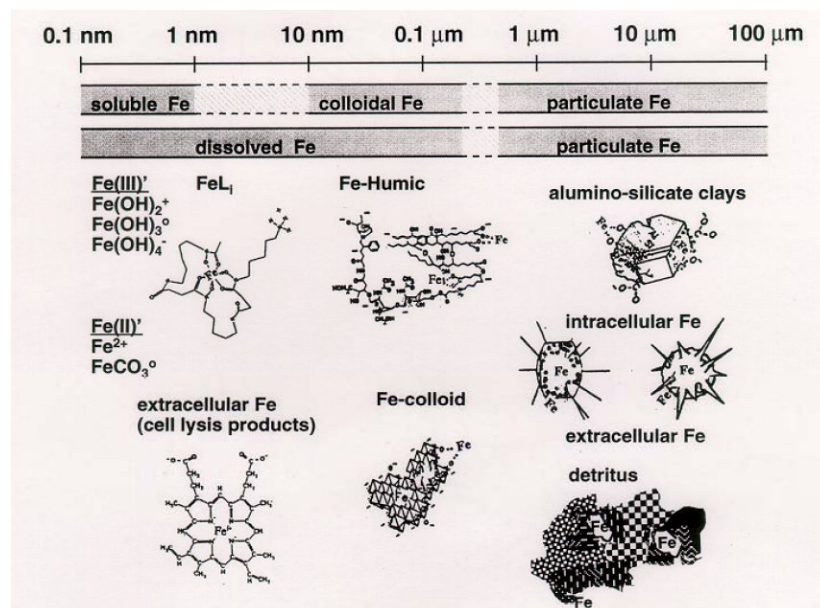


Figure 1: Various chemical forms and species of Fe which can exist in dissolved and particulate phase (Bruland & Rue, 2001).

Iron plays a special role in marine food chains, as it is an essential ingredient for growth and functioning of organisms. In phytoplankton cells, Fe plays a major role in the electron transfer processes in photosynthesis and respiration (Geider, 1993). Iron is essential for the synthesis of the photosynthetic pigment Chlorophyll *a* along with a range of enzymes (Geider & Laroche, 1994).

Iron is transported to the marine environment by four major routes - fluvial, aeolian, submarine hydrothermal, and glacial. Coastal waters receive large inputs of Fe from rivers and anoxic sediments (Johnson *et al.*, 1997a), whereas offshore regions rely mainly on atmospheric dust deposition and/or upwelling and mixing of deep waters as sources of Fe (Duce *et al.*, 1991).

Atmospheric dust accounts for a major portion of the global Fe input to the world's ocean (Martin & Fitzwater, 1988; Guieu *et al.*, 2002), away from river inputs. Dust is considered the principal source of soluble and bio-available Fe to remote open ocean surface water (Jickells *et al.*, 2005). The majority of Fe inputs via this pathway originate from arid and semi-arid landmasses, with important areas being North Africa, the Asian deserts and the Middle East. These arid and semi-arid landmasses are very sensitive to global change (Gong *et al.*, 2004), hence changes in their source strength with subsequent changes in Fe supply could have a strong impact on the ocean primary productivity and climate.

Production of dust occurs when winds above a threshold velocity transport soil grains horizontally and produce smaller particles, which are carried up into the atmosphere for long range transport. Deposition of dust occurs via dry and wet deposition, and is strongly seasonal and episodic in nature (Prospero & Carlson, 1972; Gao *et al.*, 2001). In certain regions wet and dry atmospheric deposition represents a significant source of Fe to the ocean and can alleviate Fe limitation (Duce *et al.*, 1991; Jickells *et al.*, 2005). In high latitude areas of the North Pacific, North Atlantic and Southern Ocean, the atmospheric Fe deposition is very low (Fig. 2).

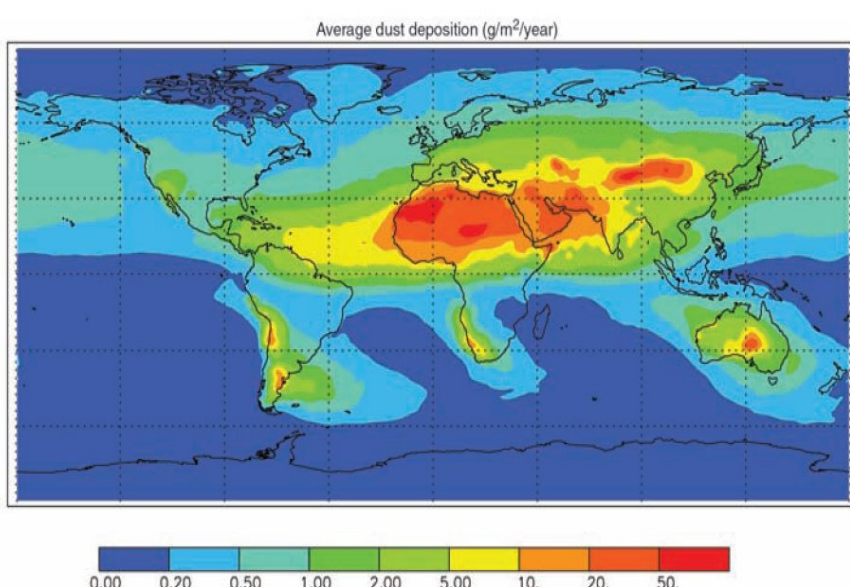


Figure 2: Modelling dust fluxes to the world's oceans (Jickells *et al.*, 2005).

1.2 Iron limiting conditions

Large scale in situ Fe enrichment experiments have been carried out in the Equatorial Pacific, Pacific Subpolar and Southern Ocean (Martin *et al.*, 1990; Martin *et al.*, 1994; Kumar *et al.*, 1995; Coale *et al.*, 1996; Falkowski *et al.*, 1998; Boyd *et al.*, 2000; Gervais *et al.*, 2002; Tsuda *et al.*, 2003; Boyd *et al.*, 2004; Coale *et al.*, 2004) (Fig. 3). Most of the experiments have shown that Fe is an important factor controlling phytoplankton growth in the high nutrient low chlorophyll (HNLC) regions. Atmospheric deposition is insufficient to compensate for the low ambient Fe concentrations (Fung *et al.*, 2000), resulting in depleted dissolved Fe concentrations (Martin & Fitzwater, 1988; Coale *et al.*, 1996; Hutchins *et al.*, 1998; Boyd *et al.*, 2000).

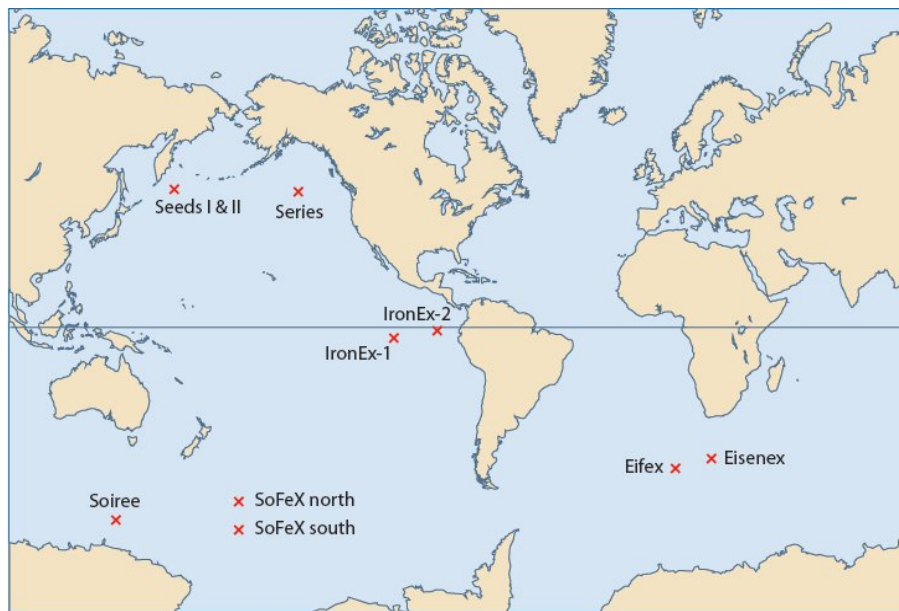


Figure 3: World map showing the locations of the ten major Fe addition experiments completed thus far. IronEx-1 (Martin *et al.*, 1994), IronEx-2 (Coale *et al.*, 1996), SOIREE (Boyd *et al.*, 2000), Eisenex (Gervais *et al.*, 2002), SEEDS I (Tsuda *et al.*, 2003), SEEDS II (Roy *et al.*, 2008), SoFeX North (Coale *et al.*, 2004), SoFeX South (Coale *et al.*, 2004), SERIES (Boyd *et al.*, 2004), and Eifex (Hoffmann *et al.*, 2006).

There have been a few studies investigating the importance of Fe on primary production conducted in North Atlantic Ocean due to the assumption that its surface waters contain enhanced Fe concentrations due to the atmospheric inputs of Saharan desert dust. Dissolved Fe concentrations in surface waters of the North Atlantic are expected to be highly variable as Fe is supplied to this region through episodic Saharan dust depositions (Duce *et al.*, 1991; De Jong *et al.*, 2000; Spokes *et al.*, 2001) and important hydrographic features such as fronts or mesoscales eddies (De Jong *et al.*, 2000). Indeed, in a study in the high latitude of North Atlantic Ocean (~50°N) Fe was not considered a limiting micronutrient due to the absence of a phytoplankton

response in Fe enrichment experiments (Martin *et al.*, 1993). Thus, despite the low atmospheric Fe inputs, this region was considered to differ from other high latitude regions including the HNLC Southern Ocean. Moreover, this region is known as an important region of deep winter mixed layers (>600 m) (Holliday & Reid, 2001; Allen *et al.*, 2005). The deep winter mixing supplies nutrients and Fe to the surface water, and allows sufficient nutrients for spring bloom development upon shoaling (Ducklow & Harris, 1993) with a rapid increase in the chlorophyll biomass (Siegel *et al.*, 2002; Sanders *et al.*, 2005).

Recent manipulations of phytoplankton communities in bottle experiments and in situ physiological measurements have however indicated the formation of the Fe limited conditions in the North Atlantic Ocean (~40°N) (Blain *et al.*, 2004; Moore *et al.*, 2006). Furthermore, Fe enrichment incubation experiments in the central Iceland Basin have also shown an increase in biomass accumulation after 24 or 48 hours during post spring bloom conditions (Nielsdottir *et al.*, 2009). Dissolved Fe profiles (Fig. 4) also indicate a very low Fe concentration in the surface water (<0.010-0.218 nM, *n*=43) in this region, with residual nitrate concentrations (1-5 µM). The surface dissolved Fe concentrations determined in the Iceland Basin are consistent with previous observations south of Iceland (Martin *et al.*, 1993; Measures *et al.*, 2008).

Nielsdottir *et al.* (2009) concluded that the supply of nitrate and phosphate to the surface water by winter overturning was not accompanied by sufficient dissolved Fe to allow complete drawdown of their concentrations and have suggested the formation of Fe limitation in the central Iceland Basin under post spring bloom conditions. Moreover, the low concentration of dissolved aluminum in this region (1-3 nM; Achterberg, unpublished data) also indicates that the atmospheric inputs of Fe are low in this region.

The biological uptake of Fe in this region is thus likely controlled by the availability of Fe (De Baar *et al.*, 1990; Martin *et al.*, 1990). The Fe bioavailability is influenced by its chemical forms, biogeochemical cycling and the different uptake strategies of the phyto- and bacterio-plankton communities (Hutchins *et al.*, 1999a; Nodwell & Price, 2001; Maldonado *et al.*, 2005; Strzepek *et al.*, 2005). In the biogeochemical cycle, Fe becomes bio-available as Fe(II) which is produced by photo or biological reduction (Weber *et al.*, 2005). In addition, inorganic Fe(III) is also available for uptake by organisms (Hudson & Morel, 1990). For these reasons, Fe speciation is an important characteristic of the biological Fe cycle that needs to be considered in this region.

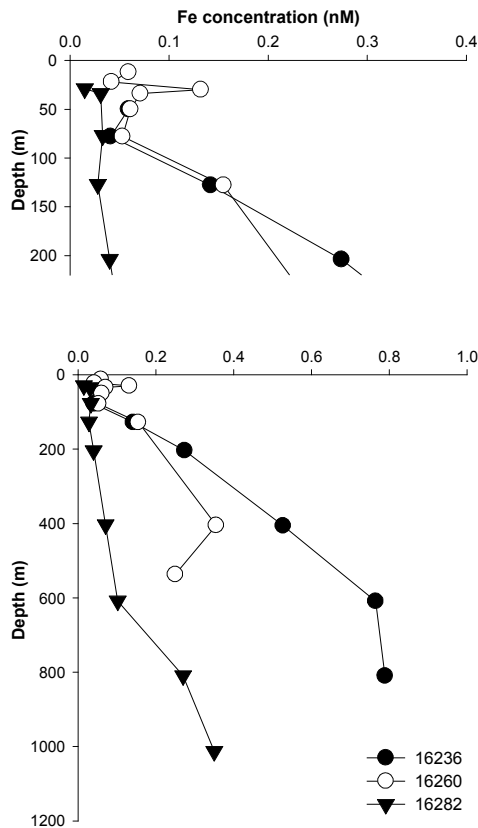


Figure 4: Vertical profile of dissolved Fe concentration in the Iceland Basin. Samples were collected at three stations located in the central Iceland Basin; (station 16236 (59.14°N, 19.31°W), station 16260 (59.19°N, 19.12°W) and station 16282 (59.40°N, 20.61°W) (Nielsdottir *et al.*, 2009).

1.3 Iron speciation

The chemistry of Fe, such as its inorganic and organic complexation in seawater (Fig. 5), is very complex and not yet fully understood. In seawater (pH~8.1), Fe(II) is rapidly oxidised to Fe(III) which has a low solubility (Liu & Millero, 1999; Waite & Nodder, 2001). The solubility of Fe in seawater is largely determined by organic complexation (Kuma *et al.*, 1996; Millero, 1996; Waite & Nodder, 2001; Liu & Millero, 2002; Tani *et al.*, 2003), which therefore plays an important role in regulating dFe concentrations in seawater (Johnson *et al.*, 1997a; Kuma *et al.*, 1998; Archer & Johnson, 2000).

1.3.1 Organic Fe(III) binding ligands

Organic Fe(III)-binding ligands have a potential to regulate the oceanic Fe cycle. The abundance of organic Fe(III)-binding ligands regulates the concentration of Fe in the water column, as more than 99% of dissolved Fe is organically complexed (Gledhill & Van Den Berg, 1994; Rue & Bruland, 1995; Van Den Berg, 1995; Croot & Johansson, 2000). Organic ligands in seawater are thought to specifically complex Fe(III) and responsible for increasing its apparent solubility. The formation of Fe(III) complexes

with organic matter resulted in the high solubility of Fe(III) in the initial seawater (Salinity=36) (0.5 nM) compared to the diluted seawater (0.2-0.3 nM) with 0.7 M sodium chloride (NaCl) (Liu & Millero, 2002). In diluted seawater the Fe(III) solubility approaches the solubility in pure NaCl (10 pM) (Liu & Millero, 1999). The formation of organic Fe(III) binding ligands could be increasing the Fe(III) solubility by 20-fold (Millero, 2001) and reduce scavenging rates (Johnson *et al.*, 1997a) in seawater.

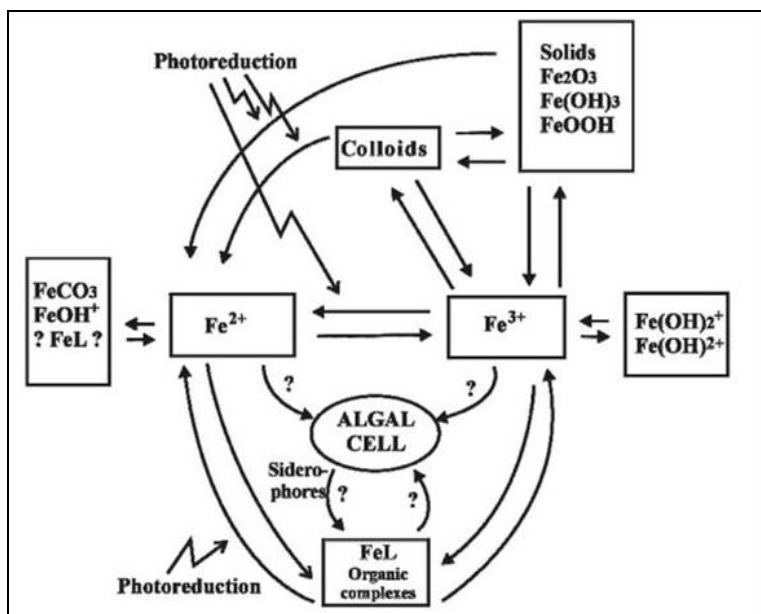


Figure 5: Schematic representation of the speciation of Fe in natural sea water and the possible uptake pathways of Fe by an algal cell (Gerringa *et al.*, 2000).

On the other hand, organic Fe complexation dramatically reduces the fraction of inorganic Fe (Fe⁺) in the seawater system (Hudson *et al.*, 1992), resulting in low concentrations of free Fe(III) (< 0.1 pM) (Rue & Bruland, 1997). Free Fe(III) concentrations could therefore fall below the concentration required for organisms, even for low-Fe adapted species (Sunda *et al.*, 1991). However, Sunda & Huntsman (1995) have been suggested that the low concentration of free Fe could support a very slow growth rate of picoplankton due to their high surface to volume ratio. In fact, this free Fe(III) could increase due to photo-reduction of Fe(III) complexes during the day (Rue & Bruland, 1997; Maldonado *et al.*, 2005; Barbeau, 2006) and consequently, maintain the growth rate of phytoplankton (Sunda & Huntsman, 1995).

The production of ligands is widely supposed to be regulated by the Fe level (Reid *et al.*, 1993; Wilhelm & Trick, 1994; Wilhelm *et al.*, 1996; Macrellis *et al.*, 2001). The vertical distribution of Fe complexing ligands have been measured in the most ocean waters (Table 1), but the sources and chemical structures of these ligands are presently

much less understood, although clearly the release of ligands is linked to microbial biomass and thus their source is thought to be biological (Boye *et al.*, 2005).

Table 1: Overview of oceanic regions with reported organic speciation of Fe: concentrations of dissolved Fe (dFe) and the organic ligands for Fe (L_i), conditional stability constants ($\sim 10^{10}$ conversion factor relates $\log K'_{Fe-L}$ to $\log K'_{Fe(III)-L_i}$).

Location	Depth(m)	[dFe] (nM)	[L_i] (nM)	$\log K'_{Fe-L}$	References
Atlantic Ocean	80 -100	1.6-1.8	3.5-4.8	19.0	(Gledhill & Van Den
	800 -1000	0.8-0.85	3.0-5.0	19.6	Berg, 1995)
Western Mediterranean	0 -165	3.1	4.0 -12	21.3-22.5	(Van Den Berg, 1995)
	400 -	2.6	6.4-7.8	19.79-	
	2500			20.38	
Northwest Atlantic Ocean		< 400	0.45 - 0.60	> 23.22	(Wu & Luther, 1995)
HNLC region of the Equatorial Pacific	Surface	0.02-	L_1 :	22.67	(Rue & Bruland, 1997)
		0.04	0.31 ± 0.01	21.81	
			L_2 :		
			0.19 ± 0.09		
Southern Ocean Pacific sector	25 - 800	0.14 ± 0.72	2.0 ± 12.0	20.6-21.6	(Nolting <i>et al.</i> , 1998)
Northwestern Atlantic	Surface	0.5-1.9	2.0-5.0	22.3-22.9	(Witter & Luther, 1998)
Southern Ocean Atlantic sector	Surface	0.25 ± 0.13	0.72 ± 0.23	22.1 ± 0.5	(Boye <i>et al.</i> , 2001)
Southern Ocean eastern Atlantic sector	Surface	1.0-3.0	0.9-3.0	21.4-23.5	(Croot <i>et al.</i> , 2004)
Eastern North Atlantic Ocean	Surface	0.31 ± 0.18	1.79 ± 0.73	19.8-22.7	(Gerringa <i>et al.</i> , 2006)
Southern Ocean (Indian sector)	Surface	0.91	0.44-1.61	21.7	(Gerringa <i>et al.</i> , 2008)
Tropical North Atlantic Ocean	Surface	0.1-0.4	0.82-1.46	22.85 ± 0.38	(Rijkenberg <i>et al.</i> , 2008)
Eastern North Atlantic Ocean	Surface	0.1-0.4	0.8-1.2	21.6-22.6	(Thuroczy <i>et al.</i> , 2010)

1.4 Specific Fe(III) chelators: Siderophores

There is a prominent hypothesis that an important fraction of natural organic Fe(III) binding ligands are bacterial siderophores (Tortell *et al.*, 1999) which alter Fe bioavailability to marine organisms (Hutchins *et al.*, 1999a). Siderophores (from the Greek “Fe carriers”) (Drechsel & Jung, 1998) are low molecular weight organic compounds (300-1500 Da) which are produced by prokaryotes as part of a specific Fe uptake mechanism (Vraspir & Butler, 2009). Figure 6 shows the schematic role of siderophores in the Fe cycle in the mixed layer as suggested by Tortell *et al.* (1999).

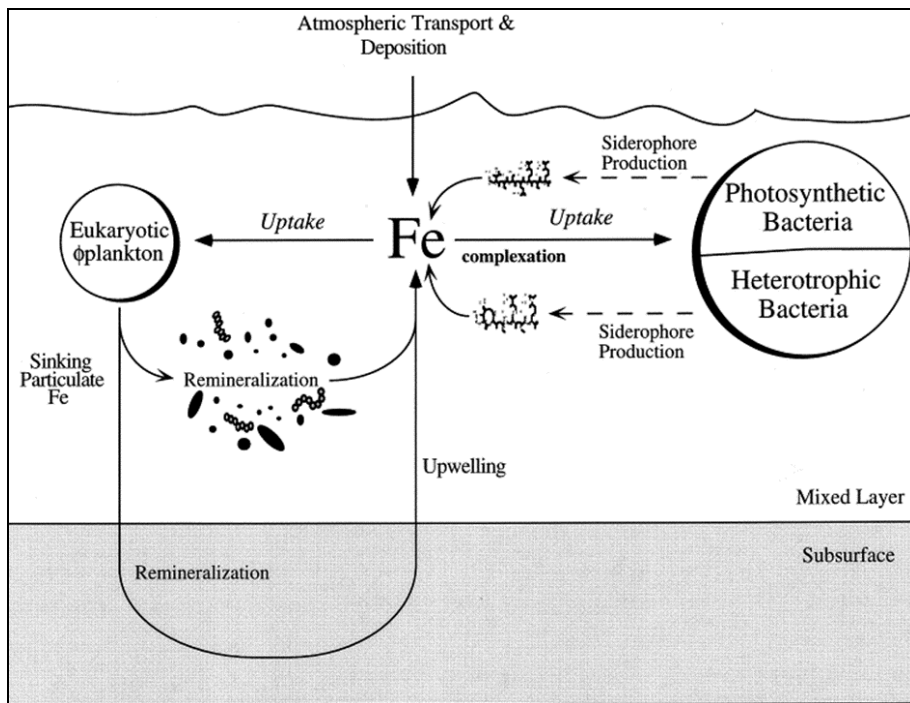


Figure 6: The role of siderophores in the Fe cycle in the upper and deep ocean (Tortell *et al.*, 1999).

The siderophore family includes hydroxamate acid, catechol or α -hydroxy carboxylic acid functional groups for Fe coordination. These specific chelators have an extraordinarily high affinity for Fe(III) (Jalal *et al.*, 1984; Matzanke *et al.*, 1991; Boukhalfa & Crumbliss, 2002), compared to other divalent ions (Kraemer, 2004). Once Fe chelation deprotonation occurs, the tricatecholates and trihydroxamates generally form 1:1 complexes with trivalent Fe with stability constants of 10^{52} (enterobactin) (Drechsel & Jung, 1998; Budzikiewicz, 2004) and $10^{30.6}$ (ferrioxamine B) (Boukhalfa & Crumbliss, 2002; Kraemer, 2004) (Fig.7).

There are several lines of indirect evidence consistent with the hypothesis that marine organic Fe(III) binding ligands include siderophores (Tortell *et al.*, 1999). Marine microorganisms, mostly heterotrophic bacteria and cyanobacteria, are reported to produce siderophores to facilitate Fe uptake under low Fe level seawater cultures (Trick, 1989; Reid *et al.*, 1993; Wilhelm & Trick, 1994; Wilhelm *et al.*, 1996). In fact, the production of several different types of siderophores by marine bacteria (Butler, 2005a) and by mixed bacterial populations in incubations of natural seawater have been documented (Gledhill *et al.*, 2004). Moreover, these siderophores have similar conditional stability constant in seawater to the natural organic Fe(III) binding ligands (Macrellis *et al.*, 2001). Several hydroxamate and catecholate siderophores have conditional stability constants between $10^{11.5}$ - $10^{12.5}$ (Lewis *et al.*, 1995). Measurements of Fe(III) binding ligands from the California coastal upwelling region have shown that

a large proportion of the ligands is similar in size (300-1000 Da) and contain functional groups similar to siderophores (Macrellis *et al.*, 2001). This similarity could give us some information about the structural nature of the organic molecules that bind Fe(III).

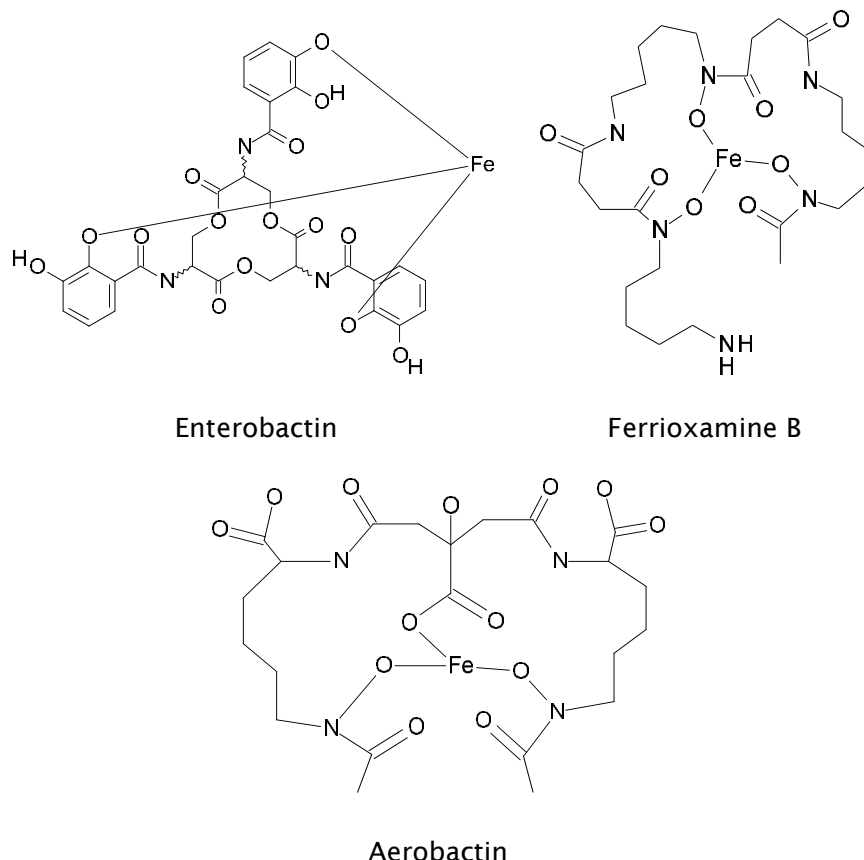


Figure 7: Examples of siderophores type ligands with enterobactin (catecholate), ferrioxamine B (hydroxamate) and aerobactin (α -hydroxy carboxylic). Three catechol rings wrap around the Fe(III) to afford a right-handed (D) coordination propeller with the highest known binding constant for ferric ion.

However, the first direct observations of siderophores in natural seawater have been reported by Mawji *et al.* (2008a) the Atlantic Ocean samples. Two types of hydroxamate siderophores, Ferrioxamine G (FOG) and ferrioxamine E (FOE) (Fig. 8) were successfully identified using a recently developed high performance liquid chromatography- mass spectrometry method (Mawji *et al.*, 2008a). The total concentrations of siderophores ranged between 3-20 pM, which was much lower than the dFe concentrations (0.58 ± 0.25 nM, $n = 118$) (Mawji *et al.*, 2008a). Thus, they were suggested to be present as Fe complexes in seawater, since this type of siderophore (ferrioxamines) are hydrophilic, stable and do not photochemically degrade in natural sunlight (Barbeau *et al.*, 2003).

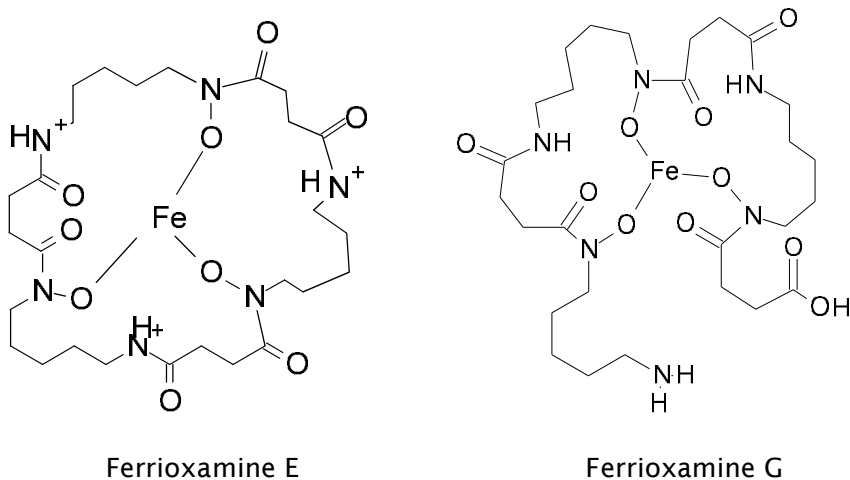


Figure 8: Structures of the two siderophores identified in Atlantic seawater samples. A less abundant cyclic ferrioxamine E and a more abundant linear ferrioxamine G (Mawji *et al.*, 2008a).

The study by Mawji *et al.* (2008a) showed that dissolved siderophore-like compounds occur in seawater, and hence play an active role as Fe-complexing agents in the natural marine environment (Macrellis *et al.*, 2001). The Fe(III) siderophore complexes are thermodynamically very stable (Renshaw *et al.*, 2002). The formation of these complexes would minimize the adsorption of Fe to particles, thereby maximizing the Fe residence time in seawater, which benefits the biological community (Johnson *et al.*, 1997a; Sunda, 1997; Sunda & Huntsman, 1997). These organic complexes with high stability constants therefore strongly influence Fe biogeochemistry in the ocean (Mawji *et al.*, 2008a; Hopkinson & Morel, 2009; Vraspir & Butler, 2009).

1.5 Future speciation study in the high latitude North Atlantic Ocean

The distribution of dissolved Fe in the water column of the high latitude North Atlantic has been studied and the low Fe concentrations yield Fe limitation of phytoplankton during post spring bloom conditions (Nielsdottir *et al.*, 2009). Measurements of dissolved Fe concentrations alone are insufficient for understanding the accessibility of Fe to microorganism. Therefore, knowledge of the chemical speciation of Fe is critical and facilitates an improved understanding of the mechanisms which microorganism utilise Fe in order to fulfil their requirements in this region. Since the solubility and bioavailability of Fe are controlled by its speciation (Sunda *et al.*, 1991; Zhu *et al.*, 1992; Kuma & Matsunaga, 1995; Rue & Bruland, 1995; Kuma *et al.*, 1996), it is important to determine Fe speciation in these waters. To our knowledge, there is no Fe speciation data available for this ocean region yet.

The nature of organic Fe(III) binding ligands in seawater is still largely unknown and little is known about their ecological significance. The high organic Fe(III)-binding affinities of the unidentified compounds strongly suggest that they could be siderophores biosynthesized by marine bacteria. Siderophores potentially facilitate Fe uptake for certain Fe limited microorganisms in high latitude North Atlantic Ocean. However, the direct determination of siderophores in natural seawater has been reported in only a limited number of locations (Mawji *et al.*, 2008a; Velasquez *et al.*, 2011) and there were no data on the occurrence of siderophore-like substances in the high latitude North Atlantic Ocean. Thus, we will determine the presence of siderophore in this region using the recently developed analytical techniques (Mawji *et al.*, 2008a). The concentrations and structures of siderophores will help us to better understand the biological availability of Fe in seawater.

1.6 Objectives of study

The overall aim of this research is to study the speciation of Fe and the role of siderophores (specific Fe chelater) in the biogeochemical cycle of Fe in the high latitude North Atlantic.

Specific objectives were to:

1. To determine the distribution of Fe speciation in the high latitude North Atlantic Ocean in order to understand the role of organic Fe(III) binding ligands in the distribution of Fe in the water column.
2. To identify and quantify the presence of dissolved siderophores in natural seawater in the high latitude North Atlantic Ocean by interfacing liquid chromatography with inductively coupled plasma mass spectrometry (LC-ICP-MS) and liquid chromatography with electro spray ionization mass spectrometry (LC-ESI-MS) methods.
3. To study the siderophore type chelates produced by marine bacterioplankton in nutrient enrichment incubation experiments from the high latitude North Atlantic Ocean seawater.

1.7 Thesis structure

In Chapter 2, I describe in detail the methods which were used in this work. The Fe speciation and Liquid Chromatography with Inductively Coupled Plasma Mass Spectrometry (LC-ICP-MS) methods were used for studies reported in the Chapter 3, Chapter 4 and Chapter 5, respectively. Each chapter includes an area specific introduction and presents work carried out in the high latitude North Atlantic.

Chapter 3 presents the first assessment of organic Fe(III) binding ligands in the high latitude North Atlantic Ocean (Iceland Basin), an ocean region which undergoes seasonal Fe limitation. The results from 2009 were compared to results from 2007 in order to obtain a better understanding of the role of organic Fe(III) binding ligands in controlling Fe concentrations throughout the water column. The ratio of $[L]/[dFe]$ was used to analyse trends in Fe speciation in the Iceland Basin and it was compared to the other regions including Hatton-Rockall and Rockall Trough.

Chapter 4 includes the identification and quantification of dissolved hydroxamate siderophores in the high latitude North Atlantic Ocean using High Performance Liquid Chromatography – Electro Spray Ionization – Mass Spectrometry (LC-ESI-MS) and liquid chromatography with inductively coupled plasma mass spectrometry (LC-ICP-MS). Samples were collected from the Iceland Basin and Irminger Basin during two cruises in summer 2010.

Chapter 5 described the siderophore type chelates produced by marine bacterioplankton in experiments where seawater was incubated with different sources of nutrients, were also examined. The effect of different additions of Fe(III) level (9 nM and 90 nM) to the incubated samples were investigated during April-May 2010 cruise, while the effect of different sources of nitrogen (ammonium and nitrate) on the production of siderophore type chelates was examined in July-August 2010.

Chapter 6 provides a synthesis of Chapter 3, Chapter 4 and Chapter 5 regarding the Fe speciation study in the high latitude North Atlantic Ocean (Iceland Basin) and highlights directions for future research.

References

Allen, J. T., Brown, L., Sanders, R., Moore, C. M., Mustard, A., Fielding, S., Lucas, M., Rixen, M., Savidge, G., Henson, S. & Mayor, D. (2005) Diatom carbon export enhanced by silicate upwelling in the northeast Atlantic. *Nature*, 437, 728-732.

Archer, D. E. & Johnson, K. (2000) A Model of the iron cycle in the ocean. *Global Biogeochemical Cycles*, 14, 269-279.

Barbeau, K. (2006) Photochemistry of organic iron(III) complexing ligands in oceanic systems. *Photochem Photobiol*, 82, 1505-16.

Barbeau, K., Rue, E. L., Trick, C. G., Bruland, K. T. & Butler, A. (2003) Photochemical reactivity of siderophores produced by marine heterotrophic bacteria and cyanobacteria based on characteristic Fe(III) binding groups. *Limnology and Oceanography*, 48, 1069-1078.

Blain, S., Guieu, U., Claustre, H., Leblanc, K., Moutin, T., Queguiner, B., Ras, J. & Sarthou, G. (2004) Availability of iron and major nutrients for phytoplankton in the northeast Atlantic Ocean. *Limnology and Oceanography*, 49, 2095-2104.

Boukhalfa, H. & Crumbiss, A. L. (2002) Chemical aspects of siderophore mediated iron transport. *Biometals*, 15, 325-339.

Boyd, P. W., Law, C. S., Wong, C. S., Nojiri, Y., Tsuda, A., Levasseur, M., Takeda, S., Rivkin, R., Harrison, P. J., Strzepek, R., Gower, J., Mckay, R. M., Abraham, E., Arychuk, M., Barwell-Clarke, J., Crawford, W., Crawford, D., Hale, M., Harada, K., Johnson, K., Kiyosawa, H., Kudo, I., Marchetti, A., Miller, W., Needoba, J., Nishioka, J., Ogawa, H., Page, J., Robert, M., Saito, H., Sastri, A., Sherry, N., Soutar, T., Sutherland, N., Taira, Y., Whitney, F., Wong, S. K. E. & Yoshimura, T. (2004) The decline and fate of an iron-induced subarctic phytoplankton bloom. *Nature*, 428, 549-553.

Boyd, P. W., Watson, A. J., Law, C. S., Abraham, E. R., Trull, T., Murdoch, R., Bakker, D. C. E., Bowie, A. R., Buesseler, K. O., Chang, H., Charette, M., Croot, P., Downing, K., Frew, R., Gall, M., Hadfield, M., Hall, J., Harvey, M., Jameson, G., Laroche, J., Liddicoat, M., Ling, R., Maldonado, M. T., Mckay, R. M., Nodder, S., Pickmere, S., Pridmore, R., Rintoul, S., Safi, K., Sutton, P., Strzepek, R., Tanneberger, K., Turner, S., Waite, A. & Zeldis, J. (2000) A mesoscale phytoplankton bloom in the polar Southern Ocean stimulated by iron fertilization. *Nature*, 407, 695-702.

Boye, M., Nishioka, J., Croot, P. L., Laan, P., Timmermans, K. R. & De Baar, H. J. W. (2005) Major deviations of iron complexation during 22 days of a mesoscale iron enrichment in the open Southern Ocean. *Marine Chemistry*, 96, 257-271.

Boye, M., Van Den Berg, C. M. G., De Jong, J. T. M., Leach, H., Croot, P. & De Baar, H. J. W. (2001) Organic complexation of iron in the Southern Ocean. *Deep-Sea Research Part I-Oceanographic Research Papers*, 48, 1477-1497.

Bruland, K. & Rue, E. (2001) Domoic acid binds iron and copper: a possible role for the toxin produced by the marine diatom *Pseudo-nitzschia*. *Marine Chemistry*, 76, 127-134.

Bruland, K. W. & Wells, S. G. (1995) The Chemistry of Iron in Seawater and Its Interaction with Phytoplankton - Introduction. *Marine Chemistry*, 50, 1-2.

Budzikiewicz, H. (2004) Selected reviews on mass spectrometric topics-CX. *Mass Spectrometry Reviews*, 23, 228-229.

Butler, A. (2005) Marine microbial iron mobilization: New marine siderophores. *Abstracts of Papers of the American Chemical Society*, 229, U893-U893.

Coale, K. H., Johnson, K. S., Chavez, F. P., Buesseler, K. O., Barber, R. T., Brzezinski, M. A., Cochlan, W. P., Millero, F. J., Falkowski, P. G., Bauer, J. E., Wanninkhof, R. H., Kudela, R. M., Altabet, M. A., Hales, B. E., Takahashi, T., Landry, M. R., Bidigare, R. R., Wang, X. J., Chase, Z., Strutton, P. G., Friederich, G. E., Gorbunov, M. Y., Lance, V. P., Hilting, A. K., Hiscock, M. R., Demarest, M., Hiscock, W. T., Sullivan, K. F., Tanner, S. J., Gordon, R. M., Hunter, C. N., Elrod, V. A., Fitzwater, S. E., Jones, J. L., Tozzi, S., Koblizek, M., Roberts, A. E., Herndon, J., Brewster, J., Ladizinsky, N., Smith, G., Cooper, D., Timothy, D., Brown, S. L., Selpf, K. E., Sheridan, C. C., Twining, B. S. & Johnson, Z. I. (2004) Southern ocean iron enrichment experiment: Carbon cycling in high- and low-Si waters. *Science*, 304, 408-414.

Coale, K. H., Johnson, K. S., Fitzwater, S. E., Gordon, R. M., Tanner, S., Chavez, F. P., Ferioli, L., Sakamoto, C., Rogers, P., Millero, F., Steinberg, P., Nightingale, P., Cooper, D., Cochlan, W. P., Landry, M. R., Constantinou, J., Rollwagen, G., Trasvina, A. & Kudela, R. (1996) A massive phytoplankton bloom induced by an ecosystem-scale iron fertilization experiment in the equatorial Pacific Ocean. *Nature*, 383, 495-501.

Croot, P. L., Andersson, K., Ozturk, M. & Turner, D. R. (2004) The distribution and specification of iron along 6 degrees E in the Southern Ocean. *Deep-Sea Research Part II-Topical Studies in Oceanography*, 51, 2857-2879.

Croot, P. L. & Johansson, M. (2000) Determination of iron speciation by cathodic stripping voltammetry in seawater using the competing ligand 2-(2-thiazolylazo)-p-cresol (TAC). *Electroanalysis*, 12, 565-576.

De Baar, H. J. W., Burna, A. G. J., Nolting, R. F., Cadee, G. C., Jacques, G. & Treguer, P. J. (1990) On Iron Limitation of the Southern-Ocean - Experimental-Observations in the Weddell and Scotia Seas. *Marine Ecology-Progress Series*, 65, 105-122.

De Jong, J. T. M., Boye, M., Schoemann, V. F., Nolting, R. F. & De Baar, H. J. W. (2000) Shipboard techniques based on flow injection analysis for measuring dissolved Fe, Mn and Al in seawater. *Journal of Environmental Monitoring*, 2, 496-502.

Drechsel, H. & Jung, G. (1998) Peptide siderophores. *Journal of Peptide Science*, 4, 147-181.

Duce, R. A., Tindale, N. & Zhuang, G. (1991) Atmospheric Iron and Its Impact on Marine Biological Productivity and Chemical Cycling. *Abstracts of Papers of the American Chemical Society*, 201, 20-Nucl.

Ducklow, H. W. & Harris, R. P. (1993) Introduction to the Jgofs North-Atlantic Bloom Experiment. *Deep-Sea Research Part II-Topical Studies in Oceanography*, 40, 1-8.

Falkowski, P. G., Barber, R. T. & Smetacek, V. (1998) Biogeochemical controls and feedbacks on ocean primary production. *Science*, 281, 200-206.

Fung, I. Y., Meyn, S. K., Tegen, I., Doney, S. C., John, J. & Bishop, J. (2000) Iron supply and demand in the upper ocean (vol 14, pg 281, 2000). *Global Biogeochemical Cycles*, 14, 697-700.

Gao, Y., Kaufman, Y. J., Tanre, D., Kolber, D. & Falkowski, P. G. (2001) Seasonal distributions of aeolian iron fluxes to the global ocean. *Geophysical Research Letters*, 28, 29-32.

Geider, R. J. (1993) Quantitative Phytoplankton Physiology - Implications for Primary Production and Phytoplankton Growth. *Measurement of Primary Production from the Molecular to the Global Scale*, 197, 52-62.

Geider, R. J. & Laroche, J. (1994) The Role of Iron in Phytoplankton Photosynthesis, and the Potential for Iron-Limitation of Primary Productivity in the Sea. *Photosynthesis Research*, 39, 275-301.

Gerringa, L. J. A., Blain, S., Laan, P., Sarthou, G., Veldhuis, M. J. W., Brussaard, C. P. D., Viollier, E. & Timmermans, K. R. (2008) Fe-binding dissolved organic ligands near the Kerguelen Archipelago in the Southern Ocean (Indian sector). *Deep-Sea Research Part II-Topical Studies in Oceanography*, 55, 606-621.

Gerringa, L. J. A., De Baar, H. J. W. & Timmermans, K. R. (2000) A comparison of iron limitation of phytoplankton in natural oceanic waters and laboratory media conditioned with EDTA. *Marine Chemistry*, 68, 335-346.

Gerringa, L. J. A., Veldhuis, M. J. W., Timmermans, K. R., Sarthou, G. & De Baar, H. J. W. (2006) Co-variance of dissolved Fe-binding ligands with phytoplankton characteristics in the Canary Basin. *Marine Chemistry*, 102, 276-290.

Gervais, F., Riebesell, U. & Gorbunov, M. Y. (2002) Changes in primary productivity and chlorophyll a in response to iron fertilization in the Southern Polar Frontal Zone. *Limnology and Oceanography*, 47, 1324-1335.

Gledhill, M., McCormack, P., Ussher, S., Achterberg, E. P., Mantoura, R. F. C. & Worsfold, P. J. (2004) Production of siderophore type chelates by mixed bacterioplankton populations in nutrient enriched seawater incubations. *Marine Chemistry*, 88, 75-83.

Gledhill, M. & Van Den Berg, C. M. G. (1994) Determination of Complexation of Iron(III) with Natural Organic Complexing Ligands in Seawater Using Cathodic Stripping Voltammetry. *Marine Chemistry*, 47, 41-54.

Gledhill, M. & Van Den Berg, C. M. G. (1995) Measurement of the Redox Speciation of Iron in Seawater by Catalytic Cathodic Stripping Voltammetry. *Marine Chemistry*, 50, 51-61.

Gong, S. L., Zhang, X. Y., Zhao, T. L. & Barrie, L. A. (2004) Sensitivity of Asian dust storm to natural and anthropogenic factors. *Geophysical Research Letters*, 31, -.

Guieu, C., Bozec, Y., Blain, S., Ridame, C., Sarthou, G. & Leblond, N. (2002) Impact of high Saharan dust inputs on dissolved iron concentrations in the Mediterranean Sea. *Geophysical Research Letters*, 29, -.

Hoffmann, L. J., Peeken, I., Lochte, K., Assmy, P. & Veldhuis, M. (2006) Different reactions of Southern Ocean phytoplankton size classes to iron fertilization. *Limnology and Oceanography*, 51, 1217-1229.

Holliday, N. P. & Reid, P. C. (2001) Is there a connection between high transport of water through the Rockall Trough and ecological changes in the North Sea? *Ices Journal of Marine Science*, 58, 270-274.

Hopkinson, B. M. & Morel, F. M. M. (2009) The role of siderophores in iron acquisition by photosynthetic marine microorganisms. *Biometals*, 22, 659-669.

Hudson, R. J. M., Covault, D. T. & Morel, F. M. M. (1992) Investigations of Iron Coordination and Redox Reactions in Seawater Using Fe-59 Radiometry and Ion-Pair Solvent-Extraction of Amphiphilic Iron Complexes. *Marine Chemistry*, 38, 209-235.

Hudson, R. J. M. & Morel, F. M. M. (1990) Iron Transport in Marine-Phytoplankton - Kinetics of Cellular and Medium Coordination Reactions. *Limnology and Oceanography*, 35, 1002-1020.

Hutchins, D. A., Ditullio, G. R., Zhang, Y. & Bruland, K. W. (1998) An iron limitation mosaic in the California upwelling regime. *Limnology and Oceanography*, 43, 1037-1054.

Hutchins, D. A., Franck, V. M., Brzezinski, M. A. & Bruland, K. W. (1999) Inducing phytoplankton iron limitation in iron-replete coastal waters with a strong chelating ligand. *Limnology and Oceanography*, 44, 1009-1018.

Jalal, M. a. F., Mocharla, R. & Vanderhelm, D. (1984) Separation of Ferrichromes and Other Hydroxamate Siderophores of Fungal Origin by Reversed-Phase Chromatography. *Journal of Chromatography*, 301, 247-252.

Jickells, T. D., An, Z. S., Andersen, K. K., Baker, A. R., Bergametti, G., Brooks, N., Cao, J. J., Boyd, P. W., Duce, R. A., Hunter, K. A., Kawahata, H., Kubilay, N., Laroche, J., Liss, P. S., Mahowald, N., Prospero, J. M., Ridgwell, A. J., I. T. & Torres, R. (2005) Global iron connections between desert dust, ocean biogeochemistry, and climate. *Science*, 308, 67-71.

Johnson, K. S., Gordon, R. M. & Coale, K. H. (1997) What controls dissolved iron concentrations in the world ocean? *Marine Chemistry*, 57, 137-161.

Kraemer, S. M. (2004) Iron oxide dissolution and solubility in the presence of siderophores. *Aquatic Sciences*, 66, 3-18.

Kuma, K., Katsumoto, A., Nishioka, J. & Matsunaga, K. (1998) Size-fractionated iron concentrations and Fe(III) hydroxide solubilities in various coastal waters. *Estuarine Coastal and Shelf Science*, 47, 275-283.

Kuma, K. & Matsunaga, K. (1995) Availability of Colloidal Ferric Oxides to Coastal Marine-Phytoplankton. *Marine Biology*, 122, 1-11.

Kuma, K., Nishioka, J. & Matsunaga, K. (1996) Controls on iron(III) hydroxide solubility in seawater: The influence of pH and natural organic chelators. *Limnology and Oceanography*, 41, 396-407.

Kumar, C. V. R. V., Sayer, M. & Pascual, R. (1995) Ferroelectric Lead Iron-Chromium-Nickel Niobate Films. *Integrated Ferroelectrics*, 8, 251-265.

Lewis, B. L., Holt, P. D., Taylor, S. W., Wilhelm, S. W., Trick, C. G., Butler, A. & Luther, G. W. (1995) Voltammetric Estimation of Iron(III) Thermodynamic Stability-Constants for Catecholate Siderophores Isolated from Marine-Bacteria and Cyanobacteria. *Marine Chemistry*, 50, 179-188.

Liu, X. W. & Millero, F. J. (1999) The solubility of iron hydroxide in sodium chloride solutions. *Geochimica Et Cosmochimica Acta*, 63, 3487-3497.

Liu, X. W. & Millero, F. J. (2002) The solubility of iron in seawater. *Marine Chemistry*, 77, 43-54.

Macrellis, H. M., Trick, C. G., Rue, E. L., Smith, G. & Bruland, K. W. (2001) Collection and detection of natural iron-binding ligands from seawater. *Marine Chemistry*, 76, 175-187.

Maldonado, M. T., Strzepek, R. F., Sander, S. & Boyd, P. W. (2005) Acquisition of iron bound to strong organic complexes, with different Fe binding groups and photochemical reactivities, by plankton communities in Fe-limited subantarctic waters. *Global Biogeochemical Cycles*, 19.

Martin, J. H., Broenkow, W. W., Fitzwater, S. E. & Gordon, R. M. (1990) Does Iron Really Limit Phytoplankton Production in the Offshore Sub-Arctic Pacific - Yes, It Does - a Reply. *Limnology and Oceanography*, 35, 775-777.

Martin, J. H., Coale, K. H., Johnson, K. S., Fitzwater, S. E., Gordon, R. M., Tanner, S. J., Hunter, C. N., Elrod, V. A., Nowicki, J. L., Coley, T. L., Barber, R. T., Lindley, S., Watson, A. J., Vanscoy, K., Law, C. S., Liddicoat, M. I., Ling, R., Stanton, T., Stockel, J., Collins, C., Anderson, A., Bidigare, R., Ondrusek, M., Latasa, M., Millero, F. J., Lee, K., Yao, W., Zhang, J. Z., Friederich, G., Sakamoto, C., Chavez, F., Buck, K., Kolber, Z., Greene, R., Falkowski, P., Chisholm, S. W., Hoge, F., Swift, R., Yungel, J., Turner, S., Nightingale, P., Hatton, A., Liss, P. & Tindale, N. W. (1994) Testing the Iron Hypothesis in Ecosystems of the Equatorial Pacific-Ocean. *Nature*, 371, 123-129.

Martin, J. H. & Fitzwater, S. E. (1988) Iron-Deficiency Limits Phytoplankton Growth in the Northeast Pacific Subarctic. *Nature*, 331, 341-343.

Martin, J. H., Fitzwater, S. E., Gordon, R. M., Hunter, C. N. & Tanner, S. J. (1993) Iron, Primary Production and Carbon Nitrogen Flux Studies during the Jgofs North-Atlantic Bloom Experiment. *Deep-Sea Research Part II-Topical Studies in Oceanography*, 40, 115-134.

Matzanke, B. F., Berner, I., Bill, E., Trautwein, A. X. & Winkelmann, G. (1991) Transport and Utilization of Ferrioxamine-E-Bound Iron in *Erwinia-Herbicola* (Pantoea-Agglomerans). *Biology of Metals*, 4, 181-185.

Mawji, E., Gledhill, M., Milton, J. A., Tarran, G. A., Ussher, S., Thompson, A., Wolff, G. A., Worsfold, P. J. & Achterberg, E. P. (2008) Hydroxamate Siderophores: Occurrence and Importance in the Atlantic Ocean. *Environmental Science & Technology*, 42, 8675-8680.

Measures, C. I., Landing, W. M., Brown, M. T. & Buck, C. S. (2008) High-resolution Al and Fe data from the Atlantic Ocean CLIVAR-CO(2) repeat hydrography A16N transect: Extensive linkages between atmospheric dust and upper ocean geochemistry. *Global Biogeochemical Cycles*, 22.

Millero, F. J. (1996) Modeling the effect of ionic interactions on radionuclides in natural waters. *Abstracts of Papers of the American Chemical Society*, 212, 85-Nucl.

Millero, F. J. (2001) Speciation of metals in natural waters. *Abstracts of Papers of the American Chemical Society*, 221, U533-U533.

Moore, C. M., Mills, M. M., Milne, A., Langlois, R., Achterberg, E. P., Lochte, K., Geider, R. J. & La Roche, J. (2006) Iron limits primary productivity during spring bloom development in the central North Atlantic. *Global Change Biology*, 12, 626-634.

Nielsdottir, M. C., Moore, C. M., Sanders, R., Hinz, D. J. & Achterberg, E. P. (2009) Iron limitation of the postbloom phytoplankton communities in the Iceland Basin. *Global Biogeochemical Cycles*, 23, 1-13.

Nodwell, L. M. & Price, N. M. (2001) Direct use of inorganic colloidal iron by marine mixotrophic phytoplankton. *Limnology and Oceanography*, 46, 765-777.

Nolting, R. F., Gerringa, L. J. A., Swagerman, M. J. W., Timmermans, K. R. & De Baar, H. J. W. (1998) Fe (III) speciation in the high nutrient, low chlorophyll Pacific region of the Southern Ocean. *Marine Chemistry*, 62, 335-352.

Prospero, J. M. & Carlson, T. N. (1972) Vertical and Areal Distribution of Saharan Dust over Western Equatorial North-Atlantic Ocean. *Journal of Geophysical Research*, 77, 5255-8.

Reid, R. T., Live, D. H., Faulkner, D. J. & Butler, A. (1993) A Siderophore from a Marine Bacterium with an Exceptional Ferric Ion Affinity Constant. *Nature*, 366, 455-458.

Renshaw, J. C., Robson, G. D., Trinci, A. P. J., Wiebe, M. G., Livens, F. R., Collison, D. & Taylor, R. J. (2002) Fungal siderophores: structures, functions and applications. *Mycological Research*, 106, 1123-1142.

Rijkenberg, M. J. A., Powell, C. F., Dall'osto, M., Nielsdottir, M. C., Patey, M. D., Hill, P. G., Baker, A. R., Jickells, T. D., Harrison, R. M. & Achterberg, E. P. (2008) Changes in iron speciation following a Saharan dust event in the tropical North Atlantic Ocean. *Marine Chemistry*, 110, 56-67.

Roy, E. G., Wells, M. L. & King, D. W. (2008) Persistence of iron(II) in surface waters of the western subarctic Pacific. *Limnology and Oceanography*, 53, 89-98.

Rue, E. L. & Bruland, K. W. (1995) Complexation of Iron(III) by Natural Organic-Ligands in the Central North Pacific as Determined by a New Competitive Ligand Equilibration Adsorptive Cathodic Stripping Voltammetric Method. *Marine Chemistry*, 50, 117-138.

Rue, E. L. & Bruland, K. W. (1997) The role of organic complexation on ambient iron chemistry in the equatorial Pacific Ocean and the response of a mesoscale iron addition experiment. *Limnology and Oceanography*, 42, 901-910.

Sanders, R., Brown, L., Henson, S. & Lucas, M. (2005) New production in the Irminger Basin during 2002. *Journal of Marine Systems*, 55, 291-310.

Siegel, D. A., Doney, S. C. & Yoder, J. A. (2002) The North Atlantic spring phytoplankton bloom and Sverdrup's critical depth hypothesis. *Science*, 296, 730-733.

Spokes, L., Jickells, T. & Jarvis, K. (2001) Atmospheric inputs of trace metals to the northeast Atlantic Ocean: the importance of southeasterly flow. *Marine Chemistry*, 76, 319-330.

Strzepek, R. F., Maldonado, M. T., Higgins, J. L., Hall, J., Safi, K., Wilhelm, S. W. & Boyd, P. W. (2005) Spinning the "Ferrous Wheel": The importance of the microbial community in an iron budget during the FeCycle experiment. *Global Biogeochemical Cycles*, 19.

Sunda, W. G. (1997) Control of dissolved iron concentrations in the world ocean: A comment. *Marine Chemistry*, 57, 169-172.

Sunda, W. G. & Huntsman, S. A. (1995) Iron Uptake and Growth Limitation in Oceanic and Coastal Phytoplankton. *Marine Chemistry*, 50, 189-206.

Sunda, W. G. & Huntsman, S. A. (1997) Interrelated influence of iron, light and cell size on marine phytoplankton growth. *Nature*, 390, 389-392.

Sunda, W. G., Swift, D. G. & Huntsman, S. A. (1991) Low Iron Requirement for Growth in Oceanic Phytoplankton. *Nature*, 351, 55-57.

Tani, F., Matsu-Ura, M., Ariyama, K., Setoyama, T., Shimada, T., Kobayashi, S., Hayashi, T., Matsuo, T., Hisaeda, Y. & Naruta, Y. (2003) Iron twin-coronet porphyrins as models of myoglobin and hemoglobin: Amphibious electrostatic effects of overhanging hydroxyl groups for successful CO/O₂ discrimination. *Chemistry-a European Journal*, 9, 862-870.

Thuroczy, C. E., Gerringa, L. J. A., Klunder, M. B., Middag, R., Laan, P., Timmermans, K. R. & De Baar, H. J. W. (2010) Speciation of Fe in the Eastern North Atlantic Ocean. *Deep-Sea Research Part I-Oceanographic Research Papers*, 57, 1444-1453.

Tortell, P. D., Maldonado, M. T., Granger, J. & Price, N. M. (1999) Marine bacteria and biogeochemical cycling of iron in the oceans. *Fems Microbiology Ecology*, 29, 1-11.

Trick, C. G. (1989) Hydroxamate-Siderophore Production and Utilization by Marine Eubacteria. *Current Microbiology*, 18, 375-378.

Tsuda, A., Takeda, S., Saito, H., Nishioka, J., Nojiri, Y., Kudo, I., Kiyosawa, H., Shiromoto, A., Imai, K., Ono, T., Shimamoto, A., Tsumune, D., Yoshimura, T., Aono, T., Hinuma, A., Kinugasa, M., Suzuki, K., Sohrin, Y., Noiri, Y., Tani, H., Deguchi, Y., Tsurushima, N., Ogawa, H., Fukami, K., Kuma, K. & Saino, T. (2003) A mesoscale iron enrichment in the western Subarctic Pacific induces a large centric diatom bloom. *Science*, 300, 958-961.

Van Den Berg, C. M. G. (1995) Evidence for Organic Complexation of Iron in Seawater. *Marine Chemistry*, 50, 139-157.

Velasquez, I., Nunn, B. L., Ibsanmi, E., Goodlett, D. R., Hunter, K. A. & Sander, S. G. (2011) Detection of hydroxamate siderophores in coastal and Sub-Antarctic water off the South Eastern Coast of New Zealand. *Marine Chemistry*, 126, 97-107.

Vraspir, J. M. & Butler, A. (2009) Chemistry of Marine Ligands and Siderophores. *Annual Review of Marine Science*, 1, 43-63.

Waite, A. M. & Nodder, S. D. (2001) The effect of in situ iron addition on the sinking rates and export flux of Southern Ocean diatoms. *Deep-Sea Research Part II-Topical Studies in Oceanography*, 48, 2635-2654.

Weber, K. A., Thieme, J., Larese-Casanova, P., Scherer, M., Achenbach, L. A. & Coates, J. D. (2005) Green rust formation under anaerobic nitrate-dependent Fe(II) oxidizing conditions. *Geochimica Et Cosmochimica Acta*, 69, A463-A463.

Wilhelm, S. W., Maxwell, D. P. & Trick, C. G. (1996) Growth, iron requirements, and siderophore production in iron-limited *Synechococcus* PCC 7002. *Limnology and Oceanography*, 41, 89-97.

Wilhelm, S. W. & Trick, C. G. (1994) Iron-Limited Growth of Cyanobacteria - Multiple Siderophore Production Is a Common Response. *Limnology and Oceanography*, 39, 1979-1984.

Witter, A. E. & Luther, G. W. (1998) Variation in Fe-organic complexation with depth in the Northwestern Atlantic Ocean as determined using a kinetic approach. *Marine Chemistry*, 62, 241-258.

Wu, J. F., Boyle, E., Sunda, W. & Wen, L. S. (2001) Soluble and colloidal iron in the oligotrophic North Atlantic and North Pacific. *Science*, 293, 847-849.

Wu, J. F. & Luther, G. W. (1995) Complexation of Fe(II) by Natural Organic-Ligands in the Northwest Atlantic-Ocean by a Competitive Ligand Equilibration Method and a Kinetic Approach. *Marine Chemistry*, 50, 159-177.

Ye, Y., Volker, C. & Wolf-Gladrow, D. A. (2009) A model of Fe speciation and biogeochemistry at the Tropical Eastern North Atlantic Time-Series Observatory site. *Biogeosciences*, 6, 2041-2061.

Zhu, X. R., Prospero, J. M., Millero, F. J., Savoie, D. L. & Brass, G. W. (1992) The Solubility of Ferric Ion in Marine Mineral Aerosol Solutions at Ambient Relative Humidities. *Marine Chemistry*, 38, 91-107.

CHAPTER 2 - Methodology

2.1 Cleaning Processes

2.1.1 Low density polyethylene bottles (Nalgene)

Trace-metal clean low density polyethylene (LDPE) 250 mL (Nalgene) bottles were used for collecting seawater samples for the determination of Fe speciation. This type of bottle was also used for storing prepared chemicals. Bottles were cleaned according to the procedures described in Achterberg *et al.* (2001). The LDPE bottles were soaked in Decon 90 (2% v/v) for 24 hours to remove any residual organic material before rinsing with reverse osmosis (Milli-RO; Millipore systems) water three times. The bottles were then soaked in hydrochloric acid (HCl) (AR grade, Fisher scientific 50% v/v, 6 M) for a week before rinsing them with Milli-Q (MQ) water ($>18.2 \text{ M}\Omega \text{ cm}^{-1}$; Millipore systems) three times. Following this pre-treatment, the LDPE bottles were submerged in a nitric acid (HNO₃) (AR grade, Fisher scientific 50% v/v, 3M) bath for another week. After that, they were rinsed with MQ water three times before filling up with MQ water. Finally, the bottles were acidified to a pH of ~2 with sub-boiled quarts distilled hydrochloric acid (HCl) (9 M) (1 mL per 1000 mL MQ water) in a Class 100 laminar flow hood in a dedicated clean room (class 1000). The bottles were tightly capped, bagged and stored in double plastic bags until they were required for use.

2.1.2 Teflon fluorinated ethylene polypropylene (FEP) (Nalgene)

Teflon FEP 30 mL bottles were used for the equilibration of samples prior to the determination of labile Fe for competitive ligands exchange-adsorptive cathodic stripping voltammetry (CLE-AdCSV) experiments and for storing the reagents. The Teflon bottles were first cleaned by rinsing with ethanol (HPLC grade), then a short wash with 10% HCl (Romil SPA grade), followed by a final rinse with MQ water.

2.1.3 Polyethylene heavy duty carboy (Nalgene)

A polyethylene heavy duty carboy 20L (Nalgene) was used for collecting seawater required for siderophore analysis from OTE (Ocean Test Equipment) samplers on board the ship. The carboy was cleaned by rinsing with RO water and soaked in 10% HCl for 2-3 days. Then, the carboys were rinsed with MQ water three times and were double bagged before storing until use. In between seawater extractions, the carboy was thoroughly rinsed with MQ water.

2.2 Sampling

Seawater samples for dissolve Fe speciation and siderophore analysis were obtained during a number of RRS *Discovery* cruises in the period between 2007-2009, in the

high latitude North Atlantic Ocean (Fig. 9). Samples for Fe speciation measurements were collected during RRS *Discovery* cruise 321 (D321) and RRS *Discovery* cruise 340 (D340) in August-September 2007 and June 2009, respectively. Meanwhile, samples for siderophore analysis, including siderophore incubation experiments, were collected during RRS *Discovery* cruise 350 (D350) in April-May 2010 and RRS *Discovery* cruise 354 (D354) in July-August 2010.

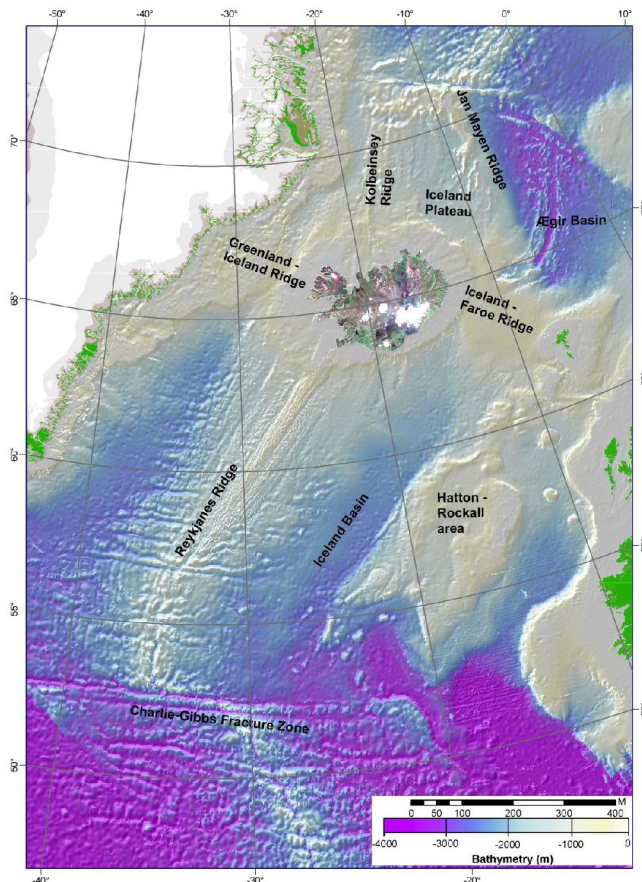


Figure 9: Overview of the study area at high latitude North Atlantic Ocean (reference: http://www.utanrikisraduneyti.is/media/Skyrslur/Icelandic_Continental_Shelf_Executive_Summary.pdf).

Seawater samples from depths >5 m were collected with a trace metal clean titanium CTD frame with 10-20 L trace metal clean Teflon coated OTE bottles, fitted with silicone O rings and plastic-coated springs (Fig. 10). Following deployment, these bottles were taken off from the titanium frame and carried to the clean container. Gentle pressure filtration with oxygen free nitrogen at 1.1 bar was used for sampling the dissolved organic Fe(III) binding ligands. A 0.2 µm pore size cartridge filters (Sartobran P-300, Sartorius) were used for filtering seawater samples from the bottles to the 250 mL LDPE bottles (Nalgene). The seawater samples were taken from 9-13 depths at each station. The same OTE bottles were also sampled for dissolved Fe (dFe),

which was determined by Maria Nielsdottir (RRS D321) and Sebastian Steigenberger (RRS D340 and D354) (see below) after acidification to pH 2 (a final concentration of 0.011 M) using ultra-pure HCl, Romil UpA grade). The samples for organic Fe(III)-binding ligands analyses were immediately frozen at -20°C (not acidified) for subsequent land based analysis. Hydrographic data were obtained from a Seabird 9/11+ CTD attached to the titanium rosette frame.

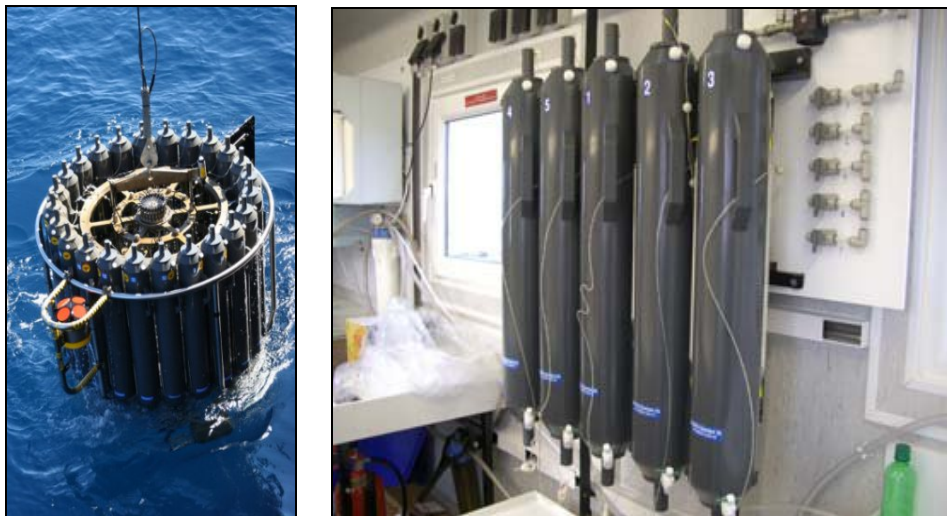


Figure 10: Titanium CTD frame fitted with 10-20 L trace metal clean Teflon OTE bottles. The OTE bottles which have been taken off from titanium CTD frame and carried to the clean container for seawater sampling.

For the siderophore samples, a seawater sample was collected at the chlorophyll *a* maximum depth and below the chlorophyll *a* maximum layer using trace metal clean teflon coated OTE bottles. Surface seawater samples (at a depth of ca. 3 m) were collected by using a trace metal clean towfish. The seawater sample was transferred into polyethylene 20 L carboy (Nalgene) in the clean container (Table 1).

2.3 Determination of total dissolved iron (dFe) concentration

Data for concentrations of total dFe for this study were provided by Maria Nielsdottir (cruise D321) and Sebastian Steigenberger (D340 and D354). The concentration of dFe was measured by using an automated flow-injection chemiluminescence method (Obata *et al.*, 1993) following modifications described by De Jong *et al.* (1998). An 8-hydroxyquinoline (8-HQ) immobilized on Toyopearl gel (Landing *et al.*, 1986; Landing & Bruland, 1987) was used as preconcentration/matrix removal resin. The detection in this method is based on the chemiluminescence (Sigma) produced by the Fe catalyzed

oxidation of luminol (3-aminophthalhydrazide, Sigma) by hydrogen peroxide (H_2O_2) (Romil UpA grade). Samples were stored for at least 24 hours prior to analysis.

Table 2: Overview of the sampling activities during the RRS *Discovery* cruises. FeL – organic Fe(III) binding ligands samples, incubation experiment – seawater nutrients enrichment experiment for siderophores production.

Cruise	Date	Latitude (°N)	Longitude (°W)	Sampling activity	Depth (m)
D321	26/08/2007	61.30	19.59	- FeL and dissolved Fe	35-2237 m, 10 depths
	06/08/2007	59.08	18.54	- FeL and dissolved Fe	10-0811 m, 9 depths
	12/08/2007	59.11	19.07	- FeL and dissolved Fe	12-0537 m, 9 depths
	08/08/2007	59.42	19.52	- FeL and dissolved Fe	50-0810 m, 7 depths
	28/08/2007	57.32	12.37	- FeL and dissolved Fe	11-1620 m, 11 depths
D340	11/06/2009	62.00	20.00	- FeL and dissolved Fe	11-1620 m, 11 depths
	12/06/2009	60.01	20.01	- FeL and dissolved Fe	05-1000 m, 10 depths
	14/06/2009	59.40	19.12	- FeL and dissolved Fe	05-1000 m, 10 depths
	15/06/2009	58.53	17.00	- FeL and dissolved Fe	05-1000 m, 10 depths
	15/06/2009	57.32	12.37	- FeL and dissolved Fe	05-1000 m, 10 depths
	19/06/2009	57.23	10.52	- FeL and dissolved Fe	05-765 m, 9 depths
D350	29/04/2010	21.51	58.34	- Incubation experiment	3
	01/05/2010	34.52	60.56	- Dissolved siderophores	25, 85
	02/05/2010	34.57	60.02	- Dissolved siderophores	27, 93
	03/05/2010	37.55	59.59	- Dissolved siderophores	27, 68
				- Incubation experiment	27
	04/05/2010	29.10	59.58	- Dissolved siderophores	24
	05/05/2010	26.02	59.54	- Dissolved siderophores	30
	06/05/2010	21.44	60.50	- Dissolved siderophores	30
	07/05/2010	20.01	61.57	- Dissolved siderophores	20
	08/05/2010	19.52	63.05	- Dissolved siderophores	23
D354	11/07/2010	19.58	60.00	- Dissolved siderophores	20, 30
	12/07/2010	19.58	60.00	- Incubation experiment	3
	14/07/2010	23.00	60.00	- Dissolved siderophores	20, 50
	15/07/2010	23.37	60.02	- Incubation experiment	20
	16/07/2010	29.00	60.02	- Dissolved siderophores	20, 75
	18/07/2010	35.00	60.02	- Incubation experiment	3
	19/07/2010	41.00	60.02	- Dissolved siderophores	20, 80
		41.35	59.59	- Incubation experiment	3
	22/07/2010	35.00	63.00	- Dissolved siderophores	20, 70
	24/07/2010	30.00	63.00	- Dissolved siderophores	20, 60
	26/07/2010	35.00	58.00	- Dissolved siderophores	40
		35.02	58.13	- Incubation experiment	40
	30/07/2010	35.04	63.49	- Dissolved siderophores	20
	31/07/2010	33.23	63.30	- Dissolved siderophores	3
	02/08/2010	23.35	63.25	- Dissolved siderophores	20
	03/08/2010	24.27	61.47	- Dissolved siderophores	30
	04/08/2010	24.45	61.14	- Dissolved siderophores	3
	06/08/2011	24.00	61.45	- Dissolved siderophores	3

2.4 Determination of natural organic Fe(III) binding ligands

The determination of Fe and the elucidation of its chemical speciation present a great analytical challenge, due to the extremely low Fe concentrations in the ocean (<0.1 nM) (Measures *et al.*, 2008; Nielsdottir *et al.*, 2009) and the high potential for contamination. Flow injection chemiluminescence (De Jong *et al.*, 1998), or preconcentration followed by high resolution inductively coupled plasma mass spectrometry (Milne *et al.*, 2010) are now methods of choice for the determination of dissolvable and total dissolved Fe. However, Fe speciation is most often assessed by competitive ligand exchange-adsorptive cathodic stripping voltammetry (CLE-AdCSV) and has been successfully used to determine the natural organics Fe(III) binding ligands in seawater in many studies (Gledhill & Van Den Berg, 1994; Rue & Bruland, 1995, 1997; Witter & Luther, 1998; Croot & Johansson, 2000; Boye *et al.*, 2001; Croot *et al.*, 2004; Boye *et al.*, 2005; Gerringa *et al.*, 2006; Gerringa *et al.*, 2008; Rijkenberg *et al.*, 2008; Thuroczy *et al.*, 2010) . One key advantage of these voltammetric methods is that they are sensitive, allow metal speciation measurements and require limited sample handling, minimising the chances of contamination.

In CLE-AdCSV experiments, the excess Fe(III) binding ligands are titrated by further additions of Fe(III), and the results of these titrations are used to calculate the concentration of the natural organic Fe(III) binding ligands and the conditional stability constant for the organic Fe(III) binding ligands complex (Ruzic, 1982; Gerringa *et al.*, 1995b). Added Fe(III) in the sample is equilibrated overnight in the presence of an added ligand, which has known thermodynamic properties, and has an ability to absorb on the mercury electrode at a preset potential with subsequent determination by cathodic stripping voltammetry. Due to slow kinetic reaction of the added Fe and added ligands with the sample which includes organic ligands (Van Den Berg, 1995), inorganic ligands and other trace metals (Nagai *et al.*, 2007), an overnight equilibration is required for sufficient equilibration in titration experiments (Hudson *et al.*, 1992; Gerringa *et al.*, 2008). The function of the added ligands is to bind Fe(III) which is present in the seawater samples to make it detectable by AdCSV. The added ligand competes with the natural ligands in the sample so, if half of the Fe(III) is bound by the added ligand, the complex stability of natural ligand is about the same as that of added ligand.

This method has been used with added ligands including 1-nitroso-2-naphthol (1N2N) (Van Den Berg *et al.*, 1991; Gledhill & Van Den Berg, 1994), salicylaldoxime (SA) (Rue & Bruland, 1995) and 2-(2-thiazolylazo)-4- methylphenol (TAC) (Croot & Johansson, 2000). The presence of an excess of the organic ligands in the seawater samples is indicated by the curvature in a plot of the measured voltammetric current (i_p) versus

the total Fe concentration (Fig. 11). Curvature is usually only observed at low Fe(III) concentrations (<1 nM). The curvature is evidence for natural organic Fe(III) binding ligands complex formation with added Fe, and as the natural ligands become saturated with Fe a straight line is observed indicating that all the added Fe is being complexed by the added ligand (Van Den Berg, 1995).

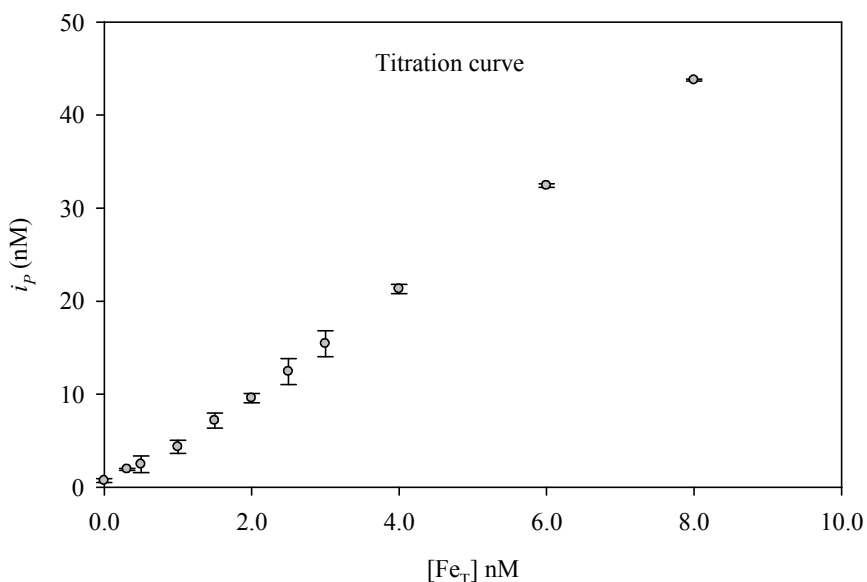


Figure 11: The current (nA) plotted versus the total amount of Fe from St. E2 (10 m depth) (Table 6, Chapter 3). The first few points of the titration indicated that about half of the natural organic complex dissociated due to the competition with the added ligand. The concentration of added ligand and Fe(III) complex is directly related to the peak heights (i_p) of the voltammetric measurements.

In this study, TAC (Fig. 12) was used as the added ligand (Croot & Johansson, 2000). TAC is sufficiently sensitive to use for open ocean seawater titrations without the use of an oxidant (like hydrogen peroxide for 1N2N; (Gledhill & Van Den Berg, 1994)), which may perturb the in-situ speciation. Furthermore the peak of Fe-TAC is free from interference at pH 8, unlike SA which often has interfering Cu-SA peak (Croot & Johansson, 2000).

The detection window is determined by the sensitivity of the CLE-AdSV analysis (the limit of detection defines the lowest determinable free or labile metal concentrations and therefore its strongest complexes) and by others aspects such as perturbation of equilibrium and its definition of the labile metal concentration (Van Den Berg & Donat, 1992). It could be varied by varying the degree of ligand competition with different added ligand concentrations (TAC). Indeed, the centre of detection window in CLE-AdCSV analysis equals to $\alpha_{Fe(TAC)_2}$ (α -coefficient for complexation of iron(III) by a TAC as added competitive ligand), with values for α_{Fe} (α -coefficient for natural organic

complexation of Fe(III)) within approximately a decade on either side of $\alpha_{\text{Fe}(\text{TAC})_2}$ being measurable. The value of $\alpha_{\text{Fe}(\text{TAC})_2}$ (250) calculated from TAC concentration and its conditional stability constant (Croot & Johansson, 2000). Furthermore, the full speciation of a Fe cannot be calculated from $\text{Fe}(\text{TAC})_2$ measurements or even from a single complexing capacity titration, as the data cannot be extrapolated outside the detection window of the CLE-AdCSV technique used. Therefore, a complexation model needed to be used for calculating the speciation of Fe.

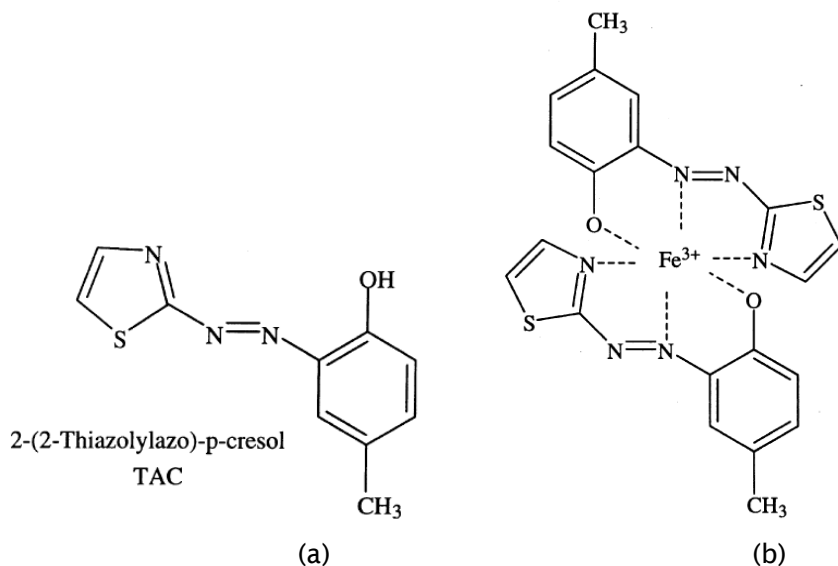


Figure 12: a) Chemical structure of 2-(2-thiazolylazo)-4-methylphenol or alternatively 2-(2-thiazolylazo)-p-cresol (common name TAC) and b) Proposed coordination of $\text{Fe}(\text{TAC})_2$ by Croot & Johansson (2000).

There are two methods for fitting of the titration data to calculate the organic Fe(III)-binding ligands concentrations and their respective conditional stability constants according to the Langmuir isotherm. These are the linear transformation of Van Den Berg/Ruzic (Ruzic, 1982) and the non linear method according to Gerringa *et al.* (1995a). The linearization method of Ruzic (1982) has been criticized as being oversimplified (Buffle *et al.*, 1992). In fact, linear methods are applicable only with caution to chemically heterogeneous complex mixtures of ligands (Miller & Bruland, 1997; Bruland & Rue, 2001). Thus, other authors (Fish & Jordan, 1983; Gerringa *et al.*, 1995a) suggested the use of non-linear curve fitting routines for direct fitting of the titration data. In fact, Gerringa *et al.* (1995a) found that there is no difference between the value for the total Fe(III)-binding ligands concentration estimated using the linear or the non linear method, but the non linear method is more suited to the error structure of the data. The standard error of the estimated parameters can be calculated consistently using the non linear method.

2.4.1 Chemical preparation

2.4.1.1 2-(2-Thiazolylazo)-p-cresol (TAC) stock solution

A 0.02 M TAC stock solution was prepared in triple quartz distilled (QD) methanol by diluting 0.43854g of TAC ($C_{10}H_9N_3OS$, Aldrich) in 100 mL methanol (HPLC grade). A final concentration of 10.0 μ M TAC was used throughout this study.

2.4.1.2 Borate buffer (H_3BO_3)

A borate buffer 1.0 M solution was prepared in 0.3 M ammonia (Suprapur, Merck) to buffer at pH 8.05. 6.184 g boric acid (H_3BO_3 , Fisher Scientific) was diluted in 25% NH_4OH (Suprapur, Merck), before make up to 100 mL with MQ water. Iron contamination was removed from this stock solution after complexation with TAC using a C_{18} (SepPak, Whatman). TAC at a final concentration of 20 μ M was added to the boric acid (pH 8.05) and left to equilibrate overnight. The C_{18} SepPak column was activated with 10 mL of MeOH (HPLC grade), followed by 10 mL of 0.6 N HCl (Romil UpA grade). Then it was rinsed with 20 mL of MQ water before loading the buffer solution using a peristaltic pump. The pH of buffer was checked before the cleaning procedure, and adjusted using HCl (Romil UPA grade) and NH_4OH (Romil UpA grade), so that a pH of ~8.05 was obtained on addition of 50 μ L buffer solution to 10 mL seawater. A final concentration of 5.0 mM borate buffer (pH 8.05) was used for seawater samples throughout this study.

2.4.1.3 Iron(III) stock solution

A 10^{-6} M Fe(III) stock solution was prepared by diluting a Fe(III) ICP-MS stock standard (1000 ppm in nitric acid, MW=55.847 g/mol, Fisher Scientific) in 0.01 M HCl (Romil UpA grade). All the chemical preparation was done on a Class 100 laminar airflow bench at room temperature (25°C).

2.4.2 Sample preparation

The seawater samples (200 mL) were buffered to pH 8.05 (1.0 mL of 1.0 M borate buffer) and left for an hour before adding 100 μ L of 0.02 M TAC so that the final concentration of TAC was 10 μ M. According to Croot & Johansson (2000), the sensitivity (S) was not significantly enhanced when the concentration of TAC $> 10 \mu$ M was used but increases in background slope in the vicinity of the $Fe(TAC)_2$ peak at higher concentrations have been observed. The sample was subdivided over 12 subsamples in the FEP bottles (Nalgene) (30 mL) containing increasing concentrations of Fe(III) between 0 and 8 nM - sufficient to saturate the natural ligands. The Fe(III) was added to all but two of the bottles, and allowed to equilibrate overnight (> 15 hours) in a room temperature (Hudson *et al.*, 1992; Gerringa *et al.*, 2008). All sample manipulations were performed on a Class 100 laminar airflow bench at room

temperature (25°C). The Teflon FEP bottles were conditioned with seawater which added with TAC, boric acid and Fe(III) twice before the equilibration experiment. The bottles were rinsed with MQ between equilibration experiments.

2.4.3 Voltammetric procedure

A model 663 VA voltammeter (Ω Metrohm, Swiss Made) (Fig. 13) was used throughout this study. The sub samples were transferred to the voltammetric cell and then were deaerated for 300s with dry nitrogen gas to remove oxygen from the samples. Subsequently, the $\text{Fe}(\text{TAC})_2$ complexes in the sample were adsorbed onto a fresh mercury (Hg) drop (Hanging Mercury Drop Electrode, HMDE) at an applied potential of -0.40V for 60s, while the sample was stirred. At pH 8.0 and above the solution is a red-orange color due to the presence of TAC (Croot & Johansson, 2000). At the completion of the adsorption period, the stirrer was stopped and the potential was scanned using a differential pulse mode from -0.40V to -0.90V at 19.5 mV s^{-1} , and the stripping current from the adsorbed $\text{Fe}(\text{TAC})_2$ recorded. The concentration of $\text{Fe}(\text{TAC})_2$ in the samples was measured in each subsample.



Figure 13: The voltammeter used for determination of organic Fe(III) binding ligands. Three electrodes electrochemical cell for voltammetric analysis was used; hanging mercury drop electrode (HMDE), reference electrode (KCl) and counter electrode. This instrument was set up on a Class 100 laminar airflow bench at room temperature (25°C).

Differential pulse mode was used as it gives low background currents, avoids interference from nickel (Ni) and results in a well defined peak for $\text{Fe}(\text{TAC})_2$ (Croot & Johansson, 2000) (Fig. 14). Every scan was repeated twice without purging, and the average of the peak heights was used for further calculations. The voltammetric cell was rinsed only with MQ water between analyses, and the subsamples were run in

order of increasing Fe(III) additions. Measurements were performed on a Class 100 laminar airflow bench at room temperature (25°C).

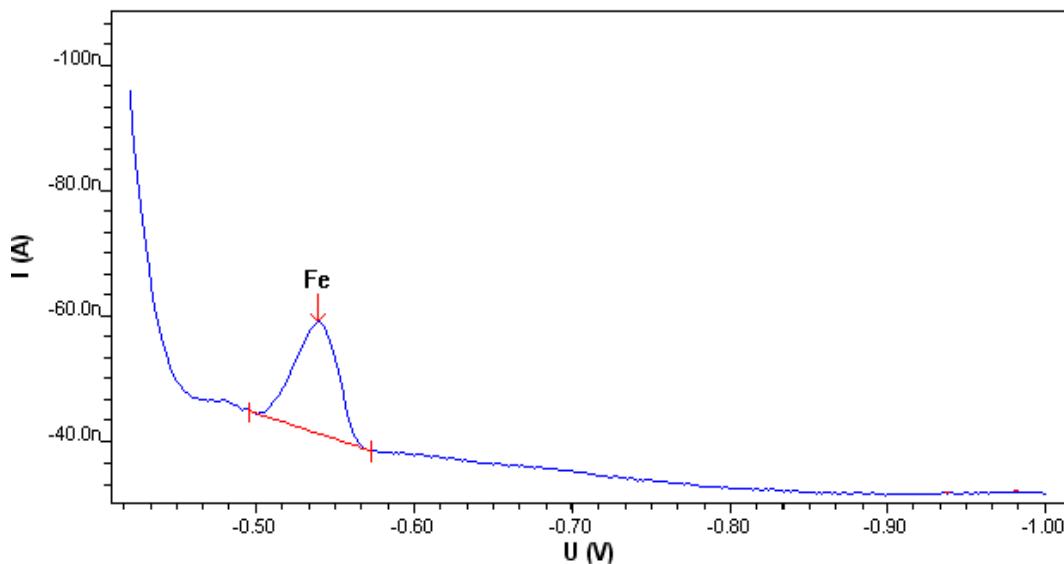


Figure 14: Voltammogram of $\text{Fe}(\text{TAC})_2$ peak under differential pulse mode from seawater sample from St. B4 (10 m depth) (Table 6, Chapter 3). Voltammetric parameters: deposition time 120s; deposition potential -0.5V; start potential -0.42V; end potential -1.0V.

2.4.4 Calculation of organic Fe(III) binding ligands

Titration data was used to calculate the conditional stability constant and the concentrations of the natural ligands. The principle of measuring the binding characteristics of dissolved organic ligands with Fe is extensively described in several publications (Gledhill & Van Den Berg, 1994; Croot & Johansson, 2000; Thuroczy *et al.*, 2010). It is possible to determine the conditional stability constant and the concentration of natural dissolved organic ligands, since the added concentration of TAC (10.0 μM) and its binding strength with Fe ($10^{22.4}\text{M}^{-2}$) (Croot & Johansson, 2000) are known. To calculate conditional stability constant ($\text{Log } K'_{\text{FeL}}$) and the concentration of total natural dissolved organic ligands ($[\text{L}_T]$), a non-linear regression of the Langmuir isotherm (Gerringa *et al.*, 1995a) was used with a single ligand model (Eq.1). It is assumed that equilibrium between all Fe(III) species exists, all binding sites between Fe and the unknown ligands are equal and that the binding is reversible.

$$\frac{K'_{\text{Fe}(\text{TAC})_2} \times [\text{TAC}]^4}{K'_{\text{FeL}} \times [\text{L}_T]} = \frac{[\text{Fe}(\text{TAC})_2]}{[\text{FeL}]} \quad (\text{Eq.1})$$

Where K' is the conditional stability constant of Fe with the ligands, (either TAC or the natural organic ligands (L)) and $[TAC]$ are the concentrations of free Fe ligands (not Fe bound), $[Fe(TAC)_2]$ and $[FeL]$ is the concentrations of Fe complexes.

The $[Fe(TAC)_2]$ was calculated by dividing the peak height, i_p (nA) over the slope (sensitivity = S) of the straight part of the titration curve (Eq. 2),

$$[Fe(TAC)_2] = \frac{i_p}{S} \quad (Eq. 2)$$

The total Fe concentration ($[Fe_T]$) consists of that dissolved Fe concentration which was measured by flow-injection method (dFe) augmented by that $Fe(III)_{added}$ during the titration (Eq. 3):

$$[Fe_T] = [dFe] + [Fe(III)_{added}] \quad (Eq. 3)$$

The concentration of Fe complex by natural organic ligands ($[FeL]$) was obtained by a difference total Fe concentration ($[Fe_T]$) and $[Fe(TAC)_2]$ (Eq. 4):

$$[FeL] = [Fe_T] - [Fe(TAC)_2] \quad (Eq. 4)$$

The concentration of $Fe(III)$ ($[Fe^{3+}]$) is directly related to the $[Fe(TAC)_2]$ by $\alpha_{Fe(TAC)_2}$ (Eq. 5):

$$[Fe^{3+}] = \frac{[Fe(TAC)_2]}{\alpha_{Fe(TAC)_2}} \quad (Eq. 5)$$

Where $\alpha_{Fe(TAC)_2}$ is the overall α -coefficient for inorganic complexation and complexation by TAC (excluding complexation by L) at a concentration of 10 μM (Eq. 6). The inorganic side reaction coefficient for Fe was taken as $\alpha_{Fe} = 10^{10}$ (Sunda *et al.*, 1991):

$$\alpha_{Fe(TAC)_2} = \beta_{Fe(TAC)_2} \times [TAC]^2 \quad (Eq. 6)$$

Where, $\beta_{Fe(TAC)_2}$ is the conditional stability constant of Fe with TAC, assuming an equilibrium as follows (Eq. 7);

$$\beta_{Fe(TAC)_2} = \frac{[Fe(TAC)_2]}{[Fe^{3+}]^2} \times [TAC]^2 \quad (Eq. 7)$$

A good agreement was found between estimates for $\beta'_{\text{Fe}(\text{TAC})_2}$ made using EDTA ($10^{12.3} \text{M}^{-2}$) and DTPA ($10^{12.4 \pm 0.3} \text{M}^{-2}$) at different TAC concentrations (Croot & Johansson, 2000). A value of $10^{12.4} \text{M}^{-2}$ (in Fe^{3+} notation $\beta'_{\text{Fe}(\text{TAC})_2} = 10^{22.4} \text{M}^{-2}$) was used throughout our studies.

Data pairs of $[\text{Fe}^{3+}]$ and $[\text{FeL}]$ resulting from CLE-AdCSV measurements are fitted to the non-linear fit directly. The non-linear fitting routine of the package SYSTAT was used to calculate L_T and K'_{FeL} (Wilkinson *et al.*, 1992). This performs a least-squares fit with the simplex algorithm. Asymptotic standard errors and the correlation between the parameters have been computed from the Hessian matrix.

To make sure the accuracy the titration method, I have analysis a few seawater samples from GEOTRACE inter-calibration iron speciation data 2008 and 2009. The result of my iron speciation data was in a range of others iron speciation measurement (Table 3).

Table 3: Comparison between iron speciation data obtained from CLE-AdCSV measurements at National Oceanography Centre Southampton (NOCS) and GEOTRACE data.

Bottle no.	Sampling date	[DFe] (nM)	Measurement at NOCS				GEOTRACE data	
			L_T (nM)	stdev	$\log K_{\text{FeL}}$	stdev	L_T (nM)	$\log K_{\text{FeL}}$
1020	22-Jun-08	0.05	0.58	0.03	22.71	0.16	0.50 - 0.80	22.1 - 23.0
1021			0.53	0.03	22.32	0.16		
1022	25-Jun-08	0.05	0.41	0.06	22.76	0.18	0.30 - 0.60	22.1 - 23.0
1023			0.41	0.03	23.15	0.38		
4186	13-May-09	0.09	1.22	0.04	22.84	0.10	1.10 - 1.40	22.1 - 23.0
4187			1.24	0.05	23.07	0.21		
4301	14-May-09	0.09	1.36	0.04	22.71	0.10	1.10 - 1.40	22.1 - 23.0
4302			1.18	0.03	23.00	0.16		
4145	13-May-09	0.06	1.00	0.05	22.98	0.25	1.10 - 1.40	22.1 - 23.0
4146			0.58	0.02	23.03	0.30		

2.5 Determination of dissolved siderophores

Siderophores have structural diversity and low concentrations in the environment. It has led to challenges in their determination, along with limitations in the analytical techniques available for their detection.

Previously, the quantification of siderophores has been done by using spectrophotometric assays like the chrome azural S test, the Arnow assay and the Csaky test (Neilands, 1983). The chrome azurol S (CAS) (Shenker *et al.*, 1995) is a universal spectrometric method which has been used for determining siderophores in

solution. The Arnow assay and Csaky assay were used to determine catecholate and hydroxamate siderophores, respectively. A catecholate structure produces a yellow colour upon reaction with nitrite-molybdate in an acid medium, and changes to an intense orange-red when the medium is basic. The absorbance of the siderophore complex is measured at 515 nm and with a detection limit for siderophores of 0.02 μM (Neilands & Nakamura, 1991). On the other hand, the Csaky test is the most sensitive assay for determination of hydroxamate acids and has a detection limit of 1.2 μM (Naito *et al.*, 2008). However, these assays are only able to identify the presence of a siderophores functional groups and thus have several major disadvantages, including matrix interference and the inability to provide any indication of the type and range of siderophores produced (Mc Cormack *et al.*, 2003).

More recently, a combination of high performance liquid chromatography-inductively coupled plasma-mass spectrometry (LC-ICP-MS) and high performance liquid chromatography-electrospray ionisation-mass spectrometry (LC-ESI-MS) method has been used successfully for identifying and quantifying siderophores in environmental samples (Mawji *et al.*, 2008a). The HPLC technique allows the siderophore type chelates present in the samples to be separated by using a chromatographic separation column before determination using ICP-MS or ESI-MS.

During ESI-MS analysis, the identification of prospective siderophore type chelates is undertaken by measuring their mass to charge ratio (m/z). This technique can also provide information on the structure of a siderophore by collision induced dissociation (CID) analysis (Mawji *et al.*, 2008b). On the other hand, LC-ICP-MS which is a hard ionisation technique, can offer quantification of siderophore type chelates according to their metal content, this is more challenging with ESI-MS as different compounds have different ionisation efficiencies. LC-ICP-MS has been reported to offer superior detection limits to ESI-MS as it destroys the organic part of the molecule thereby reducing interferences during analysis.

2.5.1 Preparation of reagents

2.5.1.1 Ammonium carbonate

A 1.0 M ammonium carbonate solution was prepared by diluting 2.37 g of ammonium carbonate stock (NH_4HCO_3 , 79 g/mol, Fisher Scientific) in 30 mL MQ water. Then, 0.336 mL of 1 M solution was diluted with 29.664 mL MQ to obtain an 11.2 mM ammonium carbonate solution. All chemical preparation in the laboratory was performed on a Class 100 laminar airflow bench at room temperature (20°C).

2.5.1.2 Extraction Solvent

A mixed extraction solvent was used to elute siderophores from polystyrene-divinylbenzene solid-phase extraction (SPE) cartridge (Isolute ENV+) cartridge. This solvent was prepared by mixing acetonitrile/propan-2-ol/Mill-Q water/formic acid with a ratio of 81:14:5:1 (v/v/v/v) in a 50 mL TPP centrifuge tube (Fisher Scientific). Solvents (Optima LC/MS grade) were purchased from Fisher Scientific, and formic acid (Aristar) was purchased from BDH Chemicals Ltd.

2.5.1.3 Mobile phase solvent

A binary gradient mobile phase was used for HPLC analysis. Solvent A was prepared by mixing 95% water: 5% methanol: 0.1% formic acid, (v/v/v) in a 500 mL glass vessel (Schott Duran, Germany). Solvent B was prepared by adding 0.1% formic acid to 99.9% methanol (v:v). Formic acid was added to the B to avoid a change of pH during gradient elution, as suggested by Gledhill *et al.* (2004).

2.5.1.4 Gallium working standard

A working standard of 0.14 M gallium was prepared from gallium standard ($\text{Ga}(\text{NO}_3)_3$, 69.72 g/mol, ICP-MS standard, VWR). It was diluted with 2% nitric acid in 50 mL TPP centrifuge tube (Fisher Scientific).

2.5.1.5 Iron (III) chloride

A 1.0 M Fe(III) chloride solution was prepared by diluting 8.109 g of Fe(III) chloride hydrate stock (FeCl_3 , 270.3 g/mol, Fisher Scientific) in 30 mL MQ water.

2.5.1.6 DFOB standard

A 7.7 mM DFOB standard solution was prepared by diluting 0.050530 g of deferrioxamine mesylate salt ($\text{C}_{25}\text{H}_{48}\text{N}_6\text{O}_8\text{CH}_4\text{O}_3\text{S}$, 656.8 g/mol, EMC micro-collection) in 10 mL of 50%:50% of formic acid: MQ water. This standard solution was stored at -20°C. It was defrosted and diluted to the working standard concentrations (0.1- 20.0 nM) with 50%:50% of formic acid: MQ water.

2.5.1.7 FOB working standard

Iron-siderophore (Ferrioxamine B, FOB) working standards were prepared by adding 1 mole of Fe(III) chloride to 1 molar equivalent of DFOB (Deferrioxamine B) standard in the 2 mL safe lock tube Amber (Eppendorf AG). Then it was left to equilibrate for 12 hours in room temperature (25°C). This working standard was made freshly each day.

2.5.1.8 Ga-FOB working standard

Gallium-siderophore (Ga-FOB) working standards were made by adding excess Ga to the DFOB standard in ratio 1:1 (v/v) in the 2 mL safe lock tube Amber (Eppendorf AG), which was left for 12 hours at room temperature (25°C). This working standard was made daily.

2.5.1.9 Nitric acid

A 2% nitric acid was prepared by adding 0.6 mL of nitric acid (BDH, Aristar) to 29.4 mL MQ water.

2.5.2 Solid phase extraction (SPE)

Solid phase extraction (SPE) is based on the reversible adsorption of substances on a solid phase, and has been used to pre-concentrate naturally occurring dissolved siderophores from large volumes of seawater (Macrellis *et al.*, 2001; Mc Cormack *et al.*, 2003). They have found that the polystyrene divinylbenzene stationary phase is successful at retaining model siderophores, with extraction recoveries from 21-37% (Mc Cormack *et al.*, 2003) up to 79-91% (Macrellis *et al.*, 2001).

Pre-concentration is necessary because of the low concentration of siderophores in the marine waters. It also reduces matrix interferences such as non-volatile salts, which are incompatible with analytical techniques like LC-ESI-MS and LC-ICP-MS. After adsorption, impurities such as salts are washed out by a solvent that allows the substance of interest to remain adsorbed. After this cleaning step, the adsorbed analytes are eluted using a non polar solvent. As non polar solvent are not compatible with HPLC separation, causing the compounds of interest to elute in the solvent front, the non polar solvent were removed by evaporation under nitrogen and the residue was dissolved in water or aqueous buffer.

Seawater samples (20 L) was sequentially filtered (3.0 and 0.2 µm) using cellulose nitrate membrane filters (Whatman). Then, the seawater was concentrated onto a polystyrene-divinylbenzene solid-phase extraction (SPE) cartridge (Isolute ENV+) (Mc Cormack *et al.*, 2003; Gledhill *et al.*, 2004; Mawji *et al.*, 2008a) with a reservoir volume of 3 mL, sorbent mass of 200 mg, average particle size of 90 µm and nominal porosity of 800 Å. The cartridges were pre-washed with 1 mL methanol (LC-MS grade, Riedel-de Haen) before pre-concentrating the seawater sample. A vacuum pump was used for filtration and extraction with flow rate 3-4 mL min⁻¹. The volume of seawater extracted through the cartridge was recorded from the corboy scale measurement. The cartridge was frozen at -20°C until further processing and analysis on shore. The diagram for filtration and extraction step is shown in Figure 15 below.

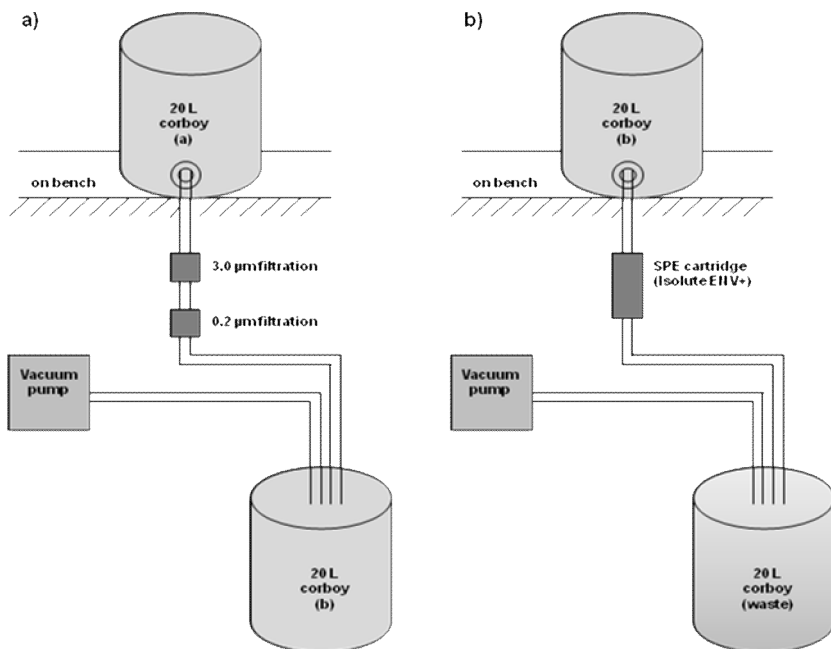


Figure 15: Diagram shows a) the filtration and b) extraction procedure for dissolved siderophores pre-concentration from sea water sample. The cellulose nitrate membrane filters were fitted to a polycarbonate 47 mm in-line filter holder (Pall Corporation).

In the land-based laboratory, the cartridges were defrosted and washed with 1 mL of 11.2 mM ammonium carbonate (Twining *et al.*, 2004) in order to remove salt from the sample. Siderophore type chelates were eluted with 5 mL of 81:14:5:1 (v/v/v/v) acetonitrile/propan-2-ol/water/formic acid (Mawji *et al.*, 2008a). The eluant was collected into 7 mL clear vials with screw top PTFE lined caps (Supelco) and blown down under nitrogen gas to 100 μ L. Then, it was diluted with 1% formic acid to make up 500 μ L solution. A 200 μ L subsample was transferred into a 2 mL eppendorf vial prior to identification and quantification of siderophores.

2.5.3 Quantification of dissolved siderophores

The high-performance liquid chromatography-inductively coupled plasma mass spectrometry (LC-ICP-MS) (Shimadzu HPLC coupled to a Thermo X-series ICP-MS) was used to quantify siderophore concentrations in natural seawater samples by monitoring the gallium-69 isotope (^{69}Ga) (Mawji *et al.*, 2008a). The ICP-MS only detects organic compounds that react with trivalent Ga (siderophores).

Gallium addition was used to displace Fe from siderophores as its determination by ICP-MS suffers from lower background interferences compared to Fe. The ^{69}Ga isotope, which has a natural abundance of 60%, is not subjected to spectral interferences from

argon. Gallium has a similar chemistry and stability constants with siderophores to Fe (Moberg *et al.*, 2004). The stability constants for Fe and Ga complex with DFOB is 30.99 and 28.17 at pH above 2 (Kiss & Farkas, 1998), respectively. In fact, Ga is an effective competitor for Fe in a siderophore transport systems, where a 10 fold excess of Ga could displace Fe from ferrichrome, ferrioxamine B and triacetyl fusarinine C (Emery & Hoffer, 1980; Emery, 1986). However, the amount of excess Ga which is needed to displace Fe is dependent on the levels of Fe in the solution and sample matrix (Gledhill *et al.*, 2004). In this study a final concentration of 10 μ M Ga was used to quantify the amount of siderophores in dissolved phase as preliminary experiments showed that this was sufficient to replace Fe after overnight equilibration (Fig. 16), whilst minimizing the elution of background Ga.

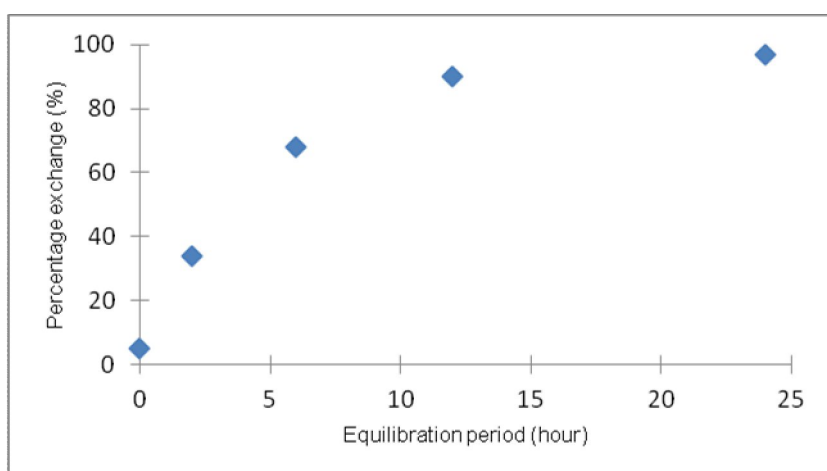


Figure 16: Percentage exchange of Ga(III) in FOB complex at the different equilibration time. A 10 μ M of Ga(III) standard was equilibrate with 1 nM FOB standard at room temperature before measuring the concentration of GaFOB complexes by LC-ICP-MS.

The ICP-MS Ga standard ($\text{Ga}(\text{NO}_3)_3$, VWR) with final concentration 10 μ M, was added to a 200 μ L sub-sample and allowed to equilibrate overnight at room temperature before analysis by the LC-ICP-MS method. The HPLC was carried out by using two pumps (LC-10ADVPM, Shimadzu) and vacuum degasser (NLG Analytical). Samples and standards (5 μ L) were manually injected onto the separation column using a metal-free injector (Rheodyne 9725i, Alsbach, Germany). The chromatographic separation was performed by using a polystyrene divinyl benzene stationary phase (PRP-H1, 100 \times 2.1 mm 5 μ m, Hamilton) column. The mobile phase was comprised of two solvents (A and B, see section 2.5.1.3). A standard gradient of 95% solvent A to 100% solvent B over 20 minutes at the beginning of chromatogram was followed by isocratic elution with 100% solvent B for 5 minutes (Mc Cormack *et al.*, 2003; Gledhill *et al.*, 2004; Mawji *et al.*, 2008a). The flow rate for the mobile phase was maintained at 150 μ L min^{-1} . Before the system returned to the starting conditions, it was re-equilibrated with 100% solvent A

for 7 minutes. Due to high concentration of free excess Ga in the sample, a 2% nitric acid was immediately injected onto the column and an additional 15 minute isocratic step at 100% solvent A was inserted after the sample injection, while the HPLC eluant line was connected to the waste. This step is important for avoiding high background Ga counts and restored the base line to initial counts during the ICP-MS analysis. Subsequently (15 minutes), the effluent line was connected to the ICP-MS via a desolvating nebulizer (MCN 6000, Cetac Technologies).

The membrane desolvation nebulizer was used to reduce the contribution of the organic solvent from the mobile phase and allow matrices with a high volatile organic content to be analysed by ICP-MS (Sutton & Caruso, 1999; Cartwright *et al.*, 2005). The optimum conditions for MCN 6000 desolvator are 100 mL min⁻¹ nebuliser gas flow (nitrogen gas), 1.0 L min⁻¹ sweep gas flow (argon gas) and 160°C membrane temperature.

Figure 17 shows a schematic diagram of the LC-ICP-MS method, which used for siderophores quantification in this study. The LC-ICP-MS system was cleaned before the determination of seawater samples in order to remove all siderophore complexes and Ga, especially from the separation column. A propan-2-ol (IPA) solution was injected onto the separation column using a metal-free injector followed by 2% nitric acid and running in chromatogram condition as described above. This cleaning procedure was carried out 2-3 times until no peak observed in the chromatogram. An injection of 1% formic acid solution was used as blank.

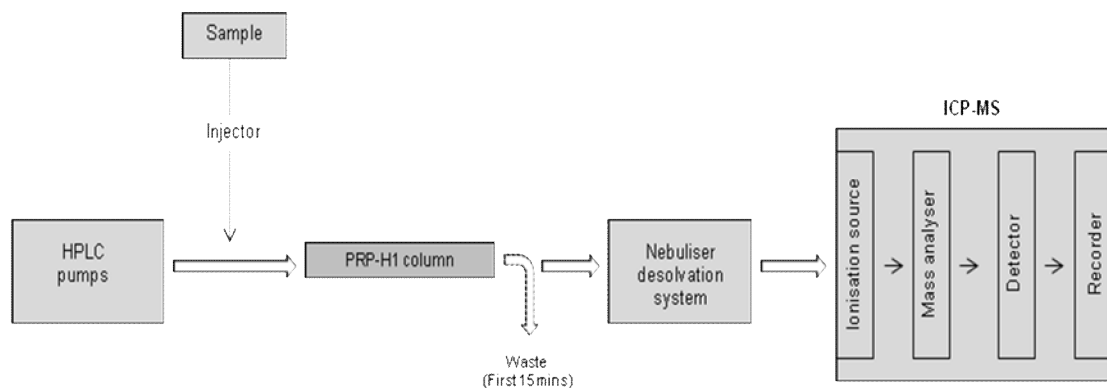


Figure 17: Diagram LC-ICP-MS method fitted with MCN-6000 microconcentric nebuliser desolvation system. Sample/working standards were manually injected into the system which fitted with polystyrene-divinylbenze reversed-phase column.

2.5.4 Identification of dissolved siderophores

Identification of different types of siderophores in the natural seawater was carried out by high-performance liquid chromatography-electrospray ionization mass spectrometry (LC-ESI-MS) (Mawji *et al.*, 2008a).

The ESI-MS is a soft ionization technique (operating at atmospheric pressure) where molecules are subject to a phase change from liquid to gas phase ions and the technique is particularly suitable for polar and nonvolatile compounds. It is ideal for the analysis of siderophores due to potential separation of these compounds (Gledhill, 2001) and provision of structural information after collision induced dissociation (CID) of parent ions (Mc Cormack *et al.*, 2003). In fact, LC-ESI-MS has been successfully applied to the analysis of catecholate (Berner *et al.*, 1991) and hydroxamate type siderophores (Gilar *et al.*, 2001; Gledhill, 2001; Martinez *et al.*, 2001; Groenewold *et al.*, 2004a; Essen *et al.*, 2006; Mawji *et al.*, 2008a). Moreover, it has been used by Gledhill *et al.* (2004) to identify previously unknown siderophore type compounds.

Samples and FOB working standards solution were transferred into 2 mL screw top vial (Thermo Scientific), and the solution was automatically injected (25 μ L volume) onto the separation column using an auto sampler (Accela, Thermo Scientific). The chromatographic separation for LC-ESI-MS analysis was carried out by using a polystyrene divinyl benzene stationary phase (PRP-H1 column, Hamilton) with dimension 100 \times 2.1 mm and particle size of 5 μ m. An Accela 1250 pump was used to pump the mobile phase which comprised of solvent A and solvent B at 150 μ L min $^{-1}$ flow rate through the system. The chromatography was started with a standard gradient of 100% solvent A to 100% solvent B over a period of 20 minutes. Then an isocratic elution with 100% solvent B was conducted for 2 minutes. Another standard gradient of 100% solvent B to 100% solvent A was performed over 3 minutes before re-equilibrating the system with 100% solvent A for 5 minutes. At the beginning of the chromatography, the ESI-MS divert valve was connected to the waste for 0.88 minutes before automatically injected sample or standard solution into the ESI system over 26 minutes. Then, the divert valve will be automatically connected to the waste within 0.88 minutes before the end of the gradient. A 1% formic acid solution was used as blank during this analysis.

The setting for the ESI source of LTQ Velos (Thermo Scientific) was as follows; spray voltage +4.0 kV, capillary voltage +35 V, tube lens 140.0 V with a vaporizer temperature of 400°C and capillary temperature of 275°C. A nitrogen sheath gas flow rate was 60 (arbitrary units). Charged droplets, produced at the heated ESI needle, underwent solvent evaporation and shrinkage resulting in droplet disintegration. These

ions were transferred to the mass spectrometer via a heated capillary and an S lens (Di Marco & Bombi, 2006). The charge was supplied to molecules by addition or removal of ions, usually protons, in order to produce the positively charged ($[M+H]^+$) or negatively charged ($[M-H]^+$) ion. However, formation of sodium, potassium and ammonium adducts ($[M+Na]^+$), ($[M+K]^+$) and ($[M+NH_4]^+$), also frequently occurred. The mass to charge ratio of each type of siderophore was determined using a linear ion trap mass spectrometer in the positive ion mode. Data was collected and interpreted using Xcalibur 2.0 software (Thermoquest). Instrument tuning and mass calibrations were carried out and checked using the automatic calibration procedure and standard calibration solutions.

The full mass spectrum (MS) was obtained by scanning between m/z 200-1500, while the ferric complexes of the siderophores were detected by selective ion monitoring (SIM) of the most abundant ion (parent ion) in the total ion mass spectra. During the SIM analysis, the instrument was set up for selective ion monitoring of masses $[M+H]^+$; m/z 614, 654, 672, 857, 883, 885, 911 and $[M+Na]^+$; m/z 636, 676, 694, 879, 905, 907, 933. The selection of these ions was based on the ferrioxamine and amphibactin siderophore complexes with the H^+ adduct ($[M+1]^+$) and the Na^+ adduct ($[M+23]^+$).

To confirm the identification of siderophores from SIM analysis, collision induced dissociation (CID) analysis of the parent ion was carried out. The instrument was set up for data dependant acquisition of CID spectra analysis. The parent ion in each total ion mass spectra undergoes fragmentation on bombardment with helium atoms at activation amplitude of 35% (Gledhill *et al.*, 2004). The obtained fragmentation pattern was then compared with the previous published data to obtain confirmation of the siderophores identity.

2.6 Nutrient enrichment experiments

In order to identify siderophores isolated from seawater and to assess the diversity of siderophores produced in the high latitude North Atlantic Ocean, nutrient enrichment experiments aimed at encouraging bacterial growth and thus siderophore production have also been carried out during this study. The nutrients, including carbon (100 μM glucose, Fisher Scientific), nitrogen (200 μM ammonium chloride, Fisher Scientific or 200 μM sodium nitrate, Fisher Scientific) and phosphate (20 μM di-sodium hydrogen orthophosphate, Fisher Scientific) (Gledhill *et al.*, 2004), were added to unfiltered seawater samples in order to stimulate bacterial growth and siderophore production.

2.6.1 Chemical preparation

2.6.1.1 Glucose solution

A 0.1 M glucose solution was prepared by diluting 4.502 g of glucose stock ($C_6H_{12}O_6$, 180.080 g/mol, Fisher Scientific) into 250 mL MQ water. A final concentration of 100 μ M of glucose was added to seawater samples. All nutrients were prepared in acid cleaned 250 mL LDPE bottle (Nalgene) in a laminar flow hood.

2.6.1.2 Ammonium chloride solution

A 2.675 g of ammonium chloride stock (NH_4Cl , 53.49 g/mol, Fisher Scientific) was diluted into 250 mL MQ water (final concentration 0.2 M). Ammonia was added to obtain a final concentration of 200 μ M for the incubated seawater.

2.6.1.3 Sodium nitrate solution

A 4.250 g of Sodium nitrate stock ($NaNO_3$, 84.99 g/mol, Fisher Scientific) was diluted into 250 mL MQ water to get 0.2 M concentration solution. Nitrate was added to obtain a final concentration of 200 μ M in the incubated seawater.

2.6.1.4 Di-sodium hydrogen orthophosphate solution

A 0.02 M di-sodium hydrogen orthophosphate solution was prepared by diluting 0.760 g of stock (Na_2HPO_4 , 156.01 g/mol, Fisher Scientific) into 250 mL MQ water. Phosphate was added to obtain a final concentration of 200 μ M in the incubated seawater.

2.6.1.5 Paraformaldehyde

The 10% paraformaldehyde solution was prepared from paraformaldehyde stock ($(C_1H_2O)_n$, 30.03 g/mol, Sigma Aldrich) in the fume hood. A 5.0 g of paraformaldehyde added to 40 mL MQ water. Then 0.5 mL of 1.0 M NaOH (Fisher Scientific) was added and heated to 60°C in water bath. The solution was allowed to cool, and the final volume was adjusted to 50 mL with MQ water. The solution was stored at -80°C. A final solution of 1 % paraformaldehyde was used to fix the flow cytometry samples.

2.6.2 Nutrient cleaning

Iron and other trace metal contaminants were removed from nutrient solutions using chelex-100 (Sigma). The chelex-100 column was cleaned with 50 mL MQ water and 50 mL 1.0 M HCl (Fisher Scientific), followed by another 50 mL MQ water. The column was conditioned with 250 mL of 0.05 M NaOH (Fisher Scientific). The pH of each nutrient was adjusted to 8 using 0.05 M NaOH or 1.0 M HCl before loading on to the column. The first 50 mL of the nutrient eluant was discharged, and the remainder was collected into 250 mL acid cleaned LDPE bottle (Nalgene) and stored at 4°C. The column was rinsed with 150 mL MQ water between nutrients.

2.6.3 Incubation conditions

Seawater samples for incubation experiments were collected from trace metal clean Teflon coated OTE bottles and the towfish. Unfiltered seawater was added to 2 L polystyrene tissue culture flask (Becton Dickinson) and was enriched with nutrients in a laminar flow hood. Incubation conditions are given in Table 4. The nutrient solutions were filter sterilized (10 mL BD Discardit™ II syringe, 0.2 µm Minisart RC-membrane, Sartorius stedim filter) on addition to the seawater. The nutrient enrichment experiments represent an assay for siderophores that may be detected in seawater.

Table 4: The final concentration for each nutrient which added into the seawater samples (2000 mL) during the enrichment experiment. The incubation experiment was carried out in duplicate.

Duplicate incubations	Fe(III) source	Carbon source	Phosphate source	Nitrogen source	
				[NH ₄ Cl] µM	[NaNO ₃] µM
Control	-	-	-	-	-
GNP	-	100	20	200	-
GNP+Fe	9	100	20	200	-
GNP++Fe	90	100	20	200	-
GNO ₃ P	-	100	20	-	200
G	-	100	-	-	-

The enriched seawater was incubated in the dark on deck in incubators at ambient surface ocean temperature (Fig. 18), with un-enriched seawater used as a control. The samples were incubated until the bacteria in the incubations had reached the late exponential or stationary growth phase (4-5 days). Bacterial growth was monitored daily using absorption measurements (Red Tide USB 650 visible spectrophotometer, Ocean Optics) at a wavelength of 600 nm (Kirchman *et al.*, 2003). Samples were collected daily for enumeration of bacteria (flow cytometric analysis) and frozen at -80°C after adding 1% (v:v) paraformaldehyde.

At the end of incubation period, samples were sequentially filtered through 3.0 and 0.2 µm cellulose acetate filters to remove bacterial cells (Sartorius polycarbonate filter unit, 45 mm nitrocellulose membrane filter, Millipore). In a laminar flow hood, the filtered supernatant was passed over pre-washed polystyrene-divinylbenzene solid phase extraction (SPE) cartridges (Isolute ENV+, 200mg x 3mL) under gentle vacuum (Supelco Visiprep™) for extraction of siderophores. Cartridges loaded with sample were frozen at -20°C until further processing and analysis on shore. Prior to analysis, SPE cartridges were defrosted and eluted with 5 mL of 81:14:5:1 (v/v/v/v) acetonitrile: propan-2-ol: water: formic acid as described in section 2.5.2 above.

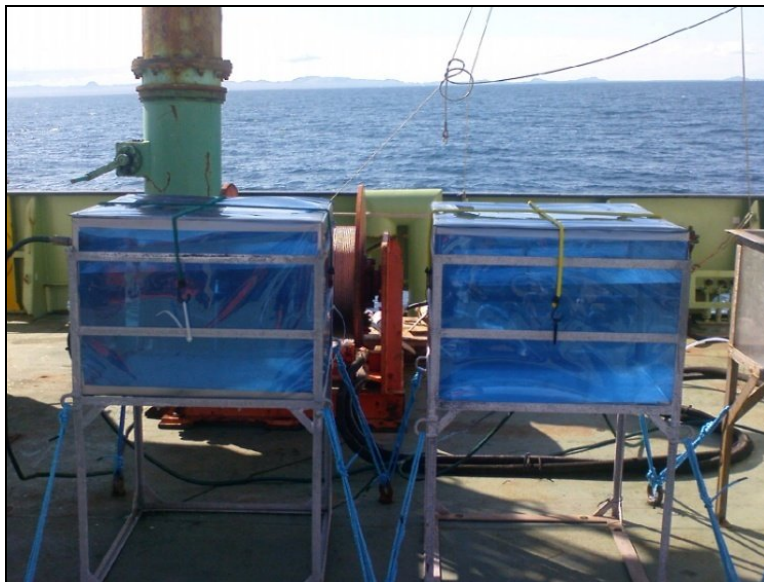


Figure 18: The incubation experiment which carried out in the dark on deck in incubators at ambient seawater temperature.

2.6.4 Determination of siderophores produced in nutrient enrichment experiments

The quantification of siderophores in the incubated seawater samples was carried out as for seawater samples (section 2.5.3), except for the concentration of added Ga. In order to ensure complete exchange of Fe with Ga, a higher final concentration of 14 mM Ga (ICP-MS standard, VWR) was added to extracts from nutrient enrichment experiments and left overnight before analysis by LC-ICP-MS.

The identifications of siderophore type compounds in the incubation samples were carried by LC-ESI-MS method in the full scans mode (m/z 200-1500) on both unamended samples and samples pre-equilibrated with 14 mM Ga (Mawji *et al.*, 2011). The analysis of samples after addition of excess Ga allows unknown siderophores to be identified in the complex mass chromatograms (Mc Cormack *et al.*, 2003). In the samples with added Ga, the Ga complexes of siderophores were determined through the distinctive isotopic ratio of Ga ($^{69}\text{Ga}/^{71}\text{Ga}$ ratio 3:2) in the full mass spectra. The identity of the siderophores was compared to the retention time for the potential Ga complex peak to peaks at similar retention times in the unamended sample, that were m/z 13 units less than the most abundant isotope in the added Ga sample (equivalent to the difference in mass between ^{56}Fe and ^{69}Ga).

Siderophores identified by Ga exchange were then characterised by collision induced dissociation (CID) analysis of the selected parent ions as described in section 2.5.4.

2.6.5 Flow cytometry analysis

Flow cytometric analysis used to enumerate bacterioplankton was based on their fluorescence and light scattering properties. Heterotrophic bacterioplankton do not possess detectable autofluorescence, and therefore fluorescent probes are added, such as DNA or protein stains. During this study, the nucleic acid stain SYBR Green I was used (Sigma-Aldrich) to determined abundance of heterotrophic bacterioplankton in the samples.

10 μ L of SYBR Green I was added to samples (1 mL) and the solution was incubated for 1 hour in the dark at room temperature. Then, the sample was analysed for total bacterial numbers using flow cytometry (FACScalibur, Becton Dickinson, Oxford, UK).

References

Achterberg, E. P., Holland, T. W., Bowie, A. R., Fauzi, R., Mantoura, C. & Worsfold, P. J. (2001) Determination of iron in seawater. *Analytica Chimica Acta*, 442, 1-14.

Berner, I., Greiner, M., Metzger, J., Jung, G. & Winkelmann, G. (1991) Identification of Enterobactin and Linear Dihydroxybenzoylserine Compounds by Hplc and Ion Spray Mass-Spectrometry (Lc/Ms and Ms/Ms). *Biology of Metals*, 4, 113-118.

Boye, M., Nishioka, J., Croot, P. L., Laan, P., Timmermans, K. R. & De Baar, H. J. W. (2005) Major deviations of iron complexation during 22 days of a mesoscale iron enrichment in the open Southern Ocean. *Marine Chemistry*, 96, 257-271.

Boye, M., Van Den Berg, C. M. G., De Jong, J. T. M., Leach, H., Croot, P. & De Baar, H. J. W. (2001) Organic complexation of iron in the Southern Ocean. *Deep-Sea Research Part I-Oceanographic Research Papers*, 48, 1477-1497.

Bruland, K. & Rue, E. (2001) Domoic acid binds iron and copper: a possible role for the toxin produced by the marine diatom *Pseudo-nitzschia*. *Marine Chemistry*, 76, 127-134.

Buffe, J., Jermann, R. & Tercier, M. L. (1992) Pressure Insensitive Solid-State Reference Electrode for Insitu Voltammetric Measurements in Lake Water. *Analytica Chimica Acta*, 269, 49-58.

Cartwright, A. J., Jones, P., Wolff, J. C. & Evans, E. H. (2005) Detection of phosphorus tagged carboxylic acids using HPLC-SF-ICP-MS. *Journal of Analytical Atomic Spectrometry*, 20, 75-80.

Croot, P. L., Andersson, K., Ozturk, M. & Turner, D. R. (2004) The distribution and specification of iron along 6 degrees E in the Southern Ocean. *Deep-Sea Research Part II-Topical Studies in Oceanography*, 51, 2857-2879.

Croot, P. L. & Johansson, M. (2000) Determination of iron speciation by cathodic stripping voltammetry in seawater using the competing ligand 2-(2-thiazolylazo)-p-cresol (TAC). *Electroanalysis*, 12, 565-576.

De Jong, J. T. M., Den Das, J., Bathmann, U., Stoll, M. H. C., Kattner, G., Nolting, R. F. & De Baar, H. J. W. (1998) Dissolved iron at subnanomolar levels in the Southern Ocean as determined by ship-board analysis. *Analytica Chimica Acta*, 377, 113-124.

Di Marco, V. B. & Bombi, G. G. (2006) Electrospray mass spectrometry (ESI-MS) in the study of metal-ligand solution equilibria. *Mass Spectrometry Reviews*, 25, 347-379.

Emery, T. (1986) Exchange of Iron by Gallium in Siderophores. *Biochemistry*, 25, 4629-4633.

Emery, T. & Hoffer, P. B. (1980) Siderophore Mediated Mechanism of Gallium Uptake Demonstrated in Microorganisms. *Journal of Nuclear Medicine*, 21, P24-P24.

Essen, S. A., Bylund, D., Holmstrom, S. J. M., Moberg, M. & Lundstrom, U. S. (2006) Quantification of hydroxamate siderophores in soil solutions of podzolic soil profiles in Sweden. *Biometals*, 19, 269-282.

Fish, A. J. & Jordan, D. (1983) An Algebraically Derived Non-Linear Control-Theory. *Journal of Dynamic Systems Measurement and Control-Transactions of the Asme*, 105, 83-91.

Gerringa, L. J. A., Blain, S., Laan, P., Sarthou, G., Veldhuis, M. J. W., Brussaard, C. P. D., Viollier, E. & Timmermans, K. R. (2008) Fe-binding dissolved organic ligands near the Kerguelen Archipelago in the Southern Ocean (Indian sector). *Deep-Sea Research Part II-Topical Studies in Oceanography*, 55, 606-621.

Gerringa, L. J. A., Herman, P. M. J. & Poortvliet, T. C. W. (1995a) Comparison of the Linear Vandenberg Ruzic Transformation and a Nonlinear Fit of the Langmuir Isotherm Applied to Cu Speciation Data in the Estuarine Environment. *Marine Chemistry*, 48, 131-142.

Gerringa, L. J. A., Rijstenbil, J. W., Poortvliet, T. C. W., Vandrie, J. & Schot, M. C. (1995b) Speciation of Copper and Responses of the Marine Diatom *Ditylum-Brightwellii* Upon Increasing Copper Concentrations. *Aquatic Toxicology*, 31, 77-90.

Gerringa, L. J. A., Veldhuis, M. J. W., Timmermans, K. R., Sarthou, G. & De Baar, H. J. W. (2006) Co-variance of dissolved Fe-binding ligands with phytoplankton characteristics in the Canary Basin. *Marine Chemistry*, 102, 276-290.

Gilar, M., Belenky, A. & Wang, B. H. (2001) High-throughput biopolymer desalting by solid-phase extraction prior to mass spectrometric analysis. *Journal of Chromatography A*, 921, 3-13.

Gledhill, M. (2001) Electrospray ionisation-mass spectrometry of hydroxamate siderophores. *Analyst*, 126, 1359-1362.

Gledhill, M., McCormack, P., Ussher, S., Achterberg, E. P., Mantoura, R. F. C. & Worsfold, P. J. (2004) Production of siderophore type chelates by mixed bacterioplankton populations in nutrient enriched seawater incubations. *Marine Chemistry*, 88, 75-83.

Gledhill, M. & Van Den Berg, C. M. G. (1994) Determination of Complexation of Iron(III) with Natural Organic Complexing Ligands in Seawater Using Cathodic Stripping Voltammetry. *Marine Chemistry*, 47, 41-54.

Groenewold, G. S., Avci, R., Karahan, C., Lefebvre, K., Fox, R. V., Cortez, M. M., Gianotto, A. K., Sunner, J. & Manner, W. L. (2004) Characterization of interlayer Cs⁺ in clay samples using secondary ion mass spectrometry with laser sample modification. *Analytical Chemistry*, 76, 2893-2901.

Hudson, R. J. M., Covault, D. T. & Morel, F. M. M. (1992) Investigations of Iron Coordination and Redox Reactions in Seawater Using Fe-59 Radiometry and Ion-Pair Solvent-Extraction of Amphiphilic Iron Complexes. *Marine Chemistry*, 38, 209-235.

Jarvis, K. E., Gray, A. L. & Houk, R. S. (1992) Handbook of Inductively Coupled Plasma Mass Spectrometry. *Chapman and Hall: New York*.

Kirchman, D. L., Hoffman, K. A., Weaver, R. & Hutchins, D. A. (2003) Regulation of growth and energetics of a marine bacterium by nitrogen source and iron availability. *Marine Ecology-Progress Series*, 250, 291-296.

Kiss, T. & Farkas, E. (1998) Metal-binding ability of desferrioxamine B. *J. Inclusion Phenomena Mol. Recog. Chem.*, 32, 385-403.

Landing, W. M. & Bruland, K. W. (1987) The Contrasting Biogeochemistry of Iron and Manganese in the Pacific-Ocean. *Geochimica Et Cosmochimica Acta*, 51, 29-43.

Landing, W. M., Haraldsson, C. & Paxeus, N. (1986) Vinyl Polymer Agglomerate Based Transition-Metal Cation Chelating Ion-Exchange Resin Containing the 8-Hydroxyquinoline Functional-Group. *Analytical Chemistry*, 58, 3031-3035.

Macrellis, H. M., Trick, C. G., Rue, E. L., Smith, G. & Bruland, K. W. (2001) Collection and detection of natural iron-binding ligands from seawater. *Marine Chemistry*, 76, 175-187.

Martinez, J. S., Haygood, M. G. & Butler, A. (2001) Identification of a natural desferrioxamine siderophore produced by a marine bacterium. *Limnology and Oceanography*, 46, 420-424.

Mawji, E., Gledhill, M., Milton, J. A., Tarran, G. A., Ussher, S., Thompson, A., Wolff, G. A., Worsfold, P. J. & Achterberg, E. P. (2008a) Hydroxamate Siderophores: Occurrence and Importance in the Atlantic Ocean. *Environmental Science & Technology*, 42, 8675-8680.

Mawji, E., Gledhill, M., Milton, J. A., Zubkov, M. V., Thompson, A., Wolff, G. A. & Achterberg, E. P. (2011) Production of siderophore type chelates in Atlantic Ocean waters enriched with different carbon and nitrogen sources. *Marine Chemistry*, 124, 90-99.

Mawji, E., Gledhill, M., Worsfold, P. J. & Achterberg, E. P. (2008b) Collision-induced dissociation of three groups of hydroxamate siderophores: ferrioxamines, ferrichromes and coprogens/fusigens. *Rapid Communications in Mass Spectrometry*, 22, 2195-2202.

McCormack, P., Worsfold, P. J. & Gledhill, M. (2003) Separation and detection of siderophores produced by marine bacterioplankton using high-performance liquid chromatography with electrospray ionization mass spectrometry. *Analytical Chemistry*, 75, 2647-2652.

Measures, C. I., Landing, W. M., Brown, M. T. & Buck, C. S. (2008) High-resolution Al and Fe data from the Atlantic Ocean CLIVAR-CO(2) repeat hydrography A16N transect: Extensive linkages between atmospheric dust and upper ocean geochemistry. *Global Biogeochemical Cycles*, 22.

Miller, L. A. & Bruland, K. W. (1997) Competitive equilibration techniques for determining transition metal speciation in natural waters: Evaluation using model data. *Analytica Chimica Acta*, 343, 161-181.

Milne, A., Landing, W., Bizimis, M. & Morton, P. (2010) Determination of Mn, Fe, Co, Ni, Cu, Zn, Cd and Pb in seawater using high resolution magnetic sector inductively coupled mass spectrometry (HR-ICP-MS). *Analytica Chimica Acta*, 665, 200-207.

Moberg, M., Nilsson, E. M., Holmstrom, S. J. M., Lundstrom, U. S., Pettersson, J. & Markides, K. E. (2004) Fingerprinting metal-containing biomolecules after reductive displacement of iron by gallium and subsequent column-switched LC-ICPMS analysis applied on siderophores. *Analytical Chemistry*, 76, 2618-2622.

Nagai, T., Imai, A., Matsushige, K., Yokoi, K. & Fukushima, T. (2007) Dissolved iron and its speciation in a shallow eutrophic lake and its inflowing rivers. *Water Research*, 41, 775-784.

Naito, K., Imai, I. & Nakahara, H. (2008) Complexation of iron by microbial siderophores and effects of iron chelates on the growth of marine microalgae causing red tides. *Phycological Research*, 56, 58-67.

Neilands, J. B. (1983) Isolation and Assay of 2,3-Dihydroxybenzoyl Derivatives of Polyamines - the Siderophores Agrobactin and Parabactin from Agrobacterium-Tumefaciens and Paracoccus-Denitrificans. *Methods in Enzymology*, 94, 437-441.

Neilands, J. B. & Nakamura, K. (1991) Detection, determination, isolation, characterization and regulation of microbial iron chelates. In: WINKELMANN, G. (Ed.). *CRC handbook of microbial iron chelates*. Florida: CRC Press, 1-14.

Nielsdottir, M. C., Moore, C. M., Sanders, R., Hinz, D. J. & Achterberg, E. P. (2009) Iron limitation of the postbloom phytoplankton communities in the Iceland Basin. *Global Biogeochemical Cycles*, 23, 1-13.

Obata, H., Karatani, H. & Nakayama, E. (1993) Automated-Determination of Iron in Seawater by Chelating Resin Concentration and Chemiluminescence Detection. *Analytical Chemistry*, 65, 1524-1528.

Rijkenberg, M. J. A., Powell, C. F., Dall'osto, M., Nielsdottir, M. C., Patey, M. D., Hill, P. G., Baker, A. R., Jickells, T. D., Harrison, R. M. & Achterberg, E. P. (2008) Changes in iron speciation following a Saharan dust event in the tropical North Atlantic Ocean. *Marine Chemistry*, 110, 56-67.

Rue, E. L. & Bruland, K. W. (1995) Complexation of Iron(III) by Natural Organic-Ligands in the Central North Pacific as Determined by a New Competitive Ligand Equilibration Adsorptive Cathodic Stripping Voltammetric Method. *Marine Chemistry*, 50, 117-138.

Rue, E. L. & Bruland, K. W. (1997) The role of organic complexation on ambient iron chemistry in the equatorial Pacific Ocean and the response of a mesoscale iron addition experiment. *Limnology and Oceanography*, 42, 901-910.

Ruzic, I. (1982) Theoretical Aspects of the Direct Titration of Natural-Waters and Its Information Yield for Trace-Metal Speciation. *Analytica Chimica Acta*, 140, 99-113.

Shenker, M., Ghirlando, R., Oliver, I., Helmann, M., Hadar, Y. & Chen, Y. (1995) Chemical-Structure and Biological-Activity of a Siderophore Produced by Rhizopus-Arrhizus. *Soil Science Society of America Journal*, 59, 837-843.

Sunda, W. G., Swift, D. G. & Huntsman, S. A. (1991) Low Iron Requirement for Growth in Oceanic Phytoplankton. *Nature*, 351, 55-57.

Sutton, K. L. & Caruso, J. A. (1999) Liquid chromatography-inductively coupled plasma mass spectrometry. *Journal of Chromatography A*, 856, 243-258.

Thuroczy, C. E., Gerrings, L. J. A., Klunder, M. B., Middag, R., Laan, P., Timmermans, K. R. & De Baar, H. J. W. (2010) Speciation of Fe in the Eastern North Atlantic Ocean. *Deep-Sea Research Part I-Oceanographic Research Papers*, 57, 1444-1453.

Twining, B. S., Baines, S. B. & Fisher, N. S. (2004) Element stoichiometries of individual plankton cells collected during the Southern Ocean Iron Experiment (SOFeX). *Limnology and Oceanography*, 49, 2115-2128.

Van Den Berg, C. M. G. (1995) Evidence for Organic Complexation of Iron in Seawater. *Marine Chemistry*, 50, 139-157.

Van Den Berg, C. M. G. & Donat, J. R. (1992) Determination and Data Evaluation of Copper Complexation by Organic-Ligands in Sea-Water Using Cathodic Stripping Voltammetry at Varying Detection Windows. *Analytica Chimica Acta*, 257, 281-291.

Van Den Berg, C. M. G., Nimmo, M., Abollino, O. & Mentasti, E. (1991) The Determination of Trace Levels of Iron in Seawater Using Adsorptive Cathodic Stripping Voltammetry. *Electroanalysis*, 3, 477-484.

Wilkinson, L., Hill, M., Welna, J. P. & Birkenbeuel, G. K. (1992) SYSTAT for Window: Statistics, Version 5 Edition. SYSTAT. Evanston, 750.

Witter, A. E. & Luther, G. W. (1998) Variation in Fe-organic complexation with depth in the Northwestern Atlantic Ocean as determined using a kinetic approach. *Marine Chemistry*, 62, 241-258.

CHAPTER 3 - Dissolved Fe(III) speciation in the high latitude North Atlantic Ocean

The present chapter is available on line: Khairul N. Mohamed, Sebastian Steigenberger, Maria C. Nielsdottir, Martha Gledhill, Eric, P. Achterberg (2011) Dissolved iron(III) speciation in the high latitude North Atlantic Ocean. *Deep-Sea Research I*, 58, 1049–1059.

3.1 Introduction

Dissolved iron concentrations ([dFe]) in surface waters of the North Atlantic Ocean are spatially and temporally highly variable due to biological activity, episodic deposition of Saharan dust, and hydrographic features including fronts and eddies (Duce *et al.*, 1991; Rijkenberg *et al.*, 2008; Nielsdottir *et al.*, 2009). The influence of the Saharan aerosol supply diminishes with latitude, with the high latitude North Atlantic receiving very low dust and hence atmospheric Fe inputs, comparable with inputs to the High Nutrient Low Chlorophyll (HNLC) North Pacific (Jickells *et al.*, 2005). Measurements of surface water dissolved aluminum as a tracer of mineral aerosol inputs showed low concentrations of ~2 nM and below in the region (Measures *et al.*, 2008), suggestive of low atmospheric dust derived Fe inputs. The dFe concentrations in the surface water of the Iceland Basin are reported to range from <0.01 to 0.22 nM (mean 0.09 nM; (Measures *et al.*, 2008; Nielsdottir *et al.*, 2009). Moreover, manipulations of phytoplankton communities in bottle experiments showed Fe limitation under post bloom conditions in the Iceland Basin (Moore *et al.*, 2006; Nielsdottir *et al.*, 2009).

The low Fe inputs and extremely low inorganic Fe solubility in seawater (Kuma *et al.*, 1996; Liu & Millero, 2002) bring in an important question: What are the chemical forms in which Fe exists in the Iceland Basin? Because the physicochemical form or speciation of Fe can affect its solubility (Zhu *et al.*, 1992; Kuma *et al.*, 1996) and bioavailability (Hutchins *et al.*, 1999a; Castruita *et al.*, 2008; Hassler & Schoemann, 2009; Hassler *et al.*, 2011), it is important to determine the organic Fe speciation in order to understand the biotic and abiotic cycles of Fe in marine systems.

It is known that more than 99% of the total dissolved Fe in seawater is complexed by dissolved organic Fe(III)-binding ligands (Gledhill & Van Den Berg, 1994; Rue & Bruland, 1995; Hunter & Boyd, 2007; Thuroczy *et al.*, 2010), which enhance the otherwise very low Fe solubility (0.08-0.2 nM) and reduce the fraction of inorganic Fe (ionic Fe and Fe-hydroxides) (Wu *et al.*, 2001; Liu & Millero, 2002). Consequently, the distribution of Fe

in the ocean is controlled by competition between Fe stabilisation by organic ligands and Fe removal processes (Wu *et al.*, 2001; Bergquist *et al.*, 2007; Boyd & Ellwood, 2010). The removal is mainly caused by biological uptake and scavenging, i.e. the precipitation and adsorption of Fe onto particles, and colloid aggregation.

The nature and origin of the Fe(III) binding organic ligands remains largely unknown. They are known to have a range of stability constants between 19 and 23 (log values; for review see Hunter & Boyd (2007), and can either be addressed as one pool of ligands (L) or as two separate ligand classes L_1 (stronger ligand class) and L_2 (weaker ligand class) (Hunter & Boyd, 2007).

Some information about the nature of the molecules that bind Fe(III) can be gained from their conditional stability constants, which are similar to those of siderophores extracted and purified from seawater cultures (Witter *et al.*, 2000; Gledhill *et al.*, 2004; Mawji *et al.*, 2008a; Mawji *et al.*, 2011). Furthermore, the strong Fe(III) binding compounds do not appear to be part of a more general group of organics such as humic acids, since the binding strength of humic-Fe complexes is lower than the strong ligands commonly observed in the ocean (Mantoura *et al.*, 1978; Laglera & Van Den Berg, 2009).

Laboratory and field studies have suggested that a fraction of the natural organic Fe(III) binding ligand pool in seawater consists of siderophores (Macrellis *et al.*, 2001; Gledhill *et al.*, 2004; Mawji *et al.*, 2008a; Mawji *et al.*, 2011; Velasquez *et al.*, 2011). Marine heterotrophic bacteria and cyanobacteria are known to excrete siderophores as part of a highly specific Fe uptake process (Reid *et al.*, 1993; Vraspir & Butler, 2009). It is less clear whether eukaryotic phytoplankton can excrete similarly strong organic ligands (Fuse *et al.*, 1993; Boye & Van Den Berg, 2000; Boye *et al.*, 2005; Buck *et al.*, 2007), although iron binding ligands have been shown to be produced when grazers consume phytoplankton (Sato *et al.*, 2007). Only in a few cases has an apparently straightforward relationship between ligand characteristics and phytoplankton biomass been found (Rue & Bruland, 1997; Boye *et al.*, 2005; Rijkenberg *et al.*, 2006). Furthermore, eukaryotes such as diatoms are thought to be able to reduce organic Fe species using membrane based Fe reducing enzymes (Maldonado *et al.*, 2001; Shaked *et al.*, 2005) prior to oxidation and transport into the cell (Maldonado *et al.*, 2006). As inorganic Fe(III) species are more readily reduced, the complexation of Fe(III) by organic ligands diminishes the rate of reduction and hence renders Fe less available. Thus the major portion of the organic ligand pool remains uncharacterised and their role in iron biogeochemistry is therefore unclear.

The distribution of dFe in the water column has been studied in the high latitude Atlantic Ocean (Martin *et al.*, 1993; Measures *et al.*, 2008; Nielsdottir *et al.*, 2009), however much less is known about the speciation of dFe. The aim of this work is to determine the distribution of dissolved Fe species in the high latitude North Atlantic and relate this to oceanographic and biological features. This study provided the first assessment of organic Fe(III) binding ligands for the study region. During this study, Fe speciation was measured using electrochemical methods to determine the concentration of organic Fe(III)-binding ligands and the strength of their complexes.

3.2 Material and methods

3.2.1 Sampling

Seawater samples were collected at North Atlantic Ocean stations situated between Iceland and Scotland (Fig. 19), during RRS *Discovery* cruises 321 (D321) and 340 (D340) in August-September 2007 and June 2009, respectively. The sampling of the depth profiles was carried out using a titanium CTD frame fitted with 10 L trace metal clean Teflon coated OTE (Ocean Test Equipment) bottles. Samples were filtered under slight N₂ gas over pressure using 0.2 µm pore size cartridge filters (Sartobran P-300, Sartorius). All 250 mL high density polyethylene bottles (Nalgene) were cleaned according to a standard protocol (Achterberg *et al.*, 2001). Samples for dFe were acidified to pH 2 (a final concentration of 0.011 M) using ultra pure HCl (Romil UPA grade). Sample bottles for Fe-binding ligand analysis were thoroughly rinsed with de-ionised water and then seawater before filling. Samples were then immediately frozen at -20°C (not acidified) for subsequent land based analysis. Hydrographic data (Fig. 20) were obtained from a Seabird 9/11+ CTD attached to the titanium rosette frame.

3.2.2 Determination of dissolved Fe

Dissolved Fe concentrations were measured using an automated flow-injection chemiluminescence method (Obata *et al.*, 1993; De Jong *et al.*, 1998) with 8-hydroxyquinoline (8-HQ) immobilized on Toyopearl gel (Landing *et al.*, 1986) as preconcentration/ matrix removal resin. The detection limit, calculated as 3 × the standard deviation of the lowest standard addition, was on average 0.027 ± 0.017 (n=11) nM dFe; the analytical blank was 0.028 ± 0.009 (n =13) nM dFe (Nielsdottir *et al.*, 2009).

3.2.3 Determination of organic Fe(III)-binding ligands

Determination of the Fe(III)-binding capacity in the samples was undertaken using competitive ligand exchange-adsorptive cathodic stripping voltammetry (CLE-AdCSV) with TAC (thiazolylazo-p-cresol; Sigma-Aldrich) as competing ligand (Croot & Johansson, 2000). All solutions were prepared with 18.2 MΩ cm⁻¹ deionized water

(Milli-Q, Millipore) and sample manipulations were performed in a Class 100 laminar flow bench at room temperature (20°C) in a clean electrochemistry laboratory. A 0.02 M stock solution of TAC was prepared in triple quartz distilled (QD) methanol (0.439 g in 100 mL methanol), and a mixed $\text{NH}_3/\text{NH}_4\text{OH}$ borate pH buffer (1.0 M; pH 8.05; Suprapur, Merck) solution was prepared by dissolution of boric acid in 0.3 M ammonia (Suprapur, Merck). Iron contamination was removed from the borate buffer using a C18 SepPak column (Whatman) after the addition of TAC to the buffer. Iron standard solutions were prepared using a 1000 mg L⁻¹ Fe ICP-MS stock solution (Fisher Scientific).

Seawater (200 mL) was buffered to pH 8.05 (5.0 mM borate buffer) and TAC added to a final concentration of 10 μM . The pH was checked on every sample following buffer addition. The sample was subdivided into 12 pre-conditioned FEP (Nalgene) bottles and Fe(III) was added in increments up to a total added Fe concentration of 8 nM, sufficient to saturate the natural organic Fe(III) binding ligands present in the samples. The Fe(III) was added to all but two of the bottles and allowed to equilibrate overnight (>15 hours).

The concentration of $\text{Fe}(\text{TAC})_2$ in each aliquot was determined by adsorptive cathodic stripping voltammetry using a μ Autolab potentiostat (Ecochemie, Netherlands) and a static mercury drop electrode (Metrohm Model VA663). The sample was deaerated for 300 s with nitrogen gas. The $\text{Fe}(\text{TAC})_2$ complex in the sample was adsorbed onto a fresh mercury (Hg) drop at an applied potential of -0.40 V for 60 s whilst the sample was stirred. The stirrer was stopped and the potential was scanned from -0.40 V to -0.90 V at 19.5 mV s⁻¹ using a differential pulse mode, and the stripping reduction current from the adsorbed $\text{Fe}(\text{TAC})_2$ was recorded. The limit of detection for the technique for dissolved Fe measurements was 0.15 nM (3 σ of blank) using a 60 s deposition time, with a blank of 0.08 nM. Details of Fe-binding ligand measurement were described in Chapter 2.

3.2.4 Calculation of Fe speciation

The titration data was used to calculate the conditional stability constants (K'_{FeL}) and concentrations of the organic binding ligands ($[\text{L}_i]$). The principle of determining the binding characteristics of dissolved organic ligands with Fe has been described in detail by Croot & Johansson (2000). A non-linear regression of the Langmuir isotherm was used to determine the concentration and conditional stability constants of the natural dissolved organic ligands, according to Gerringa *et al.* (1995a):

$$\frac{K'_{Fe(TAC)_2} \times [TAC]^2}{K'_{FeL} \times [L_T]} = \frac{[Fe(TAC)_2]}{[FeL]}$$

Where K' is the conditional stability constant of Fe with the ligands, (either TAC or the natural organic ligands (L)) and $[TAC]$ is the concentrations of free (not Fe bound) ligands. Whilst $[Fe(TAC)_2]$ and $[FeL]$ are the concentrations of the Fe complexes with TAC and natural ligands, respectively. The alpha coefficient for the inorganic speciation of Fe (Fe) used in this study was 10^{10} (Hudson *et al.*, 1992). Details of Fe speciation calculation are described in Chapter 2.

3.3 Results and discussion

3.3.1 Study area

The majority of the stations were located in the Iceland Basin, whilst station B4 was located on the Hatton-Rockall Plateau and stations A5, B5 and B6 in the Rockall Trough region (Fig. 20).

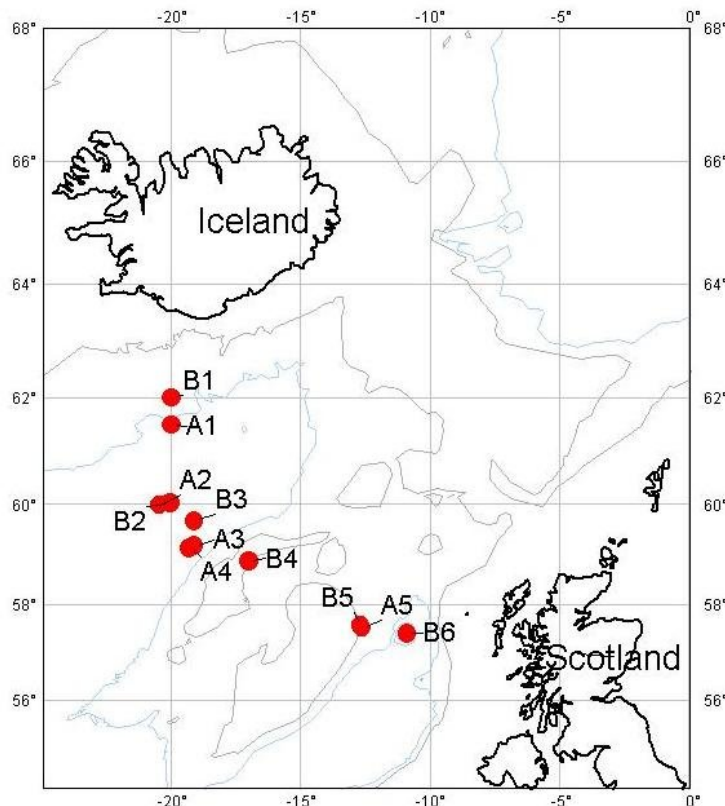


Figure 19: Sampling stations visited during cruise D321 (August/September 2007) (A1-A5) and cruise D340 (June 2009) (B1-B6). Stations were located in the Iceland Basin (A1, A2, A3, A4, B1, B2 and B3), Hatton-Rockall (B4) and Rockall Trough (A5, B5 and B6). The isobaths represent 1000 and 2000 m depth contours.

Water mass definitions by Fogelqvist *et al.* (2003) are used here to describe the three different sampling regions. In the upper water layer of the Iceland Basin the predominant flow of relatively warm and saline waters from the North Atlantic Current is in a north easterly direction. Along the edge of the Reykjanes Ridge, periodically a southerly flow can be observed. During the cruise in June 2009 (D340) the surface waters had similar physical properties in the Iceland Basin, the Hatton-Rockall region and Rockall Trough. Northeast Atlantic Water (NEAW) with a salinity of around 35.2-35.3 and a potential temperature between 9.1-10.4°C (Table , Fig. 20) was observed from the surface waters (<150 m) down to mid layer depths of ca. 500 m. Below the mid layer depths (down to ca. 1000 m depth), the potential temperature decreased to a minimum of ~5°C indicating Iceland-Scotland Overflow Water (ISOW; salinity ca. 35.0, Table 6) which travels along the deeper part of the Iceland slope (Table 6, Fig. 20) (Sherwin, unpublished data, 2009). At ca. 1500 m depth, Labrador Sea Water (LSW) was present, extending from the southern edge of the Iceland Basin and with a potential temperature of ca. 2.7°C. The bottom waters in the Iceland Basin were formed by North East Atlantic Deep Waters (NEADW) with salinities of 34.95-35.0 and potential temperatures of 2-3°C.

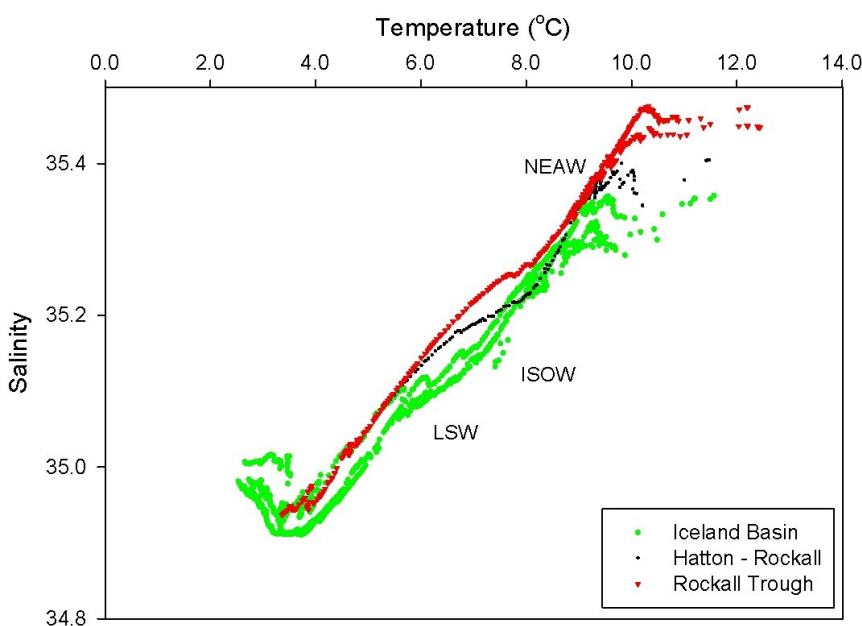


Figure 20: Potential temperature-salinity plot for CTD data from the Iceland Basin and Rockall Trough regions for the D340 cruise. NEAW: Northeast Atlantic Water; ISOW: Iceland-Scotland Overflow Water; LSW: Labrador Sea Water.

Dissolved oxygen showed enhanced concentrations in the surface layer (8.2-9.3 mg L⁻¹; Table 5) and minimum levels between ca. 600 and 900 m depth (6.5-7.5 mg L⁻¹; Table 5). The study region is characterized by the occurrence of mesoscale eddies (Kupferman *et al.*, 1986), which are important for the transfer of new nutrients into the euphotic zone.

Table 5: Physical, nutrient and chlorophyll *a* data from stations occupied during cruises D321 and D340.

Station	Depth (m)	Salinity	Pot. temp. (°C)	Oxygen (mg/L)	Phosphate (µM)	Nitrate (µM)	Silicate (µM)	Chl. a (µg/L)
A1	5	35.24	13.51	8.13	0.18	3.02	0.00	0.20
Aug. 26 2007	32	35.23	13.41	8.10	0.20	3.82	0.09	0.20
61.30 N°	75	35.34	10.58	7.98	0.72	19.52	3.63	0.13
19.59 W°	200	35.32	9.86	7.98	0.73	19.77	3.93	0.04
	610	35.28	9.27	8.18	1.06	31.42	10.69	
	800	35.28	9.27	8.19	1.06	31.38	10.82	
Depth	1000	35.22	8.55	8.00	1.02	30.54	10.68	
2220 m	1200	35.22	8.55	8.00	1.02	29.73	10.43	
	1500	35.14	7.28	6.97	1.02	29.55	11.05	
	1800	35.14	7.28	6.96	0.98	28.49	11.07	
	2100	35.07	5.88	7.17	0.90	26.80	10.13	
	2205	35.07	5.87	7.18	0.88	26.87	9.48	
A2	7	35.27	13.74	8.22	0.27	3.17	0.52	0.17
Aug. 6 2007	13	35.27	13.65	8.18	0.27	3.00	0.47	0.18
59.08 N°	23	35.27	13.62	8.12	0.28	3.08	0.47	0.22
18.54 W°	30	35.27	13.59	8.08	0.31	3.65	0.54	0.24
	34	35.28	13.11	8.04	0.38	4.58	0.73	0.25
	50	35.32	10.83	8.10	0.72	10.13	2.23	0.21
Depth	78	35.32	10.44	8.13	0.73	10.90	3.35	0.09
2680 m	129	35.30	10.07	8.08	0.81	12.45	4.87	0.04
	406	35.28	9.24	8.10	0.89	13.81	6.41	
	811	35.16	7.21	6.97				
A3	5	35.22	13.41	8.21	0.25	3.18	0.38	0.47
Aug. 12 2007	12	35.22	13.41	8.20	0.53	3.37	0.41	0.48
59.11 N°	23	35.22	12.89	8.24	0.33	4.43	0.55	0.41
19.07 W°	30	35.23	12.39	8.28	0.42	5.67	0.84	0.44
	34	35.28	10.77	8.59	0.64	8.61	1.54	0.41
	50	35.26	10.10	8.41	0.74	10.13	2.67	0.27
Depth	78	35.28	9.97	8.18	0.79	12.16	3.73	0.09
1970 m	128	35.28	9.68	8.14	0.88	13.10	4.88	
	405	35.27	9.06	8.17	0.94	14.53	6.46	
	537	35.25	8.78	8.19				
A4	7	35.22	13.38	8.15	0.25	2.37	0.23	0.17
Aug. 8 2007	12	35.22	13.22	8.14	0.27	2.30	0.23	0.18
59.42 N°	22	35.22	13.16	8.15	0.24	2.31	0.23	0.22
-19.52 W°	29	35.22	13.16	8.14	0.25	2.41	0.25	0.24
	34	35.22	13.16	8.14	0.26	2.63	0.31	0.25
	50	35.21	10.23	8.40	0.79	8.73	2.24	0.21
Depth	78	35.23	9.88	8.35	0.79	9.70	3.21	0.09
2690 m	128	35.25	9.65	8.24	0.81	13.04	4.37	0.04
	204	35.27	9.43	8.10	0.90	10.80	5.61	
	406	35.24	8.81	7.99	0.97	12.12	6.81	
	609	35.21	8.12	7.97	1.07	12.85	7.79	
	810	35.11	6.67	6.92	1.33	16.12	11.91	

Cont. Table 5

Station	Depth (m)	Salinity	Pot. temp. (°C)	Oxygen (mg/L)	Phosphate (µM)	Nitrate (µM)	Silicate (µM)	Chl. a (µg/L)
A5	10	35.22	12.88	8.26	0.04	1.44	0.09	0.33
Aug. 28 2007	20	35.22	12.80	8.27	0.09	2.15	0.12	0.40
57.32 N°	35	35.24	10.65	8.51	0.30	7.14	0.92	0.27
12.37 W°	60	35.26	9.63	8.46	0.47	12.57	2.08	0.06
	125	35.27	9.06	8.30	0.59	15.09	3.64	0.04
	600	35.28	8.95	8.41	0.71	17.53	5.73	
Depth	900	35.27	8.88	8.36	0.99	23.03	10.12	
1636 m	1100	35.15	7.45	6.87	0.98	22.00	10.01	
	1300	35.19	5.38	7.97				
	1400	35.08	5.02	8.11				
	1620	35.01	4.24	8.17				
B1	5	35.3	10.39	9.17	0.27	12.40	1.19	0.85
Jun 11 2009	40	35.29	9.07	8.83	0.30	12.90	1.07	0.41
62.00 N°	80	35.29	8.73	8.67	0.47	17.63	2.48	0.05
20.00 W°	150	35.28	8.51	8.43	0.54	18.92	3.75	0.02
	300	35.25	8.20	8.23	0.56	18.79	3.84	0.04
	500	35.23	7.89	8.14	0.66	20.80	5.92	
Depth	700	35.15	7.00	7.12	0.68	21.68	6.67	
1833 m	800	35.10	6.30	7.10	0.94	25.32	10.72	
	1000	35.05	5.08	7.90	0.89	24.55	10.32	
	1200	34.98	2.79	8.27	0.86	23.82	10.92	
	1790	35.00	2.79	8.61	0.82	23.16	11.01	
B2	5	35.36	11.57	9.31	0.23	8.70	0.15	0.68
Jun 12 2009	20	35.35	10.91	9.20	0.21	9.01	0.12	0.93
60.03 N°	50	35.33	9.72	8.55	0.25	10.30	0.10	0.33
20.01 W°	100	35.35	9.55	8.24	0.5	17.97	3.20	0.08
	150	35.34	9.36	8.24	0.54	19.05	3.68	0.02
	300	35.35	9.12	8.10	0.59	20.77	5.12	
Depth	400	35.27	8.58	7.98	0.62	22.16	5.94	
2744 m	500	35.23	8.12	8.03	0.7	23.06	6.56	
	750	35.11	6.64	6.70	0.95	28.82	11.06	
	1000	35.01	4.94	7.52	0.93	28.72	11.5	
	2000	34.91	3.21	8.33	0.87	27.49	12.2	
	2730	34.98	2.55	8.20	0.82	26.90	15.66	

Cont. Table 5

Station	Depth (m)	Salinity	Pot. temp. (°C)	Oxygen (mg/L)	Phosphate (µM)	Nitrate (µM)	Silicate (µM)	Chl. a (µg/L)
B3	5	35.35	11.21	9.15	0.21	11.02	0.08	0.42
Jun 14 2009	25	35.35	11.18	8.97	0.20	11.04	0.03	0.71
59.40 N°	50	35.31	10.70	8.52	0.32	14.42	0.28	0.32
19.12 W°	80	35.29	9.52	8.32	0.50	19.44	2.93	0.09
	100	35.30	9.45	8.33	0.52	19.71	2.91	0.06
	150	35.32	9.36	8.11	0.56	21.33	4.02	
Depth	300	35.3	9.01	8.02	0.65	22.30	5.44	
2695 m	400	35.28	8.74	7.87	0.70	22.82	6.22	
	600	35.23	8.08	7.13	0.84	24.48	8.58	
	780	35.14	6.97	6.66	0.99	25.60	11.15	
	1000	35.07	5.57	7.18	0.99	25.49	11.66	
	2000	34.91	3.41	8.30	0.91	25.00	12.32	
	2650	34.98	2.77	8.21	0.91	24.23	14.76	
B4	5	35.40	11.48	8.88	0.13	4.01	0.03	0.48
Jun 15 2009	10	35.40	11.31	8.80	0.18	5.02	0.06	0.57
58.53 N°	27	35.40	11.30	8.79	0.18	5.12	0.11	0.19
17.00 W°	80	35.37	9.85	8.32	0.54	13.44	2.79	0.07
	150	35.38	9.63	8.08	0.59	14.94	3.78	0.06
	300	35.36	9.35	8.07	0.61	15.53	4.37	
Depth	400	35.35	9.25	7.97	0.65	16.08	5.48	
1167 m	600	35.33	9.01	7.67	0.99	22.77	10.48	
	850	35.19	7.36	6.50	1.03	22.94	11.60	
	1140	35.06	5.22	7.16	1.01	22.83	16.07	
B5	5	35.45	12.43	8.99	0.13	2.89	0.22	0.22
Jun 16 2009	30	35.45	12.23	8.49	0.30	6.39	0.48	0.20
57.32 N°	50	35.44	11.02	8.26	0.36	8.62	0.51	0.16
12.37 W°	100	35.45	10.35	8.01	0.49	13.09	1.63	0.05
	150	35.43	10.01	7.80	0.58	14.46	3.51	0.04
	300	35.38	9.43	8.04	0.6	14.78	2.73	
Depth	500	35.34	8.91	7.60	0.74	17.38	6.49	
1693 m	800	35.24	7.4	6.50	0.99	22.07	10.33	
	1000	35.13	5.81	7.08	0.98	22.01	11.09	
	1640	34.94	3.38	8.09	1.00	21.45	15.87	
B6	5	35.47	12.22	8.43	0.17	3.97	0.75	0.23
Jun 19 2009	30	35.47	12.22	8.38	0.16	3.98	0.77	0.22
57.23 N°	50	35.47	12.13	8.24	0.23	6.02	0.92	0.06
10.52 W°	100	35.46	10.68	7.95	0.45	12.40	2.13	0.04
	150	35.46	10.49	7.94	0.49	13.11	2.27	0.04
	300	35.47	10.23	7.86	0.56	14.38	4.43	
Depth	500	35.41	9.77	7.77	0.63	15.5	4.90	
790 m	700	35.36	9.21	7.73	0.71	16.53	5.74	
	765	35.33	8.89	7.25	0.79	18.44	7.00	

3.3.2 Dissolved Fe (dFe) distribution

Vertical distributions of [dFe] showed sub-nanomolar concentrations at all stations during this study, with concentrations over 1 nM in near bottom samples at two stations (Fig. 21). The [dFe] in surface waters (≤ 150 m) in the Iceland Basin ranged between 0.04-0.34 nM (Table 6), with a concentration (average \pm standard deviation (1σ)) of 0.14 ± 0.08 nM ($n=19$) (Table 6) during the August-September 2007 (D321) cruise. Dissolved Fe concentrations in this region during the June 2009 (D340 cruise) ranged between 0.10-0.7 nM (Table 6) with an average value of 0.24 ± 0.17 nM ($n=14$) (Table 6). Surface waters [dFe] values were also depleted relative to deeper waters in the Rockall Trough region for both D321 and D340, with average concentrations of 0.15 ± 0.05 nM ($n=5$) and 0.25 ± 0.13 nM ($n=11$) (Table 6), respectively. However, higher [dFe] were observed in the surface waters of the Hatton-Rockall region for D340, ranging between 0.44-0.87 nM (Table 6) with an average concentration of 0.67 ± 0.15 nM ($n=5$) (Table 6). This enhanced surface water [dFe] was associated with an anticyclonic mode water eddy (Read & Pollard, 2001) present in the Hatton-Rockall region. The eddy transferred deeper waters enriched in dissolved Fe and macronutrients to the surface, thereby increasing surface [dFe] in comparison to the Iceland Basin and Rockall Trough region.

The extremely low [dFe] in the surface waters of Iceland Basin were due to low atmospheric Fe inputs, as indicated by low surface water dissolved aluminium concentration observed during D321 (1-3 nM; Achterberg, unpublished data), combined with biological uptake. In fact, the high latitude North Atlantic receives low atmospheric Fe inputs which are comparable with those in the HNLC North Pacific (Jickells *et al.*, 2005). Although the deep winter mixing in this region supplies Fe and macro-nutrients to the surface waters to fuel the spring bloom, the Fe:nitrate ratio of this supply is low and results in very low [dFe] in surface waters following the spring bloom with concomitant enhanced residual nitrate concentrations (Nielsdottir *et al.*, 2009). The resulting Fe limitation of the phytoplankton community (Nielsdottir *et al.*, 2009) may influence the production of organic Fe(III)-binding ligands (Boye *et al.*, 2005; Buck *et al.*, 2010) in the surface waters of the Iceland Basin. The dissolved Fe distribution in the surface waters of the Rockall Trough region indicate that this area of the high latitude North Atlantic is similar to the Iceland Basin, with high surface water concentrations of nitrate, phosphate and silicate (stations A5, B5 and B6, Table 5) coupled to low [dFe] likely influencing the overall levels of productivity in this region.

Table 6: Iron speciation data for the Iceland Basin from stations occupied during cruises D321 and D340. Total dissolved Fe concentration ([dFe]), total binding ligands ($[L]$) and stability constant of Fe ligand ($\log K'_{FeL}$) were determined, and free iron binding-ligand ($[L'] = [L] - [dFe]$), $\alpha_{Fe\ organic} = [L'] \times K$, $[pFe] = -\log \{dFe / (\alpha_{Fe\ organic} - \alpha_{Fe\ inorganic})\}$ were calculated. sd – standard deviation (1σ).

St.	Depth (m)	[dFe]		$[L]$		$\log K'_{FeL}$		$[L']$		\log		[pFe] (M)	$[L]/[dFe]$	FeL (%)
		nM	sd	nM	sd	mol ⁻¹	sd	nM	sd	$\alpha_{Fe\ org.}$				
A1	35	0.12	0.00	1.07	0.06	22.19	0.13	0.94	0.06	13.16	23.07	8.6	99.9	
	78	0.13	0.01	0.87	0.08	22.00	0.17	0.74	0.08	12.87	22.75	6.6	99.9	
	616	0.41	0.01	1.75	0.16	21.62	0.12	1.34	0.16	12.75	22.14	4.3	99.8	
	809	0.50	0.02	2.11	0.24	21.75	0.15	1.61	0.24	12.95	22.26	4.2	99.9	
	1014	0.44	0.01	0.66	0.09	21.76	0.22	0.22	0.09	12.1	21.45	1.5	99.2	
	1221	0.87	0.01	1.27	0.16	21.47	0.16	0.40	0.16	12.08	21.14	1.5	99.2	
	1527	0.45	0.01	0.58	0.05	21.83	0.15	0.13	0.05	11.94	21.29	1.3	98.9	
	1819	0.78	0.01	1.04	0.11	21.67	0.17	0.27	0.11	12.10	21.21	1.3	99.2	
	2133	0.74	0.06	1.59	0.18	21.64	0.15	0.85	0.19	12.57	21.7	2.1	99.7	
	2237	1.52	0.03	2.14	0.21	21.60	0.15	0.62	0.22	12.4	21.22	1.4	99.6	
A2	10	0.22	0.03	0.50	0.04	22.56	0.23	0.28	0.05	13.01	22.67	2.3	99.9	
	20	0.22	0.03	0.35	0.01	23.22	0.21	0.13	0.03	13.33	22.99	1.6	99.9	
	30	0.21	0.06	0.48	0.04	22.24	0.23	0.27	0.07	12.67	22.35	2.3	99.8	
	34	0.18	0.01	0.67	0.04	22.26	0.16	0.49	0.05	12.96	22.71	3.8	99.9	
	50	0.17	0.04	0.66	0.05	22.71	0.21	0.49	0.07	13.4	23.18	3.9	99.9	
	78	0.18	0.08	0.92	0.15	21.98	0.27	0.74	0.17	12.85	22.59	5.1	99.9	
	129	0.34	0.08	0.61	0.03	23.10	0.22	0.27	0.09	13.53	23.00	1.8	99.9	
	406	0.85	0.08	1.12	0.12	21.65	0.16	0.27	0.14	12.07	21.14	1.3	99.2	
	811	0.20	0.04	0.37	0.03	22.31	0.23	0.17	0.05	12.54	22.23	1.8	99.7	
	12	0.06	0.00	0.26	0.04	23.34	0.49	0.2	0.04	13.64	23.87	4.4	99.9	
A3	22	0.04	0.00	0.28	0.03	22.72	0.43	0.24	0.03	13.09	23.47	6.7	99.9	
	30	0.13	0.00	0.43	0.05	22.87	0.36	0.3	0.05	13.34	23.22	3.2	99.9	
	34	0.07	0.00	0.41	0.08	22.55	0.55	0.34	0.08	13.08	23.23	5.8	99.9	
	50	0.06	0.00	0.28	0.05	23.86	0.71	0.22	0.05	14.19	24.4	4.5	99.9	
	78	0.05	0.00	0.19	0.03	22.92	0.50	0.14	0.03	13.07	23.35	3.6	99.9	
	128	0.16	0.00	0.27	0.02	22.83	0.29	0.12	0.02	12.91	22.72	1.8	99.9	
	405	0.35	0.00	0.42	0.05	23.3	0.42	0.07	0.05	13.13	22.58	1.2	99.9	
	537	0.25	0.00	0.58	0.04	22.01	0.15	0.33	0.04	12.52	22.12	2.3	99.7	
	50	0.06	0.02	0.28	0.07	21.72	0.42	0.22	0.07	12.06	22.3	4.8	99.1	
	78	0.04	0.01	0.27	0.06	22.99	0.68	0.23	0.06	13.36	23.74	6.6	99.9	
A4	128	0.14	0.01	0.69	0.06	22.25	0.23	0.55	0.07	12.99	22.84	4.9	99.9	
	204	0.27	0.03	0.92	0.06	22.19	0.13	0.65	0.06	13.00	22.56	3.4	99.9	
	406	0.53	0.05	1.10	0.05	22.40	0.11	0.57	0.07	13.16	22.43	2.1	99.9	
	609	0.76	0.02	1.48	0.09	22.14	0.13	0.72	0.09	12.99	22.11	1.9	99.9	
	810	0.79	0.02	2.56	0.20	21.95	0.12	1.77	0.20	13.20	22.30	3.2	99.9	

Cont. Table 6

St.	Depth (m)	[dFe]		[L _γ]		log K' _{FeL}		[L]		log $\alpha_{Fe\ org.}$	[pFe] (M)	[L _γ]/[dFe]	FeL (%)
		nM	sd	nM	sd	mol ⁻¹	sd	nM	sd				
A5	11	0.16	0.01	0.41	0.04	22.03	0.24	0.26	0.05	12.44	22.25	2.6	99.6
	21	0.14	0.01	0.49	0.05	22.35	0.27	0.35	0.05	12.89	22.73	3.4	99.9
	36	0.09	0.00	0.52	0.02	22.78	0.13	0.43	0.02	13.42	23.47	5.8	99.9
	61	0.12	0.01	0.46	0.02	22.69	0.16	0.34	0.02	13.22	23.13	3.7	99.9
	125	0.23	0.02	0.52	0.03	23.51	0.21	0.29	0.03	13.98	23.63	2.3	99.9
	601	0.65	0.06	0.78	0.11	21.70	0.23	0.13	0.12	11.82	21.01	1.2	98.5
	901	0.39	0.02	0.48	0.04	21.98	0.18	0.09	0.05	11.92	21.33	1.2	98.8
	1100	0.08	0.00	0.24	0.02	23.11	0.28	0.16	0.02	13.31	23.41	3.0	99.9
	1300	0.59	0.01	0.72	0.03	22.19	0.11	0.13	0.03	12.30	21.54	1.2	99.5
	1400	0.68	0.04	0.86	0.08	22.89	0.49	0.18	0.09	13.15	22.32	1.3	99.9
B1	1620	0.84	0.04	1.24	0.13	22.39	0.32	0.40	0.14	12.99	22.07	1.5	99.9
	5	0.34	0.07	0.91	0.06	22.34	0.17	0.56	0.09	13.09	22.56	2.6	99.9
	40	0.70	0.01	1.30	0.05	22.35	0.10	0.61	0.05	13.14	22.29	1.9	99.9
	80	0.25	0.02	0.43	0.02	22.64	0.18	0.18	0.03	12.89	22.49	1.7	99.9
	150	0.43	0.01	0.89	0.03	22.95	0.12	0.46	0.03	13.61	22.97	2.1	99.9
	300	0.58	0.01	1.67	0.04	23.36	0.07	1.09	0.04	14.4	23.63	2.9	99.9
	500	0.83	0.02	1.22	0.02	23.28	0.11	0.39	0.03	13.87	22.95	1.5	99.9
	700	1.59	0.02	2.08	0.01	23.66	0.34	0.49	0.02	14.35	23.15	1.3	99.9
	800	2.23	0.04	2.52	0.09	22.50	0.16	0.29	0.10	12.97	21.62	1.1	99.9
	1000	1.55	0.06	2.12	0.05	23.03	0.13	0.56	0.08	13.78	22.59	1.4	99.9
B2	1200	1.51	0.06	1.95	0.07	22.5	0.13	0.44	0.09	13.15	21.97	1.3	99.9
	1790	1.42	0.03	1.87	0.08	22.95	0.21	0.45	0.09	13.61	22.45	1.3	99.9
	5	0.18	0.03	0.76	0.04	22.53	0.15	0.58	0.05	13.3	23.05	4.3	99.9
	10	0.10	0.01	0.47	0.03	22.71	0.20	0.37	0.03	13.28	23.29	4.8	99.9
	20	0.15	0.03	0.71	0.03	22.53	0.13	0.56	0.04	13.28	23.10	4.8	99.9
	80	0.21	0.02	0.49	0.04	22.46	0.39	0.28	0.05	12.90	22.58	2.3	99.9
	150	0.29	0.02	0.6	0.03	22.95	0.20	0.31	0.04	13.43	22.96	2	99.9
	300	0.38	0.01	0.87	0.04	22.51	0.15	0.50	0.04	13.21	22.63	2.3	99.9
	400	0.40	0.03	0.76	0.03	22.19	0.30	0.36	0.05	12.74	22.14	1.9	99.8
	500	0.71	0.03	1.31	0.02	23.28	0.07	0.61	0.04	14.06	23.21	1.9	99.9
B3	750	0.68	0.04	0.92	0.05	23.49	0.37	0.23	0.07	13.86	23.02	1.3	99.9
	1000	0.56	0.03	0.89	0.03	23.64	0.18	0.33	0.04	14.16	23.41	1.6	99.9

Cont. Table 6

St.	Depth (m)	[dFe]		[L _T]		log K' _{FeL}		[L]		log $\alpha_{Fe\,org.}$	[pFe] (M)	[L _T]/[dFe]	FeL (%)
		nM	sd	nM	sd	mol ⁻¹	sd	nM	sd				
B4	5	0.69	0.04	1.16	0.03	22.13	0.17	0.47	0.05	12.8	21.96	1.7	99.8
	10	0.67	0.06	1.05	0.08	22.8	0.26	0.39	0.10	13.38	22.56	1.6	99.9
	27	0.44	0.05	1.01	0.06	22.69	0.21	0.57	0.08	13.45	22.8	2.3	99.9
	80	0.67	0.08	1.12	0.09	22.06	0.17	0.45	0.12	12.71	21.88	1.7	99.8
	150	0.87	0.05	1.22	0.10	22.38	0.26	0.35	0.12	12.92	21.98	1.4	99.9
	300	0.63	0.05	1.30	0.04	22.58	0.10	0.67	0.07	13.41	22.61	2.1	99.9
	400	0.91	0.07	1.77	0.14	22.44	0.28	0.86	0.16	13.37	22.41	1.9	99.9
	600	0.93	0.06	1.69	0.1	23.03	0.38	0.75	0.12	13.90	22.94	1.8	99.9
	850	1.03	0.06	2.03	0.08	23.14	0.18	1.00	0.10	14.14	23.13	2.0	99.9
	1141	2.61	0.20	3.15	0.05	23.68	0.13	0.54	0.21	14.41	23.00	1.2	99.9
B5	5	0.23	0.03	0.57	0.02	22.16	0.09	0.35	0.04	12.7	22.34	2.5	99.8
	10	0.27	0.02	0.89	0.05	22.32	0.16	0.62	0.05	13.11	22.69	3.3	99.9
	30	0.36	0.01	0.69	0.03	22.10	0.09	0.34	0.03	12.63	22.08	1.9	99.8
	50	0.41	0.01	0.71	0.02	22.76	0.12	0.30	0.03	13.24	22.63	1.7	99.9
	100	0.25	0.00	0.84	0.04	22.37	0.13	0.60	0.04	13.14	22.75	3.4	99.9
	150	0.52	0.04	0.98	0.04	23.44	0.16	0.46	0.05	14.10	23.39	1.9	99.9
	300	0.41	0.02	1.00	0.04	22.42	0.11	0.59	0.04	13.19	22.58	2.4	99.9
	400	0.79	0.04	1.27	0.05	22.86	0.15	0.48	0.06	13.54	22.65	1.6	99.9
	800	0.86	0.03	1.40	0.04	22.57	0.09	0.54	0.05	13.3	22.37	1.6	99.9
	1000	0.82	0.03	0.96	0.04	22.85	0.21	0.14	0.05	12.99	22.08	1.2	99.9
B6	5	0.08	0.01	0.69	0.05	22.63	0.16	0.61	0.05	13.41	23.5	8.5	99.9
	30	0.18	0.03	0.55	0.06	21.82	0.18	0.37	0.06	12.39	22.13	3.1	99.6
	50	0.12	0.02	0.46	0.03	22.96	0.32	0.34	0.03	13.49	23.43	4.0	99.9
	100	0.21	0.04	0.53	0.02	22.23	0.07	0.32	0.04	12.73	22.41	2.5	99.8
	150	0.17	0.02	0.66	0.03	22.34	0.15	0.49	0.04	13.03	22.8	3.9	99.9
	300	0.27	0.04	0.8	0.06	22.19	0.18	0.53	0.07	12.92	22.48	2.9	99.9
	500	0.35	0.05	0.89	0.05	22.09	0.10	0.55	0.07	12.83	22.29	2.6	99.9
	700	0.29	0.05	0.52	0.04	22.40	0.19	0.23	0.06	12.76	22.29	1.8	99.8
	765	0.45	0.07	0.60	0.02	22.51	0.13	0.15	0.07	12.7	22.05	1.3	99.8

In the water column between 300-1000 m, the [dFe] increased with depth at all stations sampled during this study (Fig. 21). The mid layer depth [dFe] for D321 in the Iceland Basin (Stations A2, A3 and A4) ranged between 0.25-0.85 nM (Table 7), with an average value of 0.52 ± 0.24 nM ($n=10$) (Table 7). An average concentration of 0.79 ± 0.56 nM ($n=15$) (Table 7) was observed in the region during D340. In the Hatton-Rockall region, the [dFe] at mid layer depths were enhanced during D340, ranging from 0.63-1.03 nM (Table 7) with an average of 0.88 ± 0.17 nM ($n=4$) (Table 7). The [dFe] in the Rockall Trough region ranged between 0.27-0.86 nM for D340 (Table 7), with an average of 0.53 ± 0.25 nM ($n=8$) (Table 7). The increase with depth of [dFe]

(Fig. 21) suggests Fe supply by remineralisation of sinking biogenic particles, akin to nutrients such as nitrate (Boyd & Ellwood, 2010), as indicated by the strong correlations between dFe and nutrients (Table 8, Fig. 21). Iron differs from truly scavenged metals such as lead, as there is a strong biological Fe requirement with uptake by living cells, with subsequent release during their remineralisation. The relative enhanced [dFe] at mid layer depths (0.22-0.85 nM) (Table 6) for D321 and D340 in the Iceland Basin and Rockall Trough regions form an important feature of oceanic Fe distributions. The [dFe] below ca. 1000 m ranged between ca. 0.8-1 nM, with enhanced concentrations near the seafloor for Stations A5, B5 and B6 which were most likely due to benthic supplies (Laes et al., 2007). The Fe behavior at depth below the surface layers is at least partially attributable to the presence of high affinity organic ligands which specifically complex Fe(III) and increase its apparent solubility by enhancing colloid dissolution and reducing scavenging rates (Johnson *et al.*, 1997b).

Table 7: Iron speciation data averaged for parts of the water column for stations A1, A2, A3, A4, B1, B2 and B3 located in the Iceland Basin, station B4 in the Hatton-Rockall region and stations A5, B5 and B6 in the Rockall Trough region

Regions	Cruise	Depth	[dFe]		[L _{org}]		log K'		[L']		log αFe _{org}	pFe (M)	[L _{org}]/[dFe]	FeL (%)	
			(m)	nM	sd	nM	sd	mol ⁻¹	sd	nM	sd				
Iceland	D321	<150 (n=19)		0.14	0.08	0.50	0.26	22.65	0.54	0.36	0.23	13.13	23.08	4.3	99.9
		300-1000 (n=10)		0.52	0.24	1.28	0.77	22.13	0.52	0.76	0.65	12.81	22.15	2.6	99.8
		>1000 (n=6)		0.80	0.40	1.21	0.59	21.66	0.13	0.42	0.27	12.20	21.34	1.5	99.3
Basin	D340	<150 (n=14)		0.24	0.17	0.64	0.28	22.57	0.19	0.42	0.15	13.16	22.90	3.4	99.9
		300-1000 (n=15)		0.79	0.56	1.24	0.60	23.01	0.52	0.45	0.22	13.62	22.81	1.8	99.9
		>1000 (n=2)		1.46	0.06	1.91	0.06	22.73	0.32	0.45	0.09	13.38	22.21	1.3	99.9
Hatton to Rockall	D340	<150 (n=5)		0.67	0.15	1.11	0.08	22.41	0.33	0.44	0.09	13.05	22.24	1.7	99.9
		300-1000 (n=4)		0.88	0.17	1.70	0.30	22.80	0.34	0.82	0.14	13.71	22.77	1.9	99.9
		>1000 (n=1)		2.61	0.20	3.15	0.05	23.68	0.13	0.54	0.21	14.41	23.00	1.2	99.9
Rockall Trough	D321	<150 (n=5)		0.15	0.05	0.48	0.05	22.67	0.55	0.33	0.07	13.19	23.04	3.6	99.8
		300-1000 (n=2)		0.52	0.22	0.87	0.30	22.36	0.37	0.34	0.21	12.80	21.17	1.8	98.6
		>1000 (n=4)		0.55	0.33	0.76	0.41	22.64	0.42	0.22	0.13	12.94	22.33	1.8	99.8
	D340	<150 (n=11)		0.25	0.13	0.69	0.16	22.47	0.45	0.44	0.13	13.09	22.74	3.3	99.9
		300-1000 (n=8)		0.53	0.25	0.93	0.30	22.49	0.27	0.40	0.19	13.03	22.35	1.9	99.9

Table 8: The Pearson product moment correlation for the relationship between dissolved Fe and nutrients for cruises D321 and D340.

	D321			D340		
	Silicate	Nitrate	Phosphate	Silicate	Nitrate	Phosphate
Correlation Coefficient with dFe	0.672	0.602	0.529	0.585	0.466	0.678
P value	8.22E-07	1.94E-05	0.000265	9.19E-07	0.000177	2.58E-09
Number of samples	43	43	43	60	60	60

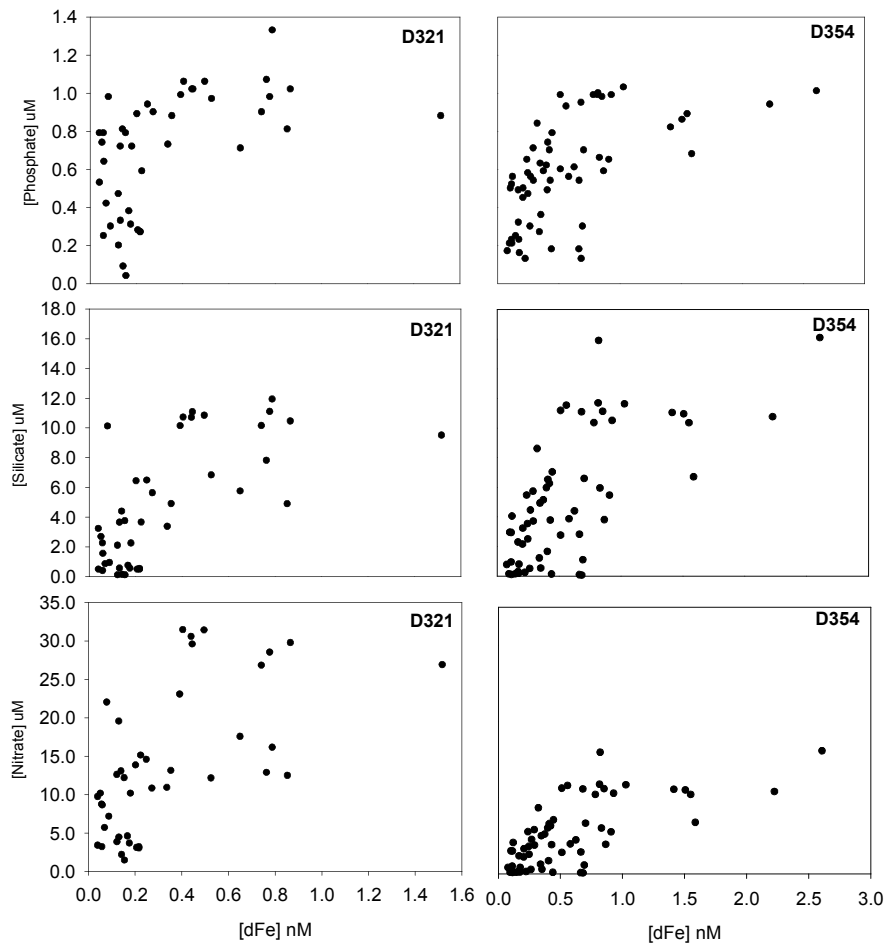


Figure 21: Correlation between dFe and nutrients during August/September 2007 (D321) cruise and June 2009 (D340) cruise.

3.3.3 Organic Fe(III)-binding ligands

This study showed relatively high and variable concentrations of Fe binding ligands in the surface waters of the study region (Table 7). The ligand concentrations were 0.50 ± 0.26 nM ($n=19$) and 0.64 ± 0.28 nM ($n=14$) in the surface waters of the Iceland Basin for the D321 and D340 cruises (Table 7), respectively. In the Hatton-Rockall and Rockall Trough regions, the ligand concentrations were 1.11 ± 0.08 nM ($n=5$) and 0.69 ± 0.16 nM ($n=11$) (Table 7) in the surface waters for D340, respectively. Furthermore, the $[L_r]$ at the mid layer depths (300-1000 m) were higher than in surface waters at all stations. In the Iceland Basin, $[L_r]$ increased to >1 nM, with average concentrations of 1.28 ± 0.77 nM ($n=10$) and 1.24 ± 0.6 nM ($n=15$) for D321 and D340 (Table 7), respectively. The highest $[L_r]$ at mid layer depths were observed in the Hatton-Rockall region (1.70 ± 0.3 nM; $n=4$) (Table 7). In the Rockall Trough region, the average $[L_r]$ were 0.87 ± 0.3 nM ($n=2$) and 0.93 ± 0.3 nM ($n=8$) for D321 and D340, respectively (Table 7). The $[L_r]$ profiles showed similar trends to those of [dFe] (Fig. 22) and the major nutrients nitrate and phosphate, suggesting that all of these constituents were

released simultaneously during remineralization of sinking biogenic particles (Wu *et al.*, 2001; Ye *et al.*, 2009). Indeed, Wu *et al.* (2001) suggested that the regeneration of sinking biogenic particles forms an important source of ligands in oceanic waters.

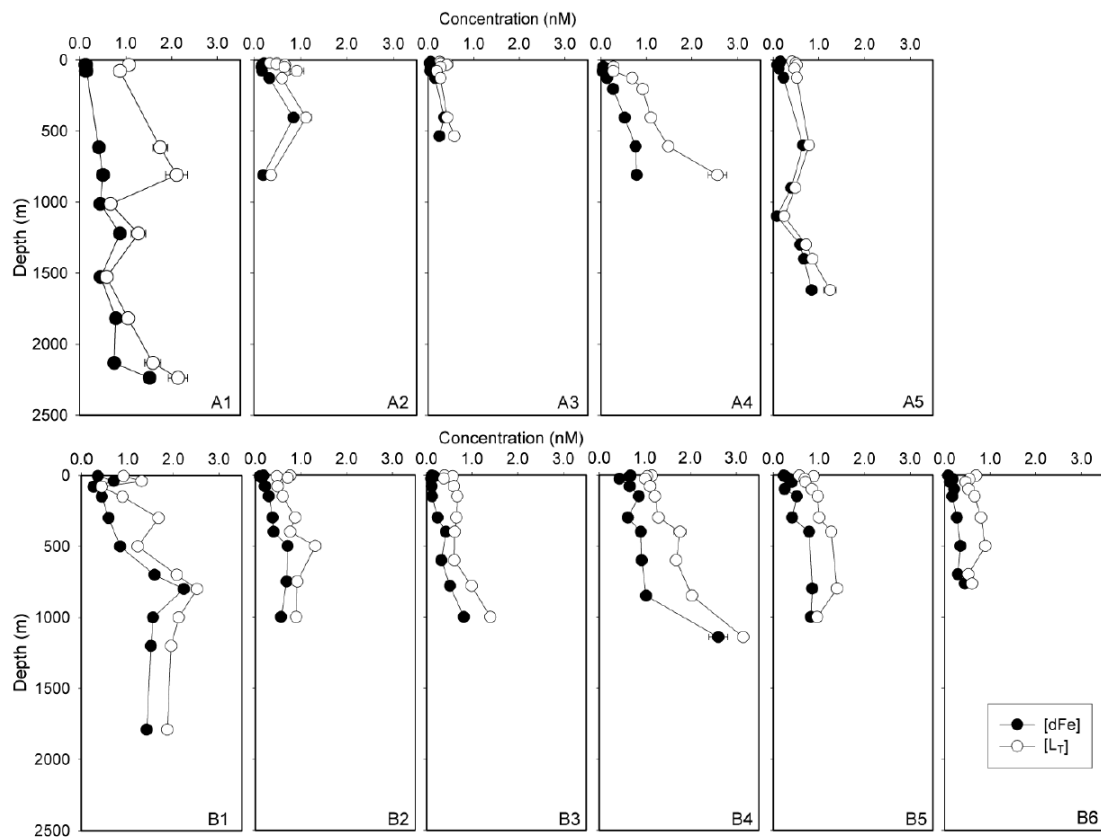


Figure 22: Vertical profiles of dissolved Fe (dFe) and ligand (L^-) concentrations for cruises D321 (Stations A1-A5) and D340 (Stations B1-B6).

The ligand concentrations were always in excess of [dFe] throughout the water column at all stations (Fig. 22). Between 99.5-99.9% of dFe was organically complexed (not considering Fe(II)) (Table 7) during both cruises. This observation agrees with other studies in the North Pacific (Rue & Bruland, 1995), Equatorial Pacific (Rue & Bruland, 1997), North Atlantic (Gledhill & Van Den Berg, 1994; Wu & Luther, 1995; Witter & Luther, 1998), South and Equatorial Atlantic (Powell & Donat, 2001), the Mediterranean Sea (Van Den Berg, 1995), the Southern Indian Ocean (Gerringa *et al.*, 2008) and the Southern Ocean (Nolting *et al.*, 1998; Boye *et al.*, 2001).

The high proportion of organic complexation is due to the high stability of the Fe(III)-ligand complexes, reflected by the high $\log K'_{FeL}$ in surface waters ($\log K'_{FeL} = 21.7-23.3$) (Table 7). The presence of strong organic Fe(III) binding ligands in the surface waters, coupled with the high inorganic side reaction coefficient of Fe^{3+} in oxic seawater i.e., $\alpha_{Fe} = 10^{10}$ (Hudson *et al.*, 1992) and low dissolved Fe concentrations, resulted in low

concentrations of free Fe^{3+} (ca. pFe^{3+} 21-23) (Table 7). Therefore, marine organisms may well have to use the organically complexed Fe to survive under depleted Fe conditions. However, the factors that affect and control an organism's ability to utilize the complexed Fe are not yet well understood.

During this study, I could not derive two classes of Fe(III)-binding ligands from the titration curves. Previous studies in the Atlantic Ocean (Gledhill & Van Den Berg, 1994; Witter & Luther, 1998) also reported one class of Fe(III)-binding ligands. Rue & Bruland (1995, 1997) reported two classes of Fe-binding ligands for the Pacific Ocean; in the Central North Pacific a strong ligand class (L_1) with a $\log K'_{\text{FeL}} = 22.7$ and a mean concentration of 0.31 nM, and a weaker class (L_2) with a $K'_{\text{FeL}} = 21.8$ and a mean concentration of 0.19 nM were observed (Rue & Bruland, 1995). Furthermore, during the Iron-Ex II experiments in the equatorial Pacific these workers observed L_1 with a $\log K'_{\text{FeL}} = 23.07$ and a mean concentration of 0.44 nM, and L_2 with a $\log K'_{\text{FeL}} = 21.48$ and a mean concentration of 1.5 nM (Rue & Bruland, 1997). Rue & Bruland (1997) used a detection window (27.5 μM of salicylaldoxime (SA), with $\alpha_{\text{Fe}^{\text{SA}}} = 73$) that was lower than the one used in this study (10.0 μM of TAC $\alpha_{\text{Fe}^{\text{TAC}}} = 250$). Consequently, it is possible that weaker ligands were not detected in titrations.

The average $\log K'_{\text{FeL}}$ value for surface waters falls within the range reported for the Northwest Atlantic Ocean ($\log K'_{\text{FeL}} = 22.3\text{-}22.9$) (Witter & Luther, 1998), Western Mediterranean ($\log K'_{\text{FeL}} = 21.3\text{-}22.5$) (Van Den Berg, 1995) and the Southeastern Atlantic Ocean ($\log K'_{\text{FeL}} = 21.4\text{-}23.5$) (Croot et al., 2004). A further study in the Atlantic Ocean Gledhill & Van Den Berg (1994) reported lower values for the conditional stability constant ($\log K'_{\text{FeL}} = 19.0$), but higher ligand concentrations of 3.5-4.8 nM than observed in the Iceland Basin. The $\log K'_{\text{FeL}}$ value in the tropical North Atlantic Ocean reported by Rijkenberg et al. (2008), using the same method and data treatment approaches, was only slightly higher (22.85 ± 0.38) than in this study. This may reflect differences between tropical and sub-polar waters in the biological ligand sources and different fractions of the Fe(III) binding ligands pool which are taken up by the microbial community (Hutchins et al., 1999a).

Nevertheless, despite differences in oceanic regimes and choices of the competitive ligands (e.g. TAC, SA) and their concentration, a remarkably similar picture has emerged for $\log K'$ of FeL complexes between present data and others. Indeed, the conditional stability constants of the organic Fe ligand complexes ($\log K'_{\text{FeL}} \approx 22\text{-}23$) for both cruises were similar to the $\log K'_{\text{FeL}}$ of strong ligands from the Pacific Ocean (Rue & Bruland, 1997), suggesting that the predominant ligand fraction in the Iceland Basin is similar to the one in the Pacific and may indicate siderophore type ligands. Siderophore

concentrations were related to the abundance of heterotrophic bacteria in the Atlantic Ocean (Mawji *et al.*, 2008a), suggesting release during the bacterially mediated organic matter mineralization processes. However, the similar stability constants of ligands and siderophores during this study are not sufficient to assume a similar chemical structure of ligands. Therefore, further studies are necessary to determine the presence of siderophore-like compounds because there is no data on the occurrence of these compounds in the study region to date.

3.3.4 Fe speciation

In order to identify trends in Fe speciation throughout the water column, I have examined the ratio of $[L]/[dFe]$ to highlight the differences in ligand saturation state (Thuroczy *et al.*, 2010; Thuroczy *et al.*, 2011). An enhanced ratio (i.e. >1) indicates a relatively large excess of ligands, and external inputs of Fe would be readily complexed by ligands. The ligands therefore have an enhanced capacity to buffer Fe. Removal of Fe by biological uptake or ligand production would increase the $[L]/[dFe]$ ratio. Conversely, a low ratio indicates a more complete saturation of the ligands with Fe, and additional external Fe inputs would be removed from the water column through precipitation and scavenging processes (Thuroczy *et al.*, 2010). The vertical profiles of the $[L]/[dFe]$ ratios in the Iceland Basin showed a similar trend as for the Hatton-Rockall and Rockall Trough regions for both cruises, with high and variable $[L]/[dFe]$ ratios in the surface waters (<150 m) and a lower and more constant ratio at depth (Fig. 23).

In the Iceland Basin, the enhanced $[L]/[dFe]$ ratios (3.4-4.3) (Table 6) in surface waters were due to the low $[dFe]$ as a result of the low atmospheric Fe inputs combined with biological uptake, and resulting in Fe stress for the phytoplankton community (Nielsdottir *et al.*, 2009). This, in turn, may have triggered the production of Fe binding ligands (low free $[Fe^{3+}]$, $pFe \approx 23$) (Table 6) by the marine microbial community to facilitate Fe uptake (Croot *et al.*, 2001; Gledhill *et al.*, 2004; Boye *et al.*, 2005; Mawji *et al.*, 2008a; Mawji *et al.*, 2011; Velasquez *et al.*, 2011).

The enhanced average ratios of $[L]/[dFe]$ found in surface waters of the Rockall Trough region of 3.6 ($n=5$) and 3.3 ($n=11$) for D321 and D340 (Table 7), respectively, were likely due to the relatively low $[dFe]$ as a consequence of biological Fe uptake, low atmospheric Fe inputs and possible ligand production by Fe stressed microorganisms. The enhanced productivity of this shallow region was most likely supported by benthic Fe inputs transferred to the surface by water column mixing processes (Johnson *et al.*, 2001).

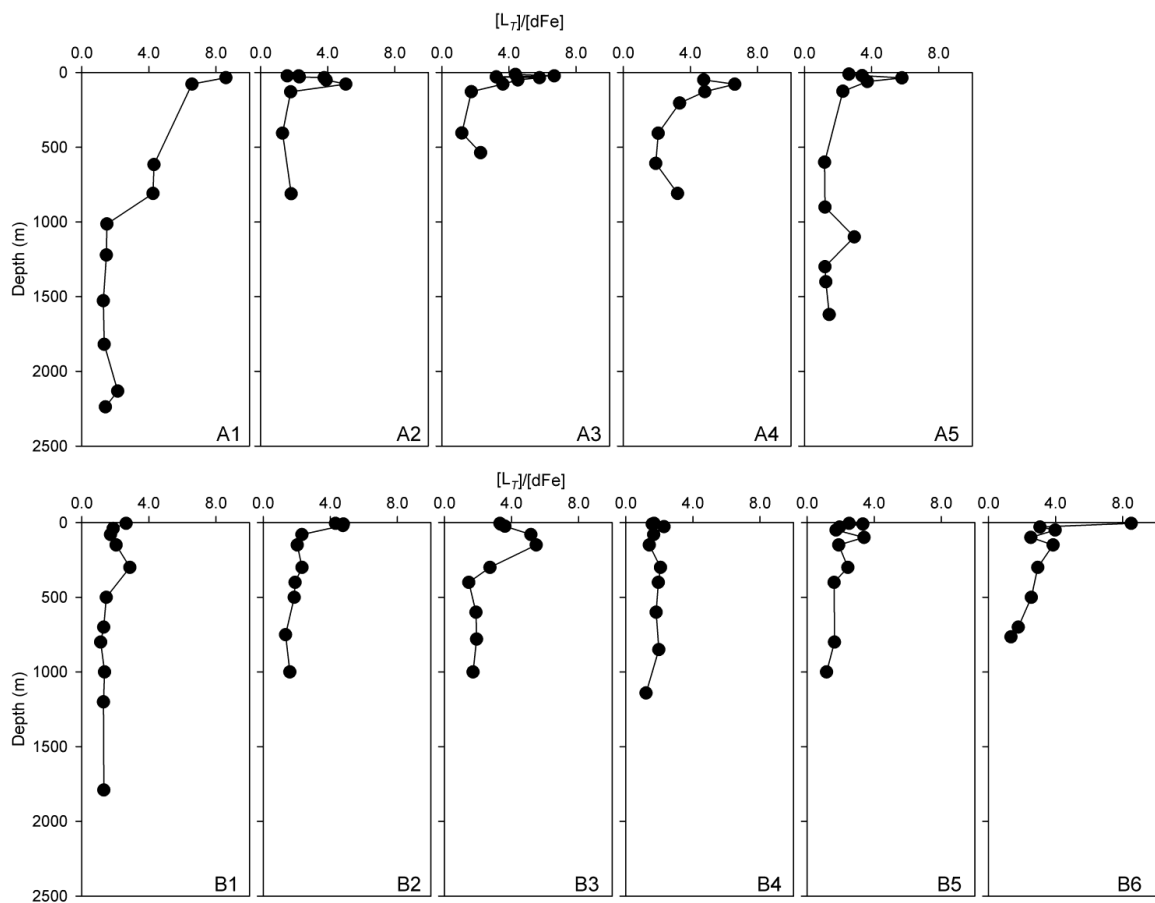


Figure 23: Depth profiles of the $[dFe]/[L_7]$ ratio for cruises D321 (Stations A1-A5) and D340 (Stations B1-B6).

The relatively low average $[L_7]/[dFe]$ ratio of 1.72 ($n=5$) (Table 7) in surface waters of the Hatton-Rockall region was the result of enhanced $[dFe]$ in this region supplied by an anticyclonic mode water eddy. It has been shown that ligands produced by phytoplankton can complex Fe (Fuse *et al.*, 1993; Boye *et al.*, 2005; Buck *et al.*, 2010). However, only a few studies have reported a clear relationship between chlorophyll α and L_7 concentrations, indicating that ligand production was related to phytoplankton biomass and associated bacteria and viruses (Rue & Bruland, 1997; Boye *et al.*, 2005; Gerringa *et al.*, 2006). In this study, I did not find a clear relationship between chlorophyll α and L_7 in surface waters ($r^2=0.0006$, $p>0.05$; $n=30$). Possibly, the standing stock of the phytoplankton and bacteria was not related to the production of ligands. The grazing of the phytoplankton cells by zooplankton could have provided an alternate source of ligand in the surface layer (Hutchins *et al.*, 1999a). Moreover, the variations in ligand concentrations in the surface layer (<150 m) are the result of a balance between production and breakdown processes (including photo-chemical degradation) (Croot *et al.*, 2001; Boye *et al.*, 2003; Rijkenberg *et al.*, 2006).

At depths between ca. 300-1000 m, the $[L]/[dFe]$ ratio decreased with depth to between 1.8-2.6 in the Iceland Basin (Table 7, Fig. 23) for both cruises. In the Hatton-Rockall and Rockall Trough regions for D340, the average ratios were respectively 1.9 ($n=4$) and 1.9 ($n=8$). The trends in ligands to dissolved Fe ratios observed in this study, agree with those reported by Thuroczy *et al.* (2010) and Thuroczy *et al.* (2011). In the Southern Ocean these authors observed enhanced $[L]/[dFe]$ ratios in the surface waters, with an average value of 4.4; lower $[L]/[dFe]$ were observed in deeper waters, with ratios ranging between 1.1 and 2.7 (Thuroczy *et al.*, 2011). The decrease of the $[L]/[dFe]$ ratio was mainly due to the increase of $[dFe]$ with depth throughout the water column (Fig. 23). This $[dFe]$ increase resulted in a progressive occupation of the Fe-binding ligand sites. The near-saturation of ligands is deemed to be consistent with the precipitation of Fe as insoluble oxyhydroxide and its removal from the deep ocean (Thuroczy *et al.*, 2010; Thuroczy *et al.*, 2011). Consequently, this indicates a steady state between dissolved organic ligands and dissolved Fe, reflecting a balance between degradation/remineralisation and scavenging in deep waters.

The relatively constant ratios of $[L]/[dFe]$ at depths below the surface mixed layer (Fig. 23) suggested that the ligands were refractory compounds that originated from degradation of sinking organic matter produced in surface waters (Kuma *et al.*, 1996; Hunter & Boyd, 2007). The microbial degradation would produce Fe binding ligands in the deep waters (Kuma *et al.*, 1996), where only one principal group of ligands is observed (Rue & Bruland, 1995; Hunter & Boyd, 2007) with a long decay time. Recalcitrant land-derived organic matter transferred from shelf seas into the deep ocean, forms an alternative ligand source (Bauer *et al.*, 2002). A recent modelling study has confirmed enhanced decay times of Fe binding ligands in deep waters in excess of 7 years (Ye *et al.*, 2009).

3.4 Conclusion

The low $[dFe]$ in surface waters of the high latitude North Atlantic Ocean coincided with excess organic ligands which prevented Fe precipitation and scavenging by forming stable chelates. This condition therefore prevented more pronounced Fe stress in the microbial surface water community. The Fe speciation analysis showed that dissolved Fe was 99.5% – 99.9% organically bound throughout the water column.

The ratio of $[L]/[dFe]$ as described by Thuroczy *et al.* (2010) , provided a useful concept to highlight the variations in ligand distributions throughout the water column and between different regimes in terms of primary production. High and variable $[L]/[dFe]$ ratios were observed in the surface waters and related to microbial ligand production and low $[dFe]$ due to the low Fe inputs combined with biological Fe uptake.

Moreover, decreasing ratios of $[L]/[dFe]$ with depth were observed to near constant ratios in the 300-1000 m depth region, reflecting a steady state between dissolved Fe and organic ligands which are possibly produced from the mineralisation of sinking biogenic particles or derived from terrestrial sources. This observation confirms the important role of organic ligands in keeping Fe in the soluble phase, and avoiding its precipitation and enhancing the residence time of Fe in the oceanic water column.

The conditional stability constants of the organic Fe ligand complexes ($\log K'_{FeL} \approx 22-23$) observed in the water column of this study region did not show a decrease with depth, as reported by Rue & Bruland (1995), and thought to be indicative of a preferential degradation of the stronger ligand types according to Hunter & Boyd (2007). The stability constants observed in this study compared well with those reported for siderophore type ligands. However, while siderophores may well have a specific role in surface waters of this study region, it is unclear whether they are sufficiently resistant to breakdown for a role in deep water Fe complexation.

References

Achterberg, E. P., Holland, T. W., Bowie, A. R., Fauzi, R., Mantoura, C. & Worsfold, P. J. 2001. Determination of iron in seawater. *Analytica Chimica Acta*, 442, 1-14.

Bauer, J. E., Druffel, E. R. M., Wolgast, D. M. & Griffin, S. 2002. Temporal and regional variability in sources and cycling of DOC and POC in the northwest Atlantic continental shelf and slope. *Deep-Sea Research Part II-Topical Studies in Oceanography*, 49, 4387-4419.

Bergquist, B. A., Wu, J. & Boyle, E. A. 2007. Variability in oceanic dissolved iron is dominated by the colloidal fraction. *Geochimica Et Cosmochimica Acta*, 71, 2960-2974.

Boyd, P. W. & Ellwood, M. J. 2010. The biogeochemical cycle of iron in the ocean. *Nature Geoscience*, 3, 675-682.

Boye, M., Aldrich, A. P., Van Den Berg, C. M. G., De Jong, J. T. M., Veldhuis, M. & De Baar, H. J. W. 2003. Horizontal gradient of the chemical speciation of iron in surface waters of the northeast Atlantic Ocean. *Marine Chemistry*, 80, 129-143.

Boye, M., Nishioka, J., Croot, P. L., Laan, P., Timmermans, K. R. & De Baar, H. J. W. 2005. Major deviations of iron complexation during 22 days of a mesoscale iron enrichment in the open Southern Ocean. *Marine Chemistry*, 96, 257-271.

Boye, M. & Van Den Berg, C. M. G. 2000. Iron availability and the release of iron-complexing ligands by *Emiliania huxleyi*. *Marine Chemistry*, 70, 277-287.

Boye, M., Van Den Berg, C. M. G., De Jong, J. T. M., Leach, H., Croot, P. & De Baar, H. J. W. 2001. Organic complexation of iron in the Southern Ocean. *Deep-Sea Research Part I-Oceanographic Research Papers*, 48, 1477-1497.

Buck, K. N., Lohan, M. C., Berger, C. J. M. & Bruland, K. W. 2007. Dissolved iron speciation in two distinct river plumes and an estuary: Implications for riverine iron supply. *Limnology and Oceanography*, 52, 843-855.

Buck, K. N., Selph, K. E. & Barbeau, K. A. 2010. Iron-binding ligand production and copper speciation in an incubation experiment of Antarctic Peninsula shelf waters from the Bransfield Strait, Southern Ocean. *Marine Chemistry*, 122, 148-159.

Castruita, M., Shaked, Y., Elmegreen, L. A., Stiefel, E. I. & Morel, F. M. M. 2008. Availability of iron from iron-storage proteins to marine phytoplankton. *Limnology and Oceanography*, 53, 890-899.

Croot, P. L., Andersson, K., Ozturk, M. & Turner, D. R. 2004. The distribution and specification of iron along 6 degrees E in the Southern Ocean. *Deep-Sea Research Part II-Topical Studies in Oceanography*, 51, 2857-2879.

Croot, P. L., Bowie, A. R., Frew, R. D., Maldonado, M. T., Hall, J. A., Safi, K. A., La Roche, J., Boyd, P. W. & Law, C. S. 2001. Retention of dissolved iron and Fe-II in an iron induced Southern Ocean phytoplankton bloom. *Geophysical Research Letters*, 28, 3425-3428.

Croot, P. L. & Johansson, M. 2000. Determination of iron speciation by cathodic stripping voltammetry in seawater using the competing ligand 2-(2-thiazolylazo)-p-cresol (TAC). *Electroanalysis*, 12, 565-576.

De Jong, J. T. M., Den Das, J., Bathmann, U., Stoll, M. H. C., Kattner, G., Nolting, R. F. & De Baar, H. J. W. 1998. Dissolved iron at subnanomolar levels in the Southern Ocean as determined by ship-board analysis. *Analytica Chimica Acta*, 377, 113-124.

Duce, R. A., Tindale, N. & Zhuang, G. 1991. Atmospheric Iron and Its Impact on Marine Biological Productivity and Chemical Cycling. *Abstracts of Papers of the American Chemical Society*, 201, 20-Nucl.

Fogelqvist, E., Blindheim, J., Tanhua, T., Osterhus, S., Buch, E. & Rey, F. 2003. Greenland-Scotland overflow studied by hydro-chemical multivariate analysis. *Deep-Sea Research Part I-Oceanographic Research Papers*, 50, 73-102.

Fuse, H., Takimura, O., Kamimura, K. & Yamaoka, Y. 1993. Marine-Algae Excrete Large Molecular-Weight Compounds Keeping Iron Dissolved. *Bioscience Biotechnology and Biochemistry*, 57, 509-510.

Gerringa, L. J. A., Blain, S., Laan, P., Sarthou, G., Veldhuis, M. J. W., Brussaard, C. P. D., Viollier, E. & Timmermans, K. R. 2008. Fe-binding dissolved organic ligands

near the Kerguelen Archipelago in the Southern Ocean (Indian sector). *Deep-Sea Research Part II-Topical Studies in Oceanography*, 55, 606-621.

Gerringa, L. J. A., Herman, P. M. J. & Poortvliet, T. C. W. 1995. Comparison of the Linear Vandenberg Ruzic Transformation and a Nonlinear Fit of the Langmuir Isotherm Applied to Cu Speciation Data in the Estuarine Environment. *Marine Chemistry*, 48, 131-142.

Gerringa, L. J. A., Veldhuis, M. J. W., Timmermans, K. R., Sarthou, G. & De Baar, H. J. W. 2006. Co-variance of dissolved Fe-binding ligands with phytoplankton characteristics in the Canary Basin. *Marine Chemistry*, 102, 276-290.

Gledhill, M., McCormack, P., Ussher, S., Achterberg, E. P., Mantoura, R. F. C. & Worsfold, P. J. 2004. Production of siderophore type chelates by mixed bacterioplankton populations in nutrient enriched seawater incubations. *Marine Chemistry*, 88, 75-83.

Gledhill, M. & Van Den Berg, C. M. G. 1994. Determination of Complexation of Iron(III) with Natural Organic Complexing Ligands in Seawater Using Cathodic Stripping Voltammetry. *Marine Chemistry*, 47, 41-54.

Hassler, C. S. & Schoemann, V. 2009. Bioavailability of organically bound Fe to model phytoplankton of the Southern Ocean. *Biogeosciences*, 6, 2281-2296.

Hassler, C. S., Schoemann, V., Nichols, C. M., Butler, E. C. V. & Boyd, P. W. 2011. Saccharides enhance iron bioavailability to Southern Ocean phytoplankton. *Proceedings of the National Academy of Sciences of the United States of America*, 108, 1076-1081.

Hudson, R. J. M., Covault, D. T. & Morel, F. M. M. 1992. Investigations of Iron Coordination and Redox Reactions in Seawater Using Fe-59 Radiometry and Ion-Pair Solvent-Extraction of Amphiphilic Iron Complexes. *Marine Chemistry*, 38, 209-235.

Hunter, K. A. & Boyd, P. W. 2007. Iron-binding ligands and their role in the ocean biogeochemistry of iron. *Environmental Chemistry*, 4, 221-232.

Hutchins, D. A., Franck, V. M., Brzezinski, M. A. & Bruland, K. W. 1999. Inducing phytoplankton iron limitation in iron-replete coastal waters with a strong chelating ligand. *Limnology and Oceanography*, 44, 1009-1018.

Jickells, T. D., An, Z. S., Andersen, K. K., Baker, A. R., Bergametti, G., Brooks, N., Cao, J. J., Boyd, P. W., Duce, R. A., Hunter, K. A., Kawahata, H., Kubilay, N., Laroche, J., Liss, P. S., Mahowald, N., Prospero, J. M., Ridgwell, A. J., I. T. & Torres, R. 2005. Global iron connections between desert dust, ocean biogeochemistry, and climate. *Science*, 308, 67-71.

Johnson, K. S., Chavez, F. P., Elrod, V. A., Fitzwater, S. E., Pennington, J. T., Buck, K. R. & Walz, P. M. 2001. The annual cycle of iron and the biological response in central California coastal waters. *Geophysical Research Letters*, 28, 1247-1250.

Johnson, K. S., Gordon, R. M. & Coale, K. H. 1997. What controls dissolved iron concentrations in the world ocean? Authors' closing comments. *Marine Chemistry*, 57, 181-186.

Kuma, K., Nishioka, J. & Matsunaga, K. 1996. Controls on iron(III) hydroxide solubility in seawater: The influence of pH and natural organic chelators. *Limnology and Oceanography*, 41, 396-407.

Kupferman, S. L., Becker, G. A., Simmons, W. F., Schauer, U., Marietta, M. G. & Nies, H. 1986. An Intense Cold Core Eddy in the Northeast Atlantic. *Nature*, 319, 474-477.

Laes, A., Blain, S., Laan, P., Ussher, S. J., Achterberg, E. P., Treguer, P. & De Baar, H. J. W. 2007. Sources and transport of dissolved iron and manganese along the continental margin of the Bay of Biscay. *Biogeosciences*, 4, 181-194.

Laglera, L. M. & Van Den Berg, C. M. G. 2009. Evidence for geochemical control of iron by humic substances in seawater. *Limnology and Oceanography*, 54, 610-619.

Landing, W. M., Haraldsson, C. & Paxeus, N. 1986. Vinyl Polymer Agglomerate Based Transition-Metal Cation Chelating Ion-Exchange Resin Containing the 8-Hydroxyquinoline Functional-Group. *Analytical Chemistry*, 58, 3031-3035.

Liu, X. W. & Millero, F. J. 2002. The solubility of iron in seawater. *Marine Chemistry*, 77, 43-54.

Macrellis, H. M., Trick, C. G., Rue, E. L., Smith, G. & Bruland, K. W. 2001. Collection and detection of natural iron-binding ligands from seawater. *Marine Chemistry*, 76, 175-187.

Maldonado, M. T., Allen, A. E., Chong, J. S., Lin, K., Leus, D., Karpenko, N. & Harris, S. L. 2006. Copper-dependent iron transport in coastal and oceanic diatoms. *Limnology and Oceanography*, 51, 1729-1743.

Maldonado, M. T., Boyd, P. W., Laroche, J., Strzepek, R., Waite, A., Bowie, A. R., Croot, P. L., Frew, R. D. & Price, N. M. 2001. Iron uptake and physiological response of phytoplankton during a mesoscale Southern Ocean iron enrichment. *Limnology and Oceanography*, 46, 1802-1808.

Mantoura, R. F. C., Dickson, A. & Riley, J. P. 1978. Complexation of Metals with Humic Materials in Natural-Waters. *Estuarine and Coastal Marine Science*, 6, 387-408.

Martin, J. H., Fitzwater, S. E., Gordon, R. M., Hunter, C. N. & Tanner, S. J. 1993. Iron, Primary Production and Carbon Nitrogen Flux Studies during the Jgofs North-Atlantic Bloom Experiment. *Deep-Sea Research Part II-Topical Studies in Oceanography*, 40, 115-134.

Mawji, E., Gledhill, M., Milton, J. A., Tarran, G. A., Ussher, S., Thompson, A., Wolff, G. A., Worsfold, P. J. & Achterberg, E. P. 2008. Hydroxamate Siderophores: Occurrence and Importance in the Atlantic Ocean. *Environmental Science & Technology*, 42, 8675-8680.

Mawji, E., Gledhill, M., Milton, J. A., Zubkov, M. V., Thompson, A., Wolff, G. A. & Achterberg, E. P. 2011. Production of siderophore type chelates in Atlantic Ocean waters enriched with different carbon and nitrogen sources. *Marine Chemistry*, 124, 90-99.

Measures, C. I., Landing, W. M., Brown, M. T. & Buck, C. S. 2008. High-resolution Al and Fe data from the Atlantic Ocean CLIVAR-CO(2) repeat hydrography A16N transect: Extensive linkages between atmospheric dust and upper ocean geochemistry. *Global Biogeochemical Cycles*, 22.

Moore, C. M., Mills, M. M., Milne, A., Langlois, R., Achterberg, E. P., Lochte, K., Geider, R. J. & La Roche, J. 2006. Iron limits primary productivity during spring bloom development in the central North Atlantic. *Global Change Biology*, 12, 626-634.

Nielsdottir, M. C., Moore, C. M., Sanders, R., Hinz, D. J. & Achterberg, E. P. 2009. Iron limitation of the postbloom phytoplankton communities in the Iceland Basin. *Global Biogeochemical Cycles*, 23, 1-13.

Nolting, R. F., Gerringa, L. J. A., Swagerman, M. J. W., Timmermans, K. R. & De Baar, H. J. W. 1998. Fe (III) speciation in the high nutrient, low chlorophyll Pacific region of the Southern Ocean. *Marine Chemistry*, 62, 335-352.

Obata, H., Karatani, H. & Nakayama, E. 1993. Automated-Determination of Iron in Seawater by Chelating Resin Concentration and Chemiluminescence Detection. *Analytical Chemistry*, 65, 1524-1528.

Powell, R. T. & Donat, J. R. 2001. Organic complexation and speciation of iron in the South and Equatorial Atlantic. *Deep-Sea Research Part II-Topical Studies in Oceanography*, 48, 2877-2893.

Read, J. F. & Pollard, R. T. 2001. A long-lived eddy in the Iceland Basin 1998. *Journal of Geophysical Research-Oceans*, 106, 11411-11421.

Reid, R. T., Live, D. H., Faulkner, D. J. & Butler, A. 1993. A Siderophore from a Marine Bacterium with an Exceptional Ferric Ion Affinity Constant. *Nature*, 366, 455-458.

Rijkenberg, M. J. A., Gerringa, L. J. A., Velzeboer, I., Timmermans, K. R., Buma, A. G. J. & De Baar, H. J. W. 2006. Iron-binding ligands in Dutch estuaries are not affected by UV induced photochemical degradation. *Marine Chemistry*, 100, 11-23.

Rijkenberg, M. J. A., Powell, C. F., Dall'osto, M., Nielsdottir, M. C., Patey, M. D., Hill, P. G., Baker, A. R., Jickells, T. D., Harrison, R. M. & Achterberg, E. P. 2008. Changes in iron speciation following a Saharan dust event in the tropical North Atlantic Ocean. *Marine Chemistry*, 110, 56-67.

Rue, E. L. & Bruland, K. W. 1995. Complexation of Iron(III) by Natural Organic-Ligands in the Central North Pacific as Determined by a New Competitive Ligand

Equilibration Adsorptive Cathodic Stripping Voltammetric Method. *Marine Chemistry*, 50, 117-138.

Rue, E. L. & Bruland, K. W. 1997. The role of organic complexation on ambient iron chemistry in the equatorial Pacific Ocean and the response of a mesoscale iron addition experiment. *Limnology and Oceanography*, 42, 901-910.

Sato, M., Takeda, S. & Furuya, K. 2007. Iron regeneration and organic iron(III)-binding ligand production during in situ zooplankton grazing experiment. *Marine Chemistry*, 106, 471-488.

Shaked, Y., Kustka, A. B. & Morel, F. M. M. 2005. A general kinetic model for iron acquisition by eukaryotic phytoplankton. *Limnology and Oceanography*, 50, 872-882.

Thuroczy, C. E., Gerringa, L. J. A., Klunder, M. B., Laan, P. & Debaar, H. J. W. 2011. Observation of consistent trends in the organic complexation of dissolved iron in the Atlantic sector of the Southern Ocean. *Deep-Sea Research II*.

Thuroczy, C. E., Gerringa, L. J. A., Klunder, M. B., Middag, R., Laan, P., Timmermans, K. R. & De Baar, H. J. W. 2010. Speciation of Fe in the Eastern North Atlantic Ocean. *Deep-Sea Research Part I-Oceanographic Research Papers*, 57, 1444-1453.

Van Den Berg, C. M. G. 1995. Evidence for Organic Complexation of Iron in Seawater. *Marine Chemistry*, 50, 139-157.

Velasquez, I., Nunn, B. L., Ibsanmi, E., Goodlett, D. R., Hunter, K. A. & Sander, S. G. 2011. Detection of hydroxamate siderophores in coastal and Sub-Antarctic water off the South Eastern Coast of New Zealand. *Marine Chemistry*, 126, 97-107.

Vraspir, J. M. & Butler, A. 2009. Chemistry of Marine Ligands and Siderophores. *Annual Review of Marine Science*, 1, 43-63.

Witter, A. E., Hutchins, D. A., Butler, A. & Luther, G. W. 2000. Determination of conditional stability constants and kinetic constants for strong model Fe-binding ligands in seawater. *Marine Chemistry*, 69, 1-17.

Witter, A. E. & Luther, G. W. 1998. Variation in Fe-organic complexation with depth in the Northwestern Atlantic Ocean as determined using a kinetic approach. *Marine Chemistry*, 62, 241-258.

Wu, J. F., Boyle, E., Sunda, W. & Wen, L. S. 2001. Soluble and colloidal iron in the oligotrophic North Atlantic and North Pacific. *Science*, 293, 847-849.

Wu, J. F. & Luther, G. W. 1995. Complexation of Fe(II) by Natural Organic-Ligands in the Northwest Atlantic-Ocean by a Competitive Ligand Equilibration Method and a Kinetic Approach. *Marine Chemistry*, 50, 159-177.

Ye, Y., Volker, C. & Wolf-Gladrow, D. A. 2009. A model of Fe speciation and biogeochemistry at the Tropical Eastern North Atlantic Time-Series Observatory site. *Biogeosciences*, 6, 2041-2061.

Zhu, X. R., Prospero, J. M., Millero, F. J., Savoie, D. L. & Brass, G. W. 1992. The Solubility of Ferric Ion in Marine Mineral Aerosol Solutions at Ambient Relative Humidities. *Marine Chemistry*, 38, 91-107.

CHAPTER 4 - Determination of dissolved hydroxamate siderophores in the high latitude North Atlantic Ocean

4.1 Introduction

Iron (Fe) is an essential element for the biochemical and physiological functioning of terrestrial and oceanic organisms. In an aqueous aerobic environment and at neutral seawater pH, iron is rapidly converted to highly insoluble oxy-hydroxides. In seawater the presence of naturally occurring organic ligands further decreases the concentration of the biologically important labile Fe species (Fe^{3+} concentrations $< 10^{-14}$ M) (Rue & Bruland, 1995; Bruland & Rue, 2001; Hunter & Boyd, 2007) which is lower than the concentrations required for the sustenance of microbial life (Neilands, 1995).

The high latitude North Atlantic is known for its deep winter overturning (>600 m). This process supplies nitrate and Fe from deeper water to the surface layer (Ducklow & Harris, 1993; Holliday & Reid, 2001; Allen *et al.*, 2005), resulting in large phytoplankton bloom (Sanders *et al.*, 2005) during the spring and subsequently significant drawdown of surface water macronutrients. However, in many regions of the open North Atlantic, including the Iceland and Irminger Basins, residual concentrations of nitrate persist into the summer, after the spring bloom has ceased. This phenomenon is due to depleted Fe concentrations which limit the summer biological production and macronutrient drawdown by phytoplankton in this region (Nielsdottir *et al.*, 2009). Thus it has been suggested that the high latitude North Atlantic forms a seasonal high-nutrient, low chlorophyll (HNLC) environment. Hence, competition for Fe between microorganisms is likely to be strong under these conditions. Although it is known that certain pathogenic microorganisms have evolved specialised mechanisms to extract Fe bound to a host-protein, a high proportion of prokaryotic microorganisms produce Fe specific chelators called siderophores to acquire Fe from their environment (Andrews *et al.*, 2003; Butler, 2004; Gledhill *et al.*, 2004; Butler & Martinez, 2007; Mawji *et al.*, 2008a; Velasquez *et al.*, 2011).

Siderophores are low molecular weight organic compounds (300 - 1500 Da) and are selective to Fe(III) (Boukhalfa & Crumbliss, 2002; Dhungana & Crumbliss, 2005). Common features of siderophores are the formation of six coordinate octahedral complexes and the incorporation of hydroxamate, catecholate and α -hydroxy-carboxylic acid chelating groups in different architectures (linear/cyclic) (Boukhalfa & Crumbliss, 2002). These compounds make Fe more available for biological uptake by

bacteria by enhancing its solubility (Trick & Wilhelm, 1995; Crumbliss & Dhungana, 2004).

Marine heterotrophic bacteria and cyanobacteria have been shown to produce siderophores to acquire Fe and take up both their own siderophores as well as those produced by other organisms when Fe limited (Reid *et al.*, 1993; Wilhelm & Trick, 1994; Wilhelm *et al.*, 1996; Martinez *et al.*, 2001; Butler, 2005b). For example, *Vibrio parahaemolyticus* can utilise siderophores produced by *Vibrio cholerae* (Holbein, 1980). Bacteria of the genus *Vibrio* represent an important component of the marine bacterioplankton community. These marine bacteria are known to produce deferrioxamine B (DFOB) and deferrioxamine G (DFOG) to bind Fe(III) and form complexes with trivalent Fe (Martinez *et al.*, 2001; Gledhill *et al.*, 2004). The Fe(III)-siderophore complexes have high stability constants and are not readily photochemically degraded in natural sunlight (Barbeau *et al.*, 2003). For example, the FOB complex has a stability constant of $10^{30.6}$ (Kraemer, 2004) compared to 10^{20} for the Fe(III)-EDTA complex (Martell *et al.*, 1994). Thus, these Fe(III)-siderophore complexes increase solubility and bioavailability of Fe(III) (Hutchins *et al.*, 1999b) to the heterotrophic bacteria in surface waters. However, there has been no evidence that eukaryotic phytoplankton actively produce siderophores (Hopkinson & Morel, 2009; Boyd & Ellwood, 2010). However, it is possible that eukaryotic phytoplankton acquire Fe from siderophores via reduction or photoreduction of Fe(III)-siderophore complexes (Barbeau *et al.*, 2001; Maldonado & Price, 2001; Rose *et al.*, 2005; Shaked *et al.*, 2005; Morel *et al.*, 2008; Hopkinson & Morel, 2009) and that siderophores contribute to synergistic relationships between phytoplankton and bacteria (Shaked *et al.*, 2005).

Although much work on the identification of siderophores has been undertaken in the laboratory (Stintzi *et al.*, 2000; Boukhalfa & Crumbliss, 2002; Dhungana & Crumbliss, 2005), there have been fewer studies on siderophores undertaken in the field (Macrellis *et al.*, 2001; Essen *et al.*, 2006; Mawji *et al.*, 2008a; Velasquez *et al.*, 2011). Many different structures (>100) of siderophores produced by terrestrial microorganisms have been reported, nevertheless, only a few structures of marine siderophores are known. In a field study have reported the presence and concentrations of ferrioxamines (FOE and FOG) produced by marine bacteria throughout the North and South Atlantic Ocean have been reported (40°N – 40°S). Their study showed that some of the siderophores are released into the bulk seawater and making a significant contribution to the natural Fe(III) binding ligands pool, as suggested by Macrellis *et al.* (2001) and Mawji *et al.* (2008a) . The method which was used during their study (Mawji *et al.*, 2008a) has been optimized by using hydroxamate-type siderophores. Therefore, only two different ferrioxamine

siderophore compounds were detected, out of more than 30 marine siderophores characterised to date.

However, it is possible that a proportion of the marine siderophores characterised to date are undetectable using the methods currently available (Mawji *et al.*, 2008a), either because they are too hydrophobic (Butler, 2004), or because their ferric complexes are hydrolysed at low pH (Raymond *et al.*, 1984). Thus, understanding of the overall contribution of siderophores to the organic Fe(III)-binding ligands pool is limited both spatially and temporally, and by the range of analytical techniques available for their analysis.

In this study, the presence of hydroxamate siderophores in the high latitude North Atlantic Ocean water has been investigated in order to extend the understanding of the spatial distribution of these types of siderophores.

4.2 Methodology

Seawater was collected from stations shown in Figure 24 during two separate sampling campaigns on board RRS *Discovery* cruises D350 (April-May 2010) and D354 (July-August 2010) in the high latitude North Atlantic Ocean. Samples were collected from within and just below the chlorophyll *a* maximum layer (Table 9) using a titanium CTD frame fitted with 10 L trace metal clean Teflon coated OTE (Ocean Technology Equipment) bottles. The seawater samples were filtered through 3.0 and 0.2 µm filters using cellulose nitrate membrane filters. The filtration was carried out under gentle vacuum, and the 0.2 µm filters were changed every 2 - 3 L in order to maintain filtration rates.

Dissolved siderophores in seawater were pre-concentrated onto polystyrene-divinylbenzene solid-phase extraction (SPE) cartridges (Isolute ENV+) (Mc Cormack *et al.*, 2003; Gledhill *et al.*, 2004; Mawji *et al.*, 2008a) with a reservoir capacity of 3 mL and 200 mg packing. The solid-phase extraction (SPE) technique has been described in detail in Chapter 2. Quantification of dissolved siderophores was performed by high-performance liquid chromatography-inductively coupled plasma mass spectrometry (LC-ICP-MS) (X series, Thermo Scientific) by monitoring the ⁶⁹Ga isotope (Mawji *et al.*, 2008a). Chromatography conditions were as described in Chapter 2. The gallium (ICP-MS standard, VWR) with final concentration 10 µM, was added to a 200 µL sub-sample and allowed to equilibrate overnight at room temperature before measurement by LC-ICP-MS.

Identification of types of siderophores in natural seawater was carried out by using high-performance liquid chromatography-electrospray ionization mass spectrometry (LC-ESI-MS) (Mc Cormack *et al.*, 2003; Gledhill *et al.*, 2004; Mawji *et al.*, 2008a). Samples and standard solutions were automatically injected (25 µL volume) onto the separation column using an auto sampler (Accela, Thermo Scientific) and the chromatographic conditions were as described in Chapter 2. The mass to charge ratio of each type of siderophores was determined using an ion trap mass spectrometer (LTQ Velos, Thermo Scientific) in positive ion mode. Details of LC-ICP-MS and LC-ESI-MS analyses were described in Chapter 2.

Table 9: The coordinate for each station during RRS *Discovery* D350 and D354 cruise in the high latitude North Atlantic Ocean. Seawater sample at each station was filtrated and dissolved siderophores was extracted by SPE technique.

Date	CTD No.	St.	Lat. (N°)	Long. (W°)	Time	Depth (m)	Extraction volume (L)
01/05/2010	T003	A1	60.56	34.52	1433	25	19
						85	19
02/05/2010	T004	A2	60.02	34.57	1207	27	19
						93	18
03/05/2010	T005	A3	59.59	37.55	1403	27	7.5
						68	16
04/05/2010	T007	A4	59.58	29.10	1530	24	15
05/05/2010	T008	A5	59.54	26.02	1345	30	16
06/05/2010	T009	A6	60.50	21.44	1426	30	17
07/05/2010	T010	A7	61.57	20.01	1251	20	17
08/05/2010	T011	A8	63.05	19.52	1118	23	12
11/07/2010	T002	B1	60.00	19.58	1800	20	18
						30	15
14/07/2010	T006	B2	60.00	23.00	850	20	18
						50	15
16/07/2010	T008	B3	60.02	29.00	740	20	12
						75	15
19/07/2010	T011	B4	60.02	41.00	1400	20	10
						80	18
22/07/2010	T016	B5	63.00	35.00	1100	20	17
						70	19
24/07/2010	T018	B6	63.00	30.00	930	20	18
						60	18
26/07/2010	T019	B7	58.00	35.00	1400	40	19
30/07/2010	T021	B8	63.49	35.04	1300	20	19
31/07/2010	Towfish	B9	63.30	33.23	1230	3	17
02/08/2010	T024	B10	63.25	23.35	1830	20	18
03/08/2010	T026	B11	61.47	24.27	1430	30	19
04/08/2010	Towfish	B12	61.14	24.45	1600	3	18
06/08/2011	Towfish	B13	61.45	24.00	1500	3	20

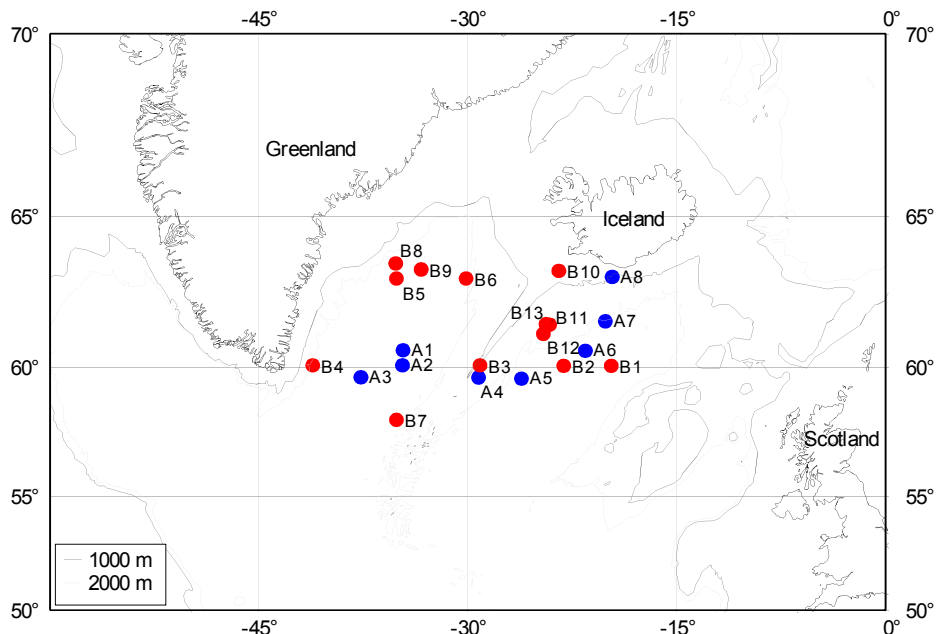


Figure 24: Map of the high latitude North Atlantic Ocean, blue and red filled circle represents the stations during D350 and D354 sampling, respectively, for dissolved siderophores determined during this study.

4.3 Results and discussion

4.3.1 Concentration of dissolved siderophores

The majority of siderophores are hexadentate ligands that complex with trivalent metals in a 1:1 ratio (Kraemer, 2004). This characteristic allows us to detect siderophores using ICP-MS and subsequently calculate the concentration of the siderophores based on an added metal concentration (Ga). By combining ICP-MS detection with LC separation, it is possible to separate the types of siderophores in the samples.

During this study, a large volume of natural seawater sample was used to concentrate dissolved siderophores onto a polystyrene-divinylbenzene solid-phase extraction (SPE) cartridge (Isolute ENV+). Then, dissolved siderophores were eluted from the column with 5 mL mix solvent of 81:14:5:1 (v/v/v/v) acetonitrile/propan-2-ol/water/formic acid (Riedel-de Haen). The large sample volume is necessary due to a low concentration of siderophores in seawater. However, such large volumes can also affect the efficiency of extraction by SPE. A $40\% \pm 6\%$ ($n = 16$) extraction efficiency of 0.5 M FOB was reported by (Mawji *et al.*, 2008a) for approaches identical to those applied in this study. The chemical characteristics and chromatographic behaviour of FOB are similar to the siderophores detected in this study (Mawji *et al.*, 2008a), allowing FOB to be

used as a model ferrioxamine for calculation of siderophore concentrations in seawater throughout this study. Table 8 showed the extraction volume of natural seawater at each station in this study.

An example of a chromatogram for siderophores quantification obtained by LC-ICP-MS analysis in this study is shown in Figure 25. Three siderophore peaks were identified as gallium complexes in the chromatograms of the seawater sample. These siderophores were identified as the hydroxamate siderophores ferrioxamine B (FOB), Ferrioxamine G (FOG) and ferrioxamine E (FOE) by LC-ESI-MS. The first peak was observed at a retention time (RT) \sim 13 minutes, similar to the retention time for FOB peak in a GaFOB standard solution, was identified as FOB. Ferrioxamine G eluted at a RT \sim 14 minutes and finally cyclic ferrioxamine FOE eluted at RT \sim 16 minutes. FOE was retained by the polystyrene divinylbenzene column to a greater extent than the linear ferrioxamines (FOB and FOG) due to its cyclic structure.

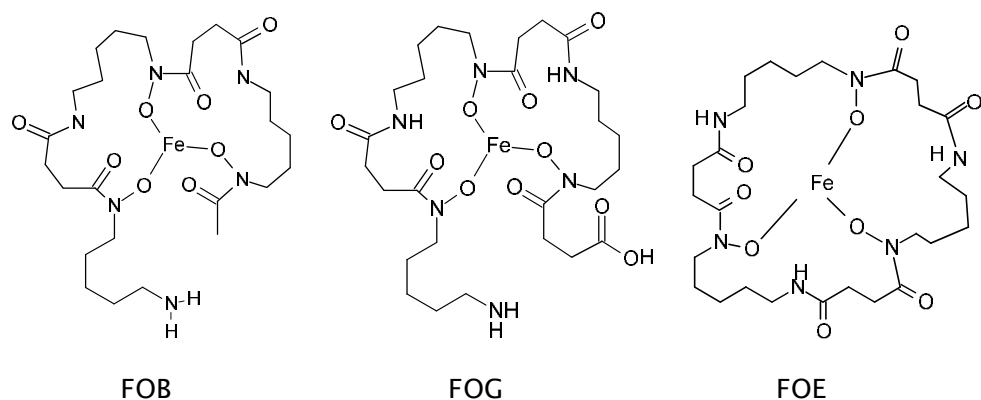


Figure 25: Structure of ferrioxamine B (FOB), ferrioxamine G (FOG) and ferrioxamine E (FOE) determined during this study in the high latitude North Atlantic Ocean.

A clear peak for FOB in the seawater sample can observe in the Fig. 26 at St.B11. Although the peak for each siderophore in the seawater sample at St. B13 is low (Fig. 27), their presence in the sample was confirmed by LC-ESI-MS. In this study, a relative retention time (RRT) was used as suggested by Mawji *et al.* (2011), in order to identify the peaks for each siderophore present in the samples as a result of the different chromatographic conditions, void volumes and pumps used for both analyses. This relative retention time is expressed relative to the retention time of FOB peak in a standard solution and obtained from the equation below:

$$t_r = \frac{(t_i - t_0)}{(t_{GaFOB} - t_0)}$$

Where t_r is the relative retention time of peak i , t_i is the absolute retention time of peak i , t_0 is the void volume of the chromatographic system and t_{GaFOB} is the retention time of GaFOB. The retention time for the GaFOB peak in the GaFOB standard solution was 13.39 minutes within the LC-ICP-MS system. For the GaFOG, GaFOG and GaFOE peaks, the t_r time were 1.0, 1.1 and 1.3, respectively.

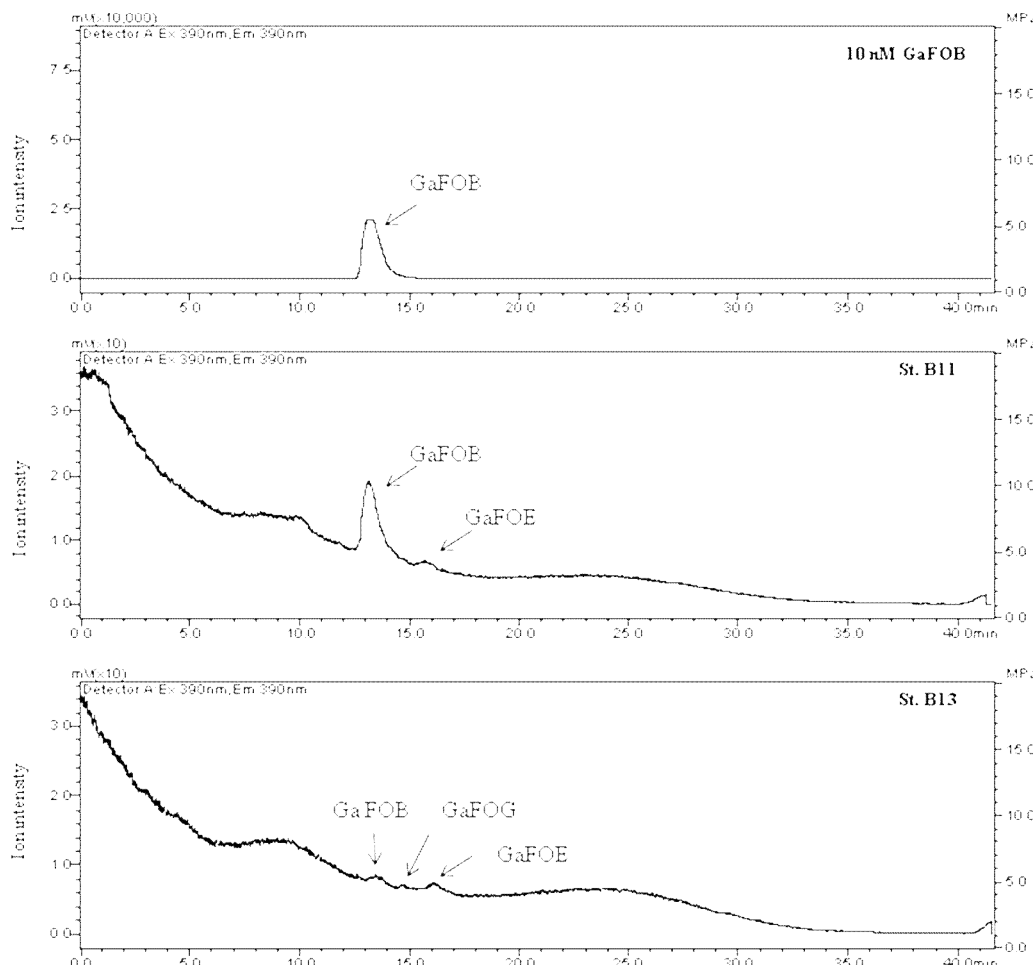


Figure 26: An example of a ^{69}Ga chromatogram from the LC-ICP-MS analysis. This chromatogram shows the peaks for GaFOB, GaFOG and GaFOE in the samples collected at St. 11 and St. 13 during RRS *Discovery* D354 cruise.

The concentration of dissolved siderophores was calculated from instrument sensitivity obtained from a calibration curve constructed by analysis of standards at beginning of each day. Concentrations were corrected for 40% of SPE extraction efficiency (Mawji *et al.*, 2008a). The concentration of dissolved FOB, FOG and FOE determined in the high-latitude North Atlantic Ocean is shown in Table 10. The concentration of dissolved hydroxamate siderophores in the seawater high-latitude North Atlantic Ocean is very low ($\times 10^{-18}$ M). Most of the seawater samples showed the presence of FOB at a concentration range of $0.63\text{--}135.56 \times 10^{-18}$ M (Table 10), with an average 16.65×10^{-18} M

($n=17$). The concentration for FOG and FOE was in the range $0.54\text{-}6.27 \times 10^{-18} \text{ M}$ and $1.24\text{-}2.79 \times 10^{-18} \text{ M}$ (Table 10), respectively.

Table 10: Types of dissolved siderophores present in the seawater of high latitude North Atlantic Ocean during RRS *Discovery* cruise D350 (April-May 2010) and D354 (July/August) cruise. Quantification and identification were carried out by LC-ICP-MS and LC-ESI-MS methods, respectively. Concentration for each siderophore is represented by the values in brackets. *n/a* is below the detection limit of LC-ICP-MS

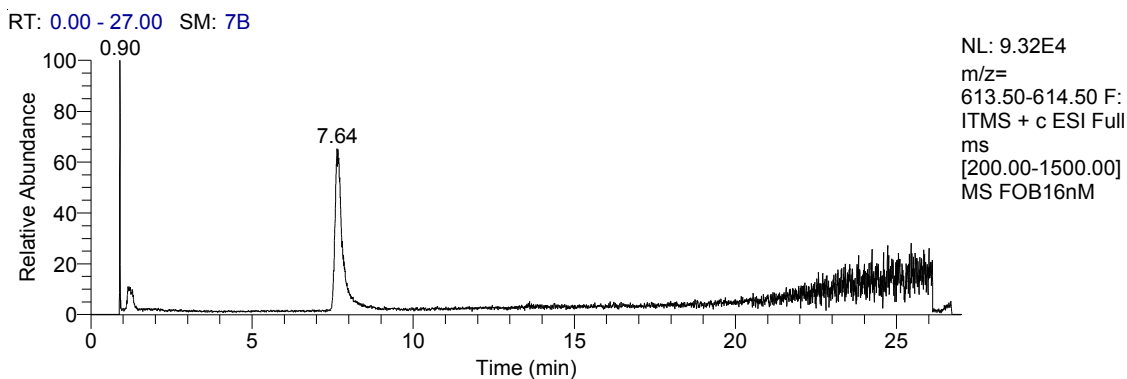
Date	St.	Depth (m)	[dFe] nM	Conc. of dissolved siderophores ($\times 10^{-18} \text{ M}$)		
				[FOB]	[FOG]	[FOE]
01/05/2010	A1	25		✓ (135.56)		
		85		✓ (1.54)		
02/05/2010	A2	27		✓ (1.77)		
		93		✓ (0.63)		
03/05/2010	A3	27				
		68				
04/05/2010	A4	24		✓ (7.79)		
05/05/2010	A5	30		✓ (44.54)		
06/05/2010	A6	30		✓ (13.49)	✓ (<i>n/a</i>)	
07/05/2010	A7	20		✓ (3.26)	✓ (<i>n/a</i>)	
08/05/2010	A8	23		✓ (5.96)	✓ (<i>n/a</i>)	
11/07/2010	B1	20	0.27	✓ (14.10)		
		30	0.20			
14/07/2010	B2	20	0.32			
		50	0.15			
16/07/2010	B3	20	0.11			
		75	0.13			
19/07/2010	B4	20	0.12			
		80	0.21			
22/07/2010	B5	20	0.14			
		70	0.24	✓ (2.44)		
24/07/2010	B6	20	0.05	✓ (1.99)	✓ (<i>n/a</i>)	
		60	0.09	✓ (7.79)	✓ (6.27)	
26/07/2010	B7	40	0.12	✓ (4.17)	✓ (0.90)	
30/07/2010	B8	20	0.08			
31/07/2010	B9	3	0.05	✓ (2.64)	✓ (<i>n/a</i>)	
02/08/2010	B10	20	0.09			
03/08/2010	B11	30	0.10	✓ (33.82)	✓ (<i>n/a</i>)	✓ (1.63)
04/08/2010	B12	3	0.08	✓ (<i>n/a</i>)	✓ (<i>n/a</i>)	✓ (1.24)
06/08/2011	B13	3	0.07	✓ (1.58)	✓ (0.54)	✓ (2.79)

4.3.2 Identification of dissolved siderophores

The combination of on-line application of LC with ESI-MS forms a powerful tool for identification of siderophores as it provides simultaneous information about chemical properties like hydrophobicity, molecular mass and structure (Feistner *et al.*, 1993; Kaltashov *et al.*, 1997; Gledhill, 2001). The retention time for the FOB standard peak

was 7.64 minutes (Fig. 27) by using the LC-ESI-MS method applied in this study. Selective ion monitoring (SIM) allowed for the detection of very low concentrations of known individual siderophores. FOB, FOG and FOE produced singly charged protonated ions ($[M+H]^+$) m/z 614 at 7.53 minutes, m/z 672 at 8.11 minutes and m/z 654 at 9.86 minutes, respectively (Fig. 28 and Fig. 29). Their identity was confirmed by comparing their fragmentation patterns with previously reported (Gledhill, 2001; Mawji *et al.*, 2008b) fragmentation patterns.

a)



b)

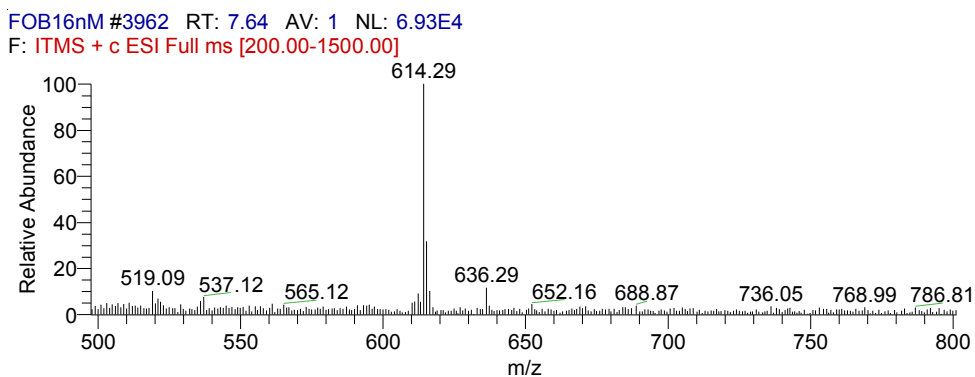
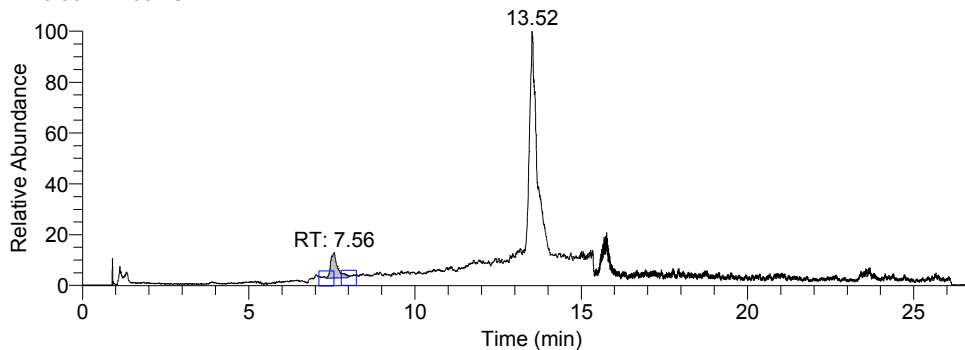


Figure 27: a) Chromatogram and b) mass spectra for a FOB standard solution (16 nM concentration) which obtained by using the LC-ESI-MS method analysis. The retention time for FOB peak was at 7.64 minutes.

a) FOB (m/z 614)

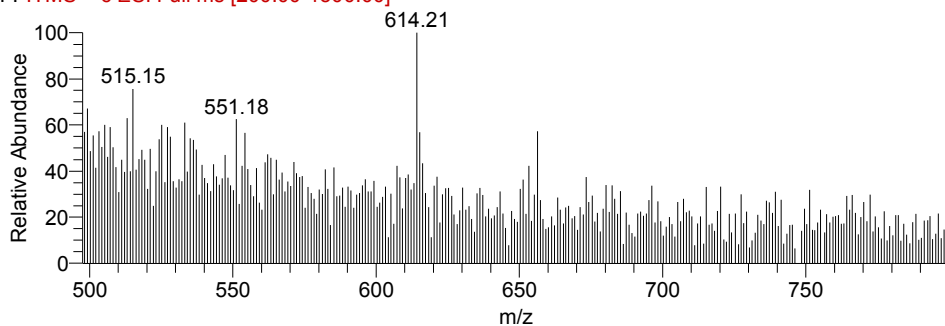
RT: 0.00 - 27.00 SM: 7B



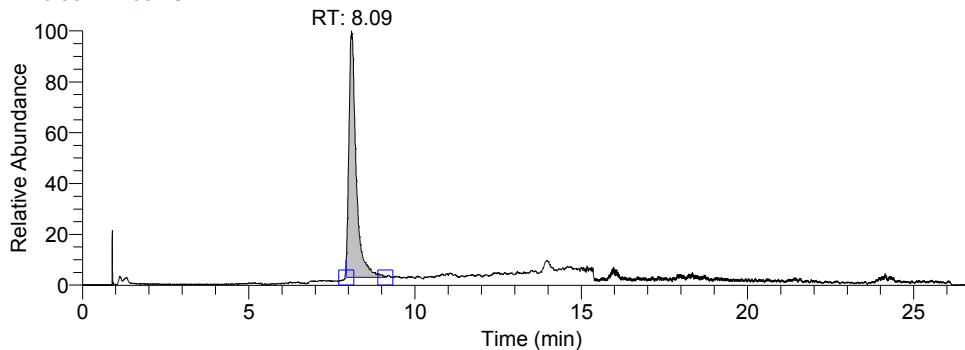
NL:
1.22E6
Base Peak m/z =
614.00-615.00+
636.00-637.00
MS D354sample
68

D354sample 68 #3475 RT: 7.56 AV: 1 NL: 1.52E5

F: ITMS + c ESI Full ms [200.00-1500.00]

b) FOG (m/z 672)

RT: 0.00 - 27.00 SM: 7B



NL:
1.95E6
Base Peak m/z =
672.00-673.00+
694.00-695.00
MS D354sample
68

D354sample 68 #3555 RT: 8.13 AV: 1 NL: 1.68E6

F: ITMS + c ESI Full ms [200.00-1500.00]

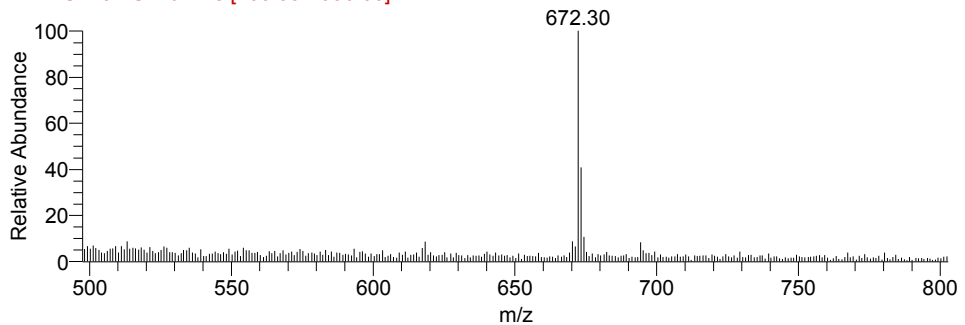


Figure 28: Full chromatogram and mass spectra for a Fe(III) complexed siderophores type compound for a) FOB, m/z 614 and b) FOG, m/z 672. The chromatogram spectra were obtained from the seawater sample collected from Station B11 during RRS *Discovery* 354 (D354).

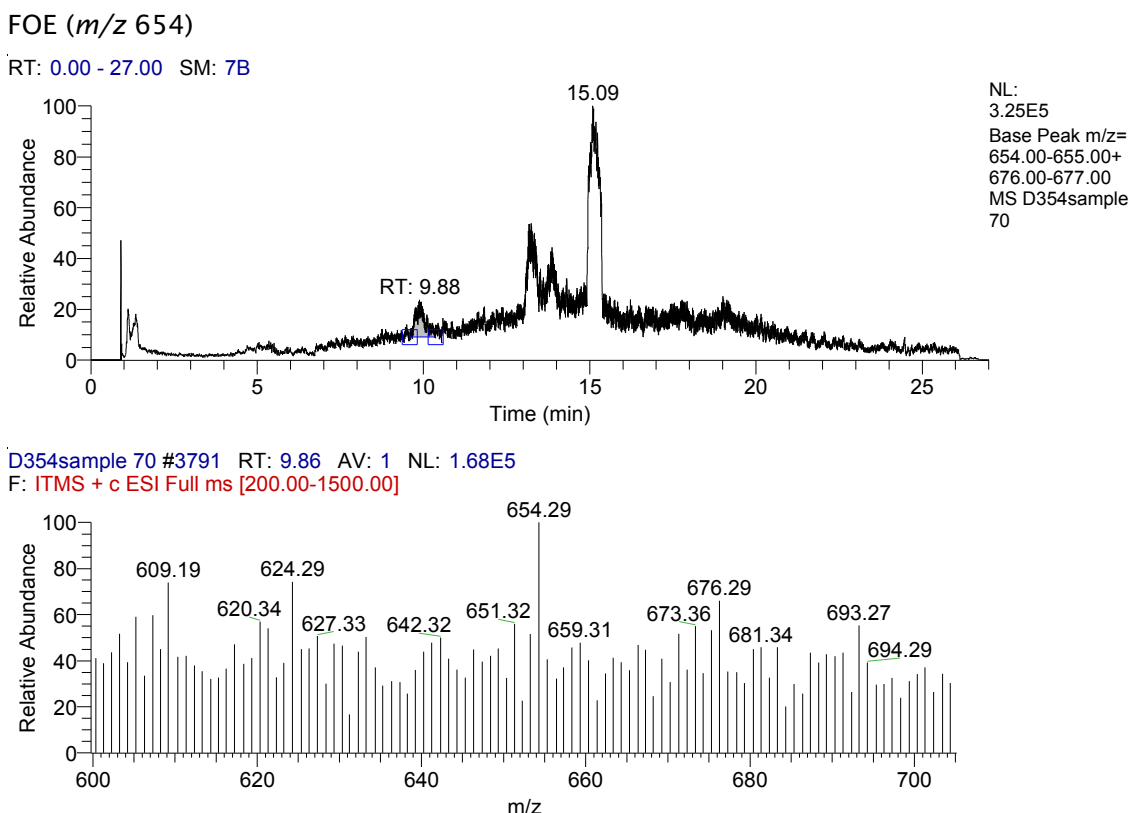
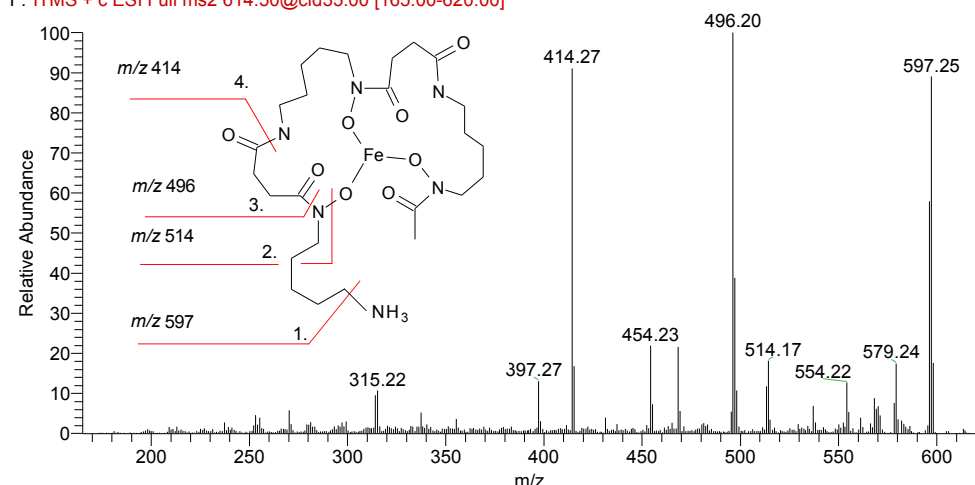


Figure 29: Full chromatogram and mass spectra for a FOE, m/z 654. The chromatograms were obtained from the seawater sample collected from Station B13 during RRS *Discover* 354 (D354). In the FOE mass spectra, the sodium adduct $[M+Na]^+$ (m/z 676) was also observed.

As observed previously, the fragmentation for FOB and FOG showed similar trends (Fig. 30) through loss of the terminal amine group (NH_3) to produce a product ion of m/z 597 for FOB (Gledhill, 2001; Groenewold *et al.*, 2004b) and 655 for FOG (Mawji *et al.*, 2008b), respectively. Further losses produced an ion of m/z 496 (FOB) and m/z 554 (FOG). Then followed rupturing of the 11-12 amide bond to produce ions at m/z 414 (FOB) and 472 (FOG). Generally, the characteristic dissociation pathways observed for linear ferrioxamines involved a loss of NH_3 and the cleavage of the 7-8 hydroxamate bonds, which produced the most abundant fragment in the spectra of both FOB and FOG. A clear neutral loss pattern is observed of m/z 17, 100, 118 and 200.

a) Ferrioxamine B (m/z 614)

D354 Sample 68_MS2 #3645 RT: 7.59 AV: 1 NL: 1.58E4
F: ITMS + c ESI Full ms2 614.50@cid35.00 [165.00-620.00]

b) Ferrioxamine G (m/z 672)

D354 Sample 68_MS2 #3820 RT: 8.15 AV: 1 NL: 5.28E5
F: ITMS + c ESI Full ms2 672.30@cid35.00 [185.00-680.00]

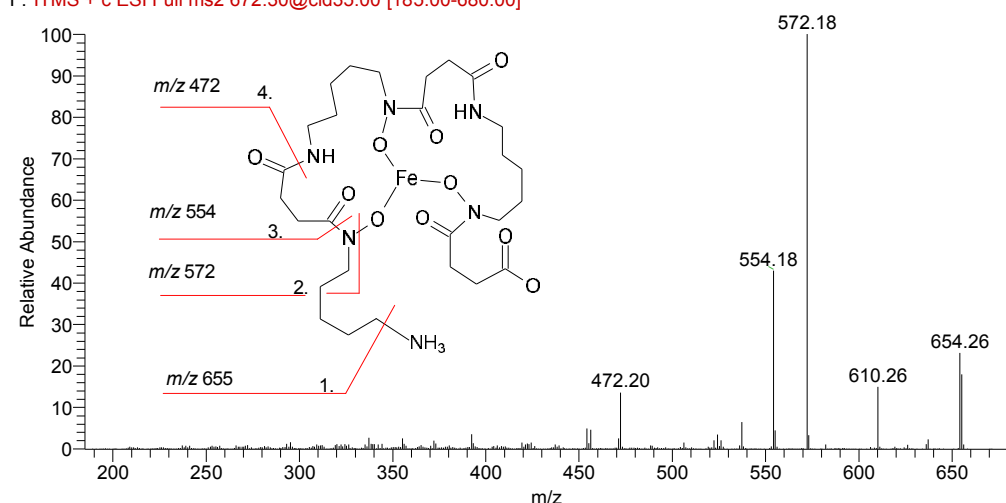


Figure 30: Structures and MS^2 spectra of a) FOB and b) FOG from Station A9 during *RRS Discovery 350* (D350) in the high latitude North Atlantic Ocean. Structure of FOB and FOG are showing the main cleavages (red line) accounting from fragments ion observed.

Incorrect programming of the ESI-MS meant that FOE was not detected by SIM or MS^2 in these seawater samples. Consequently in this study, FOE in the seawater samples is identified by extracting mass chromatograms from the total ion chromatograms for both protonated and sodium adducts ($[M+H]^+$ peak m/z 654, $[M+Na]^+$ m/z 676) (Fig. 31). The sodium adduct of siderophore complexes is commonly observed during the determination of siderophores isolated from the natural environment by ESI-MS in the positive mode. LC-ESI-MS analysis showed that FOB, FOG and FOE had a similar distribution pattern to the hydroxamate siderophores determined by LC-ICP-MS analysis (Table 10). In this study, analysis of ferrioxamine siderophores using LC-ESI-

MS with selective ion monitoring allowed FOB and FOG to be detected in more samples than analysis by LC-ICP-MS indicating that under these conditions, LC-ESI-MS was the more sensitive technique.

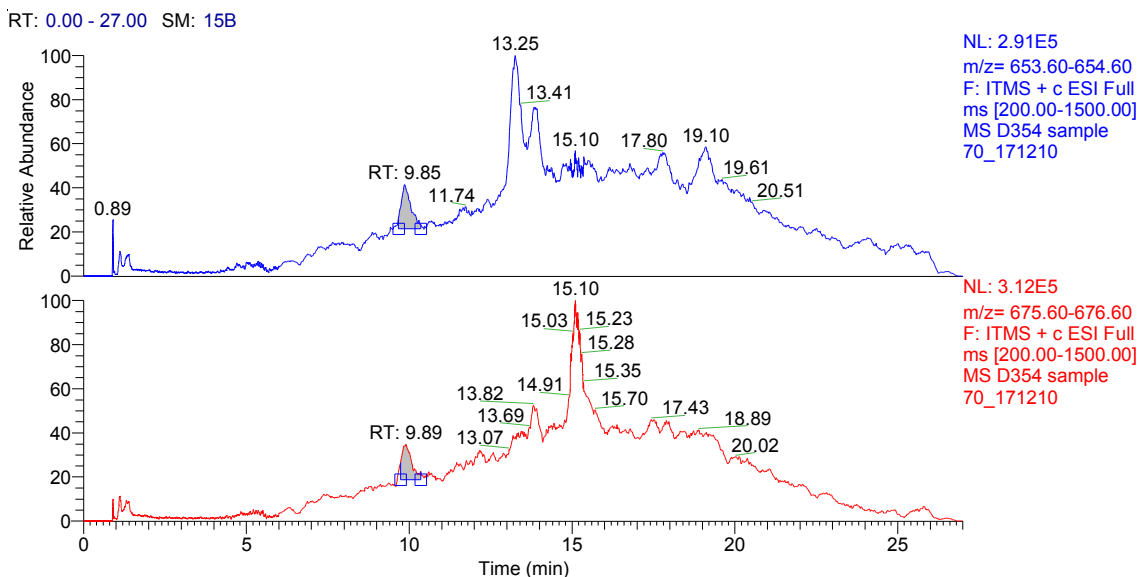


Figure 31: Determination of FOE complex by corresponding the retention time for the sodium adducts and FOE peaks. The blue and red chromatogram represents the extracted full mass chromatogram of FOE (m/z 653.6-654.6) and sodium adduct (m/z 675.6-676.6), respectively, in the seawater sample from St. B13, showing a peak at a similar retention time~9.8 minutes. The peak at this retention time is identified as FOE (m/z 654) which showed in mass spectra in Figure 29.

4.3.3 Distribution of dissolved hydroxamate siderophores in the high latitude North Atlantic Ocean

The stations sampled during the D350 and D354 cruises were labelled as A1-A8 and B1-B13, respectively (Table 9, Fig. 24). Most of the stations were located in the Iceland Basin and the Irminger Basin.

Generally, FOB was found to be widespread in early May 2010. In the Irminger Basin, the highest concentration of dissolved FOB was in the surface waters (~30 m depth) 135.56×10^{-18} M at St. A1 (Table 10, Fig. 24). Below the chlorophyll *a* maximum layer, its concentration was 1.54×10^{-18} M at St. A1 and 0.63×10^{-18} M at St. A2 (Table 10). Dissolved FOB was also detected in the chlorophyll *a* maximum layer (~30 m depth) in the Iceland Basin (St. A4, A5, A6, A7, A8) (Fig. 24) during May 2010. Its dissolved concentration was between $3.26-44.54 \times 10^{-18}$ M (Table 9). Dissolved FOG was also detected at St. A6, A7 and A8 with LC-ESI-MS analysis, but its concentration was below the detection limit of LC-ICP-MS analysis.

During the July-August sampling campaign FOB and FOG were again detected in the Iceland Basin at St. B11, B12 and B13 (Table 10). The concentration of dissolved FOB in the chlorophyll *a* maximum layer was less compared to that observed in May 2010 in the region. Dissolved FOB concentrations were between $1.58\text{--}33.82 \times 10^{-18}$ M during early August 2010 (Table 10), while dissolved FOG was 0.54×10^{-18} M at St. B13 (Table 10). Ferrioxamine E (FOE) was also detected in the Iceland Basin with concentration between $1.24\text{--}2.79 \times 10^{-18}$ M in the chlorophyll *a* maximum layer (Table 10). According to Page & Huyer (1984) and Sevinc & Page (1992), several microbes produce more than one siderophore, and in many cases the siderophores may be produced by different bacteria. A more powerful chelator with high stability constant with Fe (FOE; $\log K' = 10^{32.5}$) (Crumbiss, 1991), may only be produced when the first less powerful chelator (FOB; $\log K' = 10^{30.6}$) (Kraemer, 2004), fails to provide enough Fe to the cell due to very low Fe condition at these stations (<0.1 nM) (Table 10). This type of siderophores production has been observed in *Azotobacter vinelandii* (Page & Huyer, 1984; Sevinc & Page, 1992).

The linear ferrioxamines siderophores (FOB and FOG) were also observed in the Irminger Basin. The concentration of dissolved FOB and FOG was between $1.99\text{--}7.79 \times 10^{-18}$ M and $0.90\text{--}6.27 \times 10^{-18}$ M (Table 10), respectively. The high concentration of dissolved FOB and FOG were determined below the chlorophyll *a* maximum layer (60 m depth) at St. B6.

The concentrations observed in this study in the high latitude North Atlantic were much lower than those reported previously for dissolved ferrioxamine siderophore concentrations at lower latitudes in the Atlantic Ocean (Mawji *et al.*, 2008a). Mawji *et al.* (2008a) found that dissolved FOG was most abundant and ubiquitous with concentrations between $2.6\text{--}11.6 \times 10^{-12}$ M, while concentration of FOE in this region ranged from undetectable to 10.2×10^{-12} M which is 5-6 orders of magnitude higher than its concentrations in the high-latitude North Atlantic Ocean. The highest concentration for dissolved FOG and FOE was observed by Mawji and co-workers in the northern temperate ($>35^\circ\text{N}$) region, with concentrations between 5.7-9.2 pM and 3.1-10.2 pM (Mawji *et al.*, 2008a), respectively.

Although the concentrations of siderophores in natural seawater in the high latitude North Atlantic Ocean were very low (subfemtomolar level), siderophores were nevertheless detected in these regions and thus will be of biological significance for uptake for certain bacteria. The detected siderophores are present in the dissolved phase and will thus form a very minor portion of the natural Fe(III) binding ligands, which are likely to be present at concentrations of between 0.4-0.5 nM in the surface

waters (see Chapter 3). Clearly, as the hydroxamates detected in this study do not contribute to the overall ligands pool in a major way, the organic ligands in the high latitude North Atlantic could be made up of other organics such as exudates (Saito & Moffett, 2001) and perhaps humic materials (Laglera & Van Den Berg, 2009). If so, less than 0.1 % of identified ferrioxamines contributed to the dFe concentration (0.2 μm fraction) in the high-latitude North Atlantic Ocean. In contrast, Mawji *et al.* (2008a) showed that 0.2-4.6 % of dFe was likely to be complexed by the identified ferrioxamines at lower latitudes in the Atlantic Ocean, despite the higher concentration of dFe (0.11-0.41 nM). However, this percentage is based on 0.2 μm fraction of dFe, which is not truly soluble Fe fraction (0.02 μm) (Bergquist *et al.*, 2007). Hydroxamate siderophores and the Fe complexed to them is likely present in the truly dissolved phase.

4.3.4 Production of dissolved hydroxamate siderophores

Desferrioxamines B, E, and G are known to be produced by gram-negative bacteria such as *Vibrio* species (Martinez *et al.*, 2001) and by gram-positive *Actinomycetes* species (Mucha *et al.*, 1999; Ghanem *et al.*, 2000). During this study, the distribution of specific bacteria species has not been determined.

Previous studies (Trick, 1989; Wilhelm & Trick, 1994; Lewis *et al.*, 1995; Neilands, 1995; Jung & Drechsel, 1998; Cabaj & Kosakowska, 2009) have suggested that the production of siderophores was stimulated by low concentrations of dFe. The measurement of surface (<150 m depth) dFe concentration (0.2 μm fraction) (Steigeneuriger *et al.*, unpublished data) in this region has shown the concentration was between 0.11-0.32 nM in the Iceland Basin (St. B1, B2 and B3) and 0.12-0.24 nM in the Irminger Basin (St. B4 and B5) in early July 2010 (Fig. 24, Table 10). However, due to the formation of the spring bloom (Ducklow & Harris, 1993) with a rapid increase in the chlorophyll biomass (Siegel *et al.*, 2002; Sanders *et al.*, 2005) in these regions, the dFe concentration decreased to 0.07-0.10 nM in the Iceland Basin (St. B11, B12 and B13) and 0.05-0.10 nM in the Irminger Basin (St. B6, B7, B8 and B9), by the end of July to August 2010 (Table 10).

As a response to the Fe limited condition, it is possible that heterotrophic bacteria will actively produce siderophores (Vala *et al.*, 2006) to sequester Fe from the various Fe pools (Winkelmann, 1992) due to high Fe requirements for growth compared to the phytoplankton in open-ocean (Tortell *et al.*, 1996; Tortell *et al.*, 1999). Due to diffusion of siderophores away from the organisms that produced them (Hutchins *et al.*, 1991; Morel *et al.*, 1991), researchers have argued that organisms do not use siderophores as a means of keeping their competitors from acquiring Fe, but rather use them as a

means to acquire Fe from refractory sources. Thus, this study suggests that bacteria in the high latitude North Atlantic Ocean may be Fe deficient, as is the case for phytoplankton (Nielsdottir *et al.*, 2009). Kirchman *et al.* (2000) has suggested that in the regions where phytoplankton are clearly Fe limited, heterotrophic bacteria growth is also likely faced with Fe limitation.

In the Iceland Basin, siderophores were present in the surface layer at the end of July to August 2010, when the dissolved concentration of Fe was <0.1 nM at St. B11, B12 and B13 (Table 9). However, siderophores were not detected in early July 2010 in the Iceland Basin (St. B2 and B3), when the dissolved concentrations was more than 0.1 nM, with the exception of St. B1. This indicated that Fe concentration could influence the production of siderophores in these waters. Iron concentrations between 0 to 1 μ M have been found to induce the siderophore production by nearly all microorganisms (Neilands, 1995). In addition, Cabaj & Kosakowska (2009) found the highest concentration of FOB was produced by *Micrococcus luteus* and *Bacillus silvestris* at a concentration of 0.04 μ M Fe in Fe-deficient low nutrient artificial sea water based liquid medium (IDSM). However, these levels of Fe concentration (μ M level) are higher than the concentrations of Fe observed in the Iceland Basin. Thus, the influence of Fe concentrations on siderophores production in the marine environment is still unclear.

An alternative hypothesis is that the production of siderophores is not just affected by Fe concentrations. Siderophores have been found in podzolic soils (Essen *et al.*, 2006), which are generally not considered a low Fe environment. Siderophore production may be affected by other factors such as organic carbon concentrations. In podzolic soils the highest concentration of siderophores (ferricrocin) was determined in the upper soils containing a high level of dissolved organic carbon (DOC). Furthermore it has been observed that a concentration of 0.05-0.30 M carbon produces maximum concentration of siderophores (Bendale *et al.*, 2009). Bacteria may require more DOC at low Fe concentrations due to the effect of Fe on DOC catabolism. Thus, Fe and DOC may interact and co-limit the heterotrophic bacteria production (Kirchman, 1996; Tortell *et al.*, 1999; Kirchman *et al.*, 2000). In previous experiments the highest stimulation of bacterial production was observed when both Fe and DOC were added (Maldonado *et al.*, 2006). In other studies, the addition of organic carbon but not Fe, stimulated bacterial growth rates in the Antarctic Polar Front (Church *et al.*, 2000), subArctic Pacific (Kirchman, 1990) and equatorial Pacific (Kirchman & Rich, 1997). In addition, the highest concentration and diversity of siderophore type chelates were also found in glucose amended seawater (Mawji *et al.*, 2011). This could suggest that the production of siderophores and Fe uptake by heterotrophic bacteria is likely limited, like bacteria growth, by the supply of organic carbon in the surface ocean.

The low temperature of surface seawater in the high latitude in the North Atlantic Ocean (9.1-10.4°C) may also play a vital role in the bacteria growth and siderophores production. In fact, the influence of temperature on siderophores production has been previously observed for several bacteria (Garibaldi, 1972; Worsham & Konisky, 1984). The highest hydroxamate siderophore production by *Vibrio salmonicida* was found at temperatures of 6°C under Fe limited conditions. However, the optimum growth rate for this species was reported to be 12°C and at this temperature a very low siderophores production was found (Colquhoun & Sorum, 2001). In addition to the temperature (Thompson *et al.*, 2004; Schets *et al.*, 2010; Vezzulli *et al.*, 2010), salinity, phytoplankton and nutrients may also influence the abundance of siderophores producing bacteria as suggested by Martinez-Urtaza *et al.* (2008) and Turner *et al.* (2009). Nevertheless, investigations on the distribution of species such as *Vibrio* sp., known to produce hydroxamate siderophores, in cold water temperature (8°C) are rare and to the best of my knowledge, there was no available data on abundance of this species in the high latitude North Atlantic Ocean, yet. That is due to fact that at low temperature (<10°C), *Vibrio* bacteria enter a viable but non-culturable state (Ravel *et al.*, 1995; Oliver, 2005). Thus, it is possible the cold temperatures (9-12°C) in this region would reduce the growth of potential siderophores producing bacteria and thereby reduce hydroxamate siderophore production.

4.4 Conclusion

This first study on the determination of dissolved siderophores in the high latitude North Atlantic Ocean has confirmed the presence of dissolved hydroxamate-type siderophores (ferrioxamine B, ferrioxamine G and ferrioxamine E) in natural seawater of that region.

The linear ferrioxamines FOB and FOG were detected on cruises in April-May 2010 and late July to August 2010 in these regions, but their total concentrations were lower (0 - 135.56 x10⁻¹⁸ M). In contrast, we did not observe dissolved ferrioxamines in early July 2010. Less than 0.1% dFe (0.2 µm fraction) in this region could be complexed by these siderophores, thus they are unlikely to influence the general bioavailability of Fe in the chlorophyll *a* maximum layer in this region. The low concentration of dissolved siderophores detected in the high latitude of the Atlantic Ocean suggests that siderophore distributions are both spatially and temporally variable.

The report of formation of Fe limited conditions in this region (Iceland Basin) might influence the production of siderophores by heterotrophic bacteria and release of siderophores into the bulk dissolved phase forming portion of the natural Fe(III) binding ligands pool. However, previous observations of dissolved siderophores at

lower latitudes in the Atlantic Ocean (Mawji *et al.*, 2008a) resulted in concentrations considerably higher than the concentrations observed in the high latitude North Atlantic, despite higher Fe concentrations observed at lower latitudes. Moreover, siderophores are also found in podzolic soils (Essen *et al.*, 2006), that are not generally considered to be Fe stressed. Thus, the production of siderophores might not only be affected by Fe concentrations. The source of carbon might be a potential factor influencing siderophore production due to the importance of organic carbon to the growth of heterotrophic bacteria, which produced siderophores. On the other hand, the low seawater temperatures in this study region may also play a role in decreasing a growth of heterotrophic bacteria and thereby siderophores production.

Only three siderophores were detected in this study and they were all soluble hydroxamate siderophores, possibly amongst the most stable and soluble of the potential marine siderophores. Considering the amphiphilic character of many marine siderophores it is possible that siderophores are associated with the particulate phase. Thus, determination of siderophores in the particulate phase is needed in order to obtain more information about the abundance of siderophores in the seawater, and it is still missing in the present study. Due to the selective method for this study, it is possible that siderophores with other functional groups (e.g., catecholate or carboxylate functional groups) could not be detected. In fact, more information on the presence and distribution on other types of siderophores, coupled with other parameter like Fe speciation would help us to understand the Fe biogeochemical cycle in the ocean.

References

Allen, J. T., Brown, L., Sanders, R., Moore, C. M., Mustard, A., Fielding, S., Lucas, M., Rixen, M., Savidge, G., Henson, S. & Mayor, D. (2005) Diatom carbon export enhanced by silicate upwelling in the northeast Atlantic. *Nature*, 437, 728-732.

Andrews, S. C., Robinson, A. K. & Rodriguez-Quinones, F. (2003) Bacterial iron homeostasis. *Fems Microbiology Reviews*, 27, 215-237.

Barbeau, K., Rue, E. L., Bruland, K. W. & Butler, A. (2001) Photochemical cycling of iron in the surface ocean mediated by microbial iron(III)-binding ligands. *Nature*, 413, 409-413.

Barbeau, K., Rue, E. L., Trick, C. G., Bruland, K. T. & Butler, A. (2003) Photochemical reactivity of siderophores produced by marine heterotrophic bacteria and cyanobacteria based on characteristic Fe(III) binding groups. *Limnology and Oceanography*, 48, 1069-1078.

Bendale, M. S., Chaudhari, B. L. & Chincholkar, S. B. (2009) Influence of Environmental Factors on siderophore production by *Streptomyces fulvissimus* ATCC 27431. *Current Trends in Biotechnology and Pharmacy*, 3 (4), 362 - 371.

Bergquist, B. A., Wu, J. & Boyle, E. A. (2007) Variability in oceanic dissolved iron is dominated by the colloidal fraction. *Geochimica Et Cosmochimica Acta*, 71, 2960-2974.

Boukhalfa, H. & Crumbliss, A. L. (2002) Chemical aspects of siderophore mediated iron transport. *Biometals*, 15, 325-339.

Boyd, P. W. & Ellwood, M. J. (2010) The biogeochemical cycle of iron in the ocean. *Nature Geoscience*, 3, 675-682.

Bruland, K. & Rue, E. (2001) Domoic acid binds iron and copper: a possible role for the toxin produced by the marine diatom *Pseudo-nitzschia*. *Marine Chemistry*, 76, 127-134.

Butler, A. (2004) Amphiphilic and alpha-hydroxy acid-containing siderophores from marine bacteria. *Abstracts of Papers of the American Chemical Society*, 227, U1106-U1106.

Butler, A. (2005) Marine siderophores and microbial iron mobilization. *Biometals*, 18, 369-374.

Butler, A. & Martinez, J. S. (2007) Marine amphiphilic siderophores: Marinobactin structure, uptake, and microbial partitioning. *Journal of Inorganic Biochemistry*, 101, 1692-1698.

Cabaj, A. & Kosakowska, A. (2009) Iron-dependent growth of and siderophore production by two heterotrophic bacteria isolated from brackish water of the southern Baltic Sea. *Microbiological Research*, 164, 570-577.

Church, M. J., Hutchins, D. A. & Ducklow, H. W. (2000) Limitation of bacterial growth by dissolved organic matter and iron in the Southern Ocean. *Applied and Environmental Microbiology*, 66, 455-466.

Colquhoun, D. J. & Sorum, H. (2001) Temperature dependent siderophore production in *Vibrio salmonicida*. *Microbial Pathogenesis*, 31, 213-219.

Crumbliss, A. L. (1991) Handbook of microbial iron chelate. 2nd Edition G. Winkelmann CRC. Press. New York.

Crumbliss, A. L. & Dhungana, S. (2004) Iron redox processes in siderophore mediated iron transport. *Abstracts of Papers of the American Chemical Society*, 227, U1204-U1204.

Dhungana, S. & Crumbliss, A. L. (2005) Coordination chemistry and redox processes in siderophore-mediated iron transport. *Geomicrobiology Journal*, 22, 87-98.

Ducklow, H. W. & Harris, R. P. (1993) Introduction to the Jgofs North-Atlantic Bloom Experiment. *Deep-Sea Research Part II-Topical Studies in Oceanography*, 40, 1-8.

Essen, S. A., Bylund, D., Holmstrom, S. J. M., Moberg, M. & Lundstrom, U. S. (2006) Quantification of hydroxamate siderophores in soil solutions of podzolic soil profiles in Sweden. *Biometals*, 19, 269-282.

Feistner, G. J., Stahl, D. C. & Gabrik, A. H. (1993) Proferrioxamine Siderophores of *Erwinia-Amylovora* - a Capillary Liquid-Chromatographic Electrospray Tandem Mass-Spectrometric Study. *Organic Mass Spectrometry*, 28, 163-175.

Garibald.Ja (1972) Influence of Temperature on Biosynthesis of Iron Transport Compounds by *Salmonella-Typhimurium*. *Journal of Bacteriology*, 110, 262-&.

Ghanem, N. B., Sabry, S. A., El-Sherif, Z. M. & Abu El-Ela, G. A. (2000) Isolation and enumeration of marine actinomycetes from seawater and sediments in Alexandria. *Journal of General and Applied Microbiology*, 46, 105-111.

Gledhill, M. (2001) Electrospray ionisation-mass spectrometry of hydroxamate siderophores. *Analyst*, 126, 1359-1362.

Gledhill, M., Mccormack, P., Ussher, S., Achterberg, E. P., Mantoura, R. F. C. & Worsfold, P. J. (2004) Production of siderophore type chelates by mixed bacterioplankton populations in nutrient enriched seawater incubations. *Marine Chemistry*, 88, 75-83.

Groenewold, G. S., Van Stipdonk, M. J., Gresham, G. L., Chien, W., Bulleigh, K. & Howard, A. (2004) Collision-induced dissociation tandem mass spectrometry of desferrioxamine siderophore complexes from electrospray ionization of UO22+, Fe3+ and Ca2+ solutions. *Journal of Mass Spectrometry*, 39, 752-761.

Holbein, B. E. (1980) Iron-Controlled Infection with *Neisseria-Meningitidis* in Mice. *Infection and Immunity*, 29, 886-891.

Holliday, N. P. & Reid, P. C. (2001) Is there a connection between high transport of water through the Rockall Trough and ecological changes in the North Sea? *Ices Journal of Marine Science*, 58, 270-274.

Hopkinson, B. M. & Morel, F. M. M. (2009) The role of siderophores in iron acquisition by photosynthetic marine microorganisms. *Biometals*, 22, 659-669.

Hunter, K. A. & Boyd, P. W. (2007) Iron-binding ligands and their role in the ocean biogeochemistry of iron. *Environmental Chemistry*, 4, 221-232.

Hutchins, D. A., Rueter, J. G. & Fish, W. (1991) Siderophore Production and Nitrogen-Fixation Are Mutually Exclusive Strategies in *Anabaena* 7120. *Limnology and Oceanography*, 36, 1-12.

Hutchins, D. A., Witter, A. E., Butler, A. & Luther, G. W. (1999) Competition among marine phytoplankton for different chelated iron species. *Nature*, 400, 858-861.

Jung, G. & Drechsel, H. (1998) Peptide siderophores. *Journal of Peptide Science*, 4, 147-181.

Kaltashov, I. A., Cotter, R. J., Feinstone, W. H., Ketner, G. W. & Woods, A. S. (1997) Ferrichrome: Surprising stability of a cyclic peptide Fe-III complex revealed by mass spectrometry. *Journal of the American Society for Mass Spectrometry*, 8, 1070-1077.

Kirchman, D. L. (1990) Limitation of Bacterial-Growth by Dissolved Organic-Matter in the Sub-Arctic Pacific. *Marine Ecology-Progress Series*, 62, 47-54.

Kirchman, D. L. (1996) Oceanography - Microbial ferrous wheel. *Nature*, 383, 303-304.

Kirchman, D. L., Meon, B., Cottrell, M. T., Hutchins, D. A., Weeks, D. & Bruland, K. W. (2000) Carbon versus iron limitation of bacterial growth in the California upwelling regime. *Limnology and Oceanography*, 45, 1681-1688.

Kirchman, D. L. & Rich, J. H. (1997) Regulation of bacterial growth rates by dissolved organic carbon and temperature in the equatorial Pacific Ocean. *Microbial Ecology*, 33, 11-20.

Kraemer, S. M. (2004) Iron oxide dissolution and solubility in the presence of siderophores. *Aquatic Sciences*, 66, 3-18.

Laglera, L. M. & Van Den Berg, C. M. G. (2009) Evidence for geochemical control of iron by humic substances in seawater. *Limnology and Oceanography*, 54, 610-619.

Lewis, B. L., Holt, P. D., Taylor, S. W., Wilhelm, S. W., Trick, C. G., Butler, A. & Luther, G. W. (1995) Voltammetric Estimation of Iron(III) Thermodynamic Stability-Constants for Catecholate Siderophores Isolated from Marine-Bacteria and Cyanobacteria. *Marine Chemistry*, 50, 179-188.

Macrellis, H. M., Trick, C. G., Rue, E. L., Smith, G. & Bruland, K. W. (2001) Collection and detection of natural iron-binding ligands from seawater. *Marine Chemistry*, 76, 175-187.

Maldonado, M. T., Allen, A. E., Chong, J. S., Lin, K., Leus, D., Karpenko, N. & Harris, S. L. (2006) Copper-dependent iron transport in coastal and oceanic diatoms. *Limnology and Oceanography*, 51, 1729-1743.

Maldonado, M. T. & Price, N. M. (2001) Reduction and transport of organically bound iron by *Thalassiosira oceanica* (Bacillariophyceae). *Journal of Phycology*, 37, 298-309.

Martell, A. E., Motekaitis, R. J., Sun, Y. Z. & Clarke, E. T. (1994) Ligand Design of Chelating-Agents Effective in the Coordination of Fe(III) and for the Removal of Iron in Cases of Iron Overload. *Development of Iron Chelators for Clinical Use*, 329-351.

Martinez-Urtaza, J., Lozano-Leon, A., Varela-Pet, J., Trinanes, J., Pazos, Y. & Garcia-Martin, O. (2008) Environmental determinants of the occurrence and distribution of *Vibrio parahaemolyticus* in the rias of Galicia, Spain. *Applied and Environmental Microbiology*, 74, 265-274.

Martinez, J. S., Haygood, M. G. & Butler, A. (2001) Identification of a natural desferrioxamine siderophore produced by a marine bacterium. *Limnology and Oceanography*, 46, 420-424.

Mawji, E., Gledhill, M., Milton, J. A., Tarran, G. A., Ussher, S., Thompson, A., Wolff, G. A., Worsfold, P. J. & Achterberg, E. P. (2008a) Hydroxamate Siderophores: Occurrence and Importance in the Atlantic Ocean. *Environmental Science & Technology*, 42, 8675-8680.

Mawji, E., Gledhill, M., Milton, J. A., Zubkov, M. V., Thompson, A., Wolff, G. A. & Achterberg, E. P. (2011) Production of siderophore type chelates in Atlantic Ocean waters enriched with different carbon and nitrogen sources. *Marine Chemistry*, 124, 90-99.

Mawji, E., Gledhill, M., Worsfold, P. J. & Achterberg, E. P. (2008b) Collision-induced dissociation of three groups of hydroxamate siderophores: ferrioxamines, ferrichromes and coprogens/fusigens. *Rapid Communications in Mass Spectrometry*, 22, 2195-2202.

Mc Cormack, P., Worsfold, P. J. & Gledhill, M. (2003) Separation and detection of siderophores produced by marine bacterioplankton using high-performance liquid chromatography with electrospray ionization mass spectrometry. *Analytical Chemistry*, 75, 2647-2652.

Morel, F. M. M., Kustka, A. B. & Shaked, Y. (2008) The role of unchelated Fe in the iron nutrition of phytoplankton. *Limnology and Oceanography*, 53, 400-404.

Morel, I., Cillard, J., Lescoat, G., Pasdeloup, N., Brissot, P. & Cillard, P. (1991) Antioxidant Activity of the New Iron Chelating-Agents Hydroxypyridin-4-Ones (Cp20-Cp22) on Iron Loaded Hepatocyte Cultures - Study of Their Free-Radical Scavenging Properties. *Hepatology*, 14, A274-A274.

Mucha, P., Rekowski, P., Kosakowska, A. & Kupryszecki, G. (1999) Separation of siderophores by capillary electrophoresis. *Journal of Chromatography A*, 830, 183-189.

Neilands, J. B. (1995) Siderophores - Structure and Function of Microbial Iron Transport Compounds. *Journal of Biological Chemistry*, 270, 26723-26726.

Nielsdottir, M. C., Moore, C. M., Sanders, R., Hinz, D. J. & Achterberg, E. P. (2009) Iron limitation of the postbloom phytoplankton communities in the Iceland Basin. *Global Biogeochemical Cycles*, 23, -.

Oliver, J. D. (2005) The viable but nonculturable state in bacteria. *Journal of Microbiology*, 43, 93-100.

Page, W. J. & Huyer, M. (1984) Derepression of the *Azotobacter-Vinelandii* Siderophore System, Using Iron-Containing Minerals to Limit Iron Repletion. *Journal of Bacteriology*, 158, 496-502.

Ravel, J., Knight, I. T., Monahan, C. E., Hill, R. T. & Colwell, R. R. (1995) Temperature-Induced Recovery of *Vibrio-Cholerae* from the Viable but Nonculturable State - Growth or Resuscitation. *Microbiology-UK*, 141, 377-383.

Raymond, K. N., Muller, G. & Matzanke, B. F. (1984) Complexation of Iron by Siderophores - a Review of Their Solution and Structural Chemistry and Biological Function. *Topics in Current Chemistry*, 123, 49-102.

Reid, R. T., Live, D. H., Faulkner, D. J. & Butler, A. (1993) A Siderophore from a Marine Bacterium with an Exceptional Ferric Ion Affinity Constant. *Nature*, 366, 455-458.

Rose, A. L., Salmon, T. P., Lukondeh, T., Neilan, B. A. & Waite, T. D. (2005) Use of superoxide as an electron shuttle for iron acquisition by the marine

cyanobacterium *Lyngbya majuscula*. *Environmental Science & Technology*, 39, 3708-3715.

Rue, E. L. & Bruland, K. W. (1995) Complexation of Iron(III) by Natural Organic-Ligands in the Central North Pacific as Determined by a New Competitive Ligand Equilibration Adsorptive Cathodic Stripping Voltammetric Method. *Marine Chemistry*, 50, 117-138.

Saito, M. A. & Moffett, J. W. (2001) Complexation of cobalt by natural organic ligands in the Sargasso Sea as determined by a new high-sensitivity electrochemical cobalt speciation method suitable for open ocean work. *Marine Chemistry*, 75, 49-68.

Sanders, R., Brown, L., Henson, S. & Lucas, M. (2005) New production in the Irminger Basin during 2002. *Journal of Marine Systems*, 55, 291-310.

Schets, F. M., Van Den Berg, H. H. J. L., Rutjes, S. A. & Husman, A. M. D. (2010) Pathogenic Vibrio Species in Dutch Shellfish Destined for Direct Human Consumption. *Journal of Food Protection*, 73, 734-738.

Sevinc, M. S. & Page, W. J. (1992) Generation of Azotobacter-Vinelandii Strains Defective in Siderophore Production and Characterization of a Strain Unable to Produce Known Siderophores. *Journal of General Microbiology*, 138, 587-596.

Shaked, Y., Kustka, A. B. & Morel, F. M. M. (2005) A general kinetic model for iron acquisition by eukaryotic phytoplankton. *Limnology and Oceanography*, 50, 872-882.

Siegel, D. A., Doney, S. C. & Yoder, J. A. (2002) The North Atlantic spring phytoplankton bloom and Sverdrup's critical depth hypothesis. *Science*, 296, 730-733.

Stintzi, A., Barnes, C., Xu, L. & Raymond, K. N. (2000) Microbial iron transport via a siderophore shuttle: A membrane ion transport paradigm. *Proceedings of the National Academy of Sciences of the United States of America*, 97, 10691-10696.

Thompson, J. R., Polz, M. F., Randa, M. A., Marcelino, L. A., Tomita-Mitchell, A. & Lim, E. (2004) Diversity and dynamics of a north Atlantic coastal Vibrio community. *Applied and Environmental Microbiology*, 70, 4103-4110.

Tortell, P. D., Maldonado, M. T., Granger, J. & Price, N. M. (1999) Marine bacteria and biogeochemical cycling of iron in the oceans. *Fems Microbiology Ecology*, 29, 1-11.

Tortell, P. D., Maldonado, M. T. & Price, N. M. (1996) The role of heterotrophic bacteria in iron-limited ocean ecosystems. *Nature*, 383, 330-332.

Trick, C. G. (1989) Hydroxamate-Siderophore Production and Utilization by Marine Eubacteria. *Current Microbiology*, 18, 375-378.

Trick, C. G. & Wilhelm, S. W. (1995) Physiological-Changes in the Coastal Marine Cyanobacterium *Synechococcus* Sp Pcc-7002 Exposed to Low Ferric Ion Levels. *Marine Chemistry*, 50, 207-217.

Turner, J. W., Lipp, E. K., Good, B. & Cole, D. (2009) Plankton composition and environmental factors contribute to Vibrio seasonality. *Isme Journal*, 3, 1082-1092.

Vala, A. K., Dave, B. P. & Dube, H. C. (2006) Chemical characterization and quantification of siderophores produced by marine and terrestrial aspergilli. *Canadian Journal of Microbiology*, 52, 603-607.

Velasquez, I., Nunn, B. L., Ibsanmi, E., Goodlett, D. R., Hunter, K. A. & Sander, S. G. (2011) Detection of hydroxamate siderophores in coastal and Sub-Antarctic water off the South Eastern Coast of New Zealand. *Marine Chemistry*, 126, 97-107.

Vezzulli, L., Previati, M., Pruzzo, C., Marchese, A., Bourne, D. G., Cerrano, C. & Consortium, V. (2010) Vibrio infections triggering mass mortality events in a warming Mediterranean Sea. *Environmental Microbiology*, 12, 2007-2019.

Wilhelm, S. W., Maxwell, D. P. & Trick, C. G. (1996) Growth, iron requirements, and siderophore production in iron-limited *Synechococcus* PCC 7002. *Limnology and Oceanography*, 41, 89-97.

Wilhelm, S. W. & Trick, C. G. (1994) Iron-Limited Growth of Cyanobacteria - Multiple Siderophore Production Is a Common Response. *Limnology and Oceanography*, 39, 1979-1984.

Winkelmann, G. (1992) Structures and Functions of Fungal Siderophores Containing Hydroxamate and Complexone Type Iron-Binding Ligands. *Mycological Research*, 96, 529-534.

Worsham, P. L. & Konisky, J. (1984) Effect of Growth Temperature on the Acquisition of Iron by *Salmonella-Typhimurium* and *Escherichia-Coli*. *Journal of Bacteriology*, 158, 163-168.

CHAPTER 5 - Diversity of siderophores in surface waters of the high latitude North Atlantic Ocean

5.1 Introduction

Prokaryotes are known to have higher cellular Fe:C ratios and therefore higher iron (Fe) requirements than phytoplankton (Tortell *et al.*, 1999). The Fe:C ratios of eukaryotic phytoplankton and heterotrophic bacteria are 3.7 ± 2.3 and $6.1 \pm 2.5 \text{ } \mu\text{mol Fe mol C}^{-1}$, respectively (Tortell *et al.*, 1996; Maldonado & Price, 1999). In response to Fe deficiency marine prokaryotes secrete siderophores to solubilise and facilitate acquisition of Fe(III) in the environment. Iron stress has been reported for the phytoplankton community in the high latitude North Atlantic Ocean (Nielsdottir *et al.*, 2009). Both cyanobacteria and heterotrophic bacteria have been found to produce siderophores under Fe limited conditions (Wilhelm & Trick, 1994; Ito & Butler, 2005; Martinez & Butler, 2007; Vraspir & Butler, 2009). However, production of siderophores by phytoplankton has been the subject of much research, and up until now there has been no evidence that phytoplankton is actively producing siderophores (Hopkinson & Morel, 2009; Boyd & Ellwood, 2010). In a recent study, Mawji *et al.* (2008a) reported a significant correlation between total ferrioxamine siderophores concentration and heterotrophic bacterial abundance ($r=0.47$, $n=19$, $p<0.05$) in the low latitude North Atlantic Ocean. On the other hand, these workers did not observe a significant correlation between the total ferrioxamine concentration and autotrophic bacteria or picoeukaryote phytoplankton ($< 2 \text{ } \mu\text{m}$) abundances.

Recently, our understanding of siderophore production by heterotrophic bacteria in the marine environment has been largely based on bacteria that can either be cultured in the laboratory (Butler, 2004, 2005a; Butler & Martinez, 2007; Butler & Theisen, 2010) or grown successfully in nutrient enriched seawater samples (Gledhill *et al.*, 2004; Mawji *et al.*, 2008a; Mawji *et al.*, 2011), as this allows for the production of sufficient quantities of siderophores for further characterisation. The influence of different sources of carbon (glucose, glycine and chitin) along with nitrogen (ammonium) and phosphorus (phosphate) on the siderophore production has been examined by Mawji *et al.* (2011). These workers found that the easily available carbon source (glucose; $\text{C}_6\text{H}_{12}\text{O}_6$) produced the highest concentration and diversity of hydroxamate siderophores, compared to other carbon sources (glycine; $\text{C}_2\text{H}_5\text{NO}_2$ and chitin; $\text{C}_8\text{H}_{13}\text{NO}_5\text{}_n$) (Mawji *et al.*, 2011). The total concentration of siderophore produced in glucose incubations ranged between 0.2-69.0 nM with 12-14 different siderophores

identified in waters from the low latitude of Atlantic Ocean (43.7°N – 31.8°S) (Mawji *et al.*, 2011). Furthermore, these workers observed a positive correlation between siderophore concentrations and bacterial cell abundance in the glucose incubations. In contrast, there was no relationship between these variables in the chitin and glycine incubations. A high number of siderophore type chelates (10-12) was determined in the chitin incubation, but at low concentrations (0.1-0.6 nM) (Mawji *et al.*, 2011). In the glycine incubations, a constant number of siderophore type chelates (3-8) was observed at low concentrations, suggesting that the lack of readily available nitrogen in glycine incubations might have affected siderophore production (Mawji *et al.*, 2011), since glycine was used as a source of both nitrogen and carbon by the bacteria.

In this study, the influence of different sources of nitrogen and iron concentrations on siderophore production and types of siderophore secreted by heterotrophic bacteria was examined. High latitude North Atlantic seawater was enriched with sodium nitrate (NaNO_3) and ammonium chloride (NH_4Cl) as nitrogen sources, along with glucose and phosphate. Moreover, two different concentrations of Fe(III) (9 and 90 nM) were used. The seawater enrichment experiments were carried out in the high latitude North Atlantic Ocean during RRS *Discovery* cruise 350 (D350) and RRS *Discovery* cruise 354 (D354) in April-May 2010 and July-August 2010, respectively.

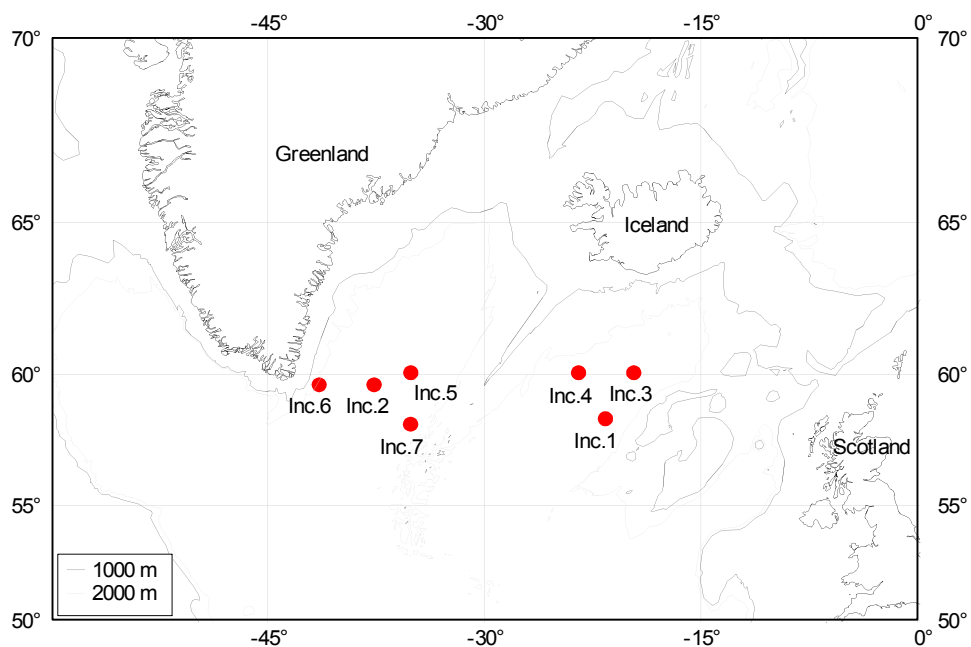
5.2 Methodology

Seawater samples for the enrichment experiments were collected in the high latitude North Atlantic Ocean (Fig. 32) into 2 L polystyrene tissue culture flasks (Becton Dickinson, USA).

The aliquots of unfiltered seawater (2 L) were enriched with nitrogen (200 μM ammonium chloride, Fisher Scientific or 200 μM sodium nitrate, Fisher Scientific), glucose (100 μM , Fisher Scientific), phosphate (20 μM di-sodium hydrogen orthophosphate, Fisher Scientific) and iron(III) (Ferric Chloride, Fisher Scientific) (Table 11). This experiment was done in duplicate, and the enriched seawater sample was incubated in the dark on deck in incubators at ambient seawater temperatures. Non enriched seawater was used as a control.

The samples were incubated until the bacteria in the incubations had reached the stationary growth phase (4-5 days). Bacterial growth was monitored daily using absorption measurements (Red Tide USB 650, Ocean Optic) at a wavelength of 600 nm. Samples for enumeration of bacteria (flow cytometry analysis) were sampled daily into 2 mL polypropylene low temperature freezer vial (VWR International) and stored at -

80°C after adding 1% paraformaldehyde (w/v) for analysis on shore. The flow cytometry analysis was described in detail in Chapter 2.



Scale: 1:38962558 at Latitude 0°

Source: GEBCO.

Figure 32: Location for enriched seawater experiments during RRS *Discovery* cruise D350 and D354 in the high latitude North Atlantic Ocean.

At the end of incubation period, samples were filtered to remove bacterial cells and the eluant was preconcentrated onto polystyrene-divinylbenzene solid phase extraction (SPE) cartridges (Isolute ENV+, 200mg x 3mL) for the extraction of siderophores. The extraction was carried out by using a Supelco Visiprep™ manifold coupled to a 5L reservoir and connected to a peristaltic vacuum pump. Cartridges loaded with preconcentrated siderophores sample were frozen at -20°C until further processing and analysis on shore. Prior to analysis at National Oceanography Centre Southampton (NOCS), SPE cartridges were defrosted and eluted with 5 mL of 81:14:5:1 (v/v/v/v) acetonitrile: propan-2-ol: water: formic acid. The enriched seawater experiments have been described in detail in Chapter 2.

The identification and quantification of siderophore type chelates in enriched samples were carried out as for seawater samples, except for the addition of Ga. A final concentration of 14 mM $\text{Ga}(\text{NO}_3)_3$ (ICP-MS standard, VWR) was used in all incubation samples and the samples with added Ga were left overnight to equilibrate before analysis by LC-ICP-MS. Siderophore type compounds were identified using LC-ESI-MS (Mc Cormack *et al.*, 2003; Mawji *et al.*, 2008a; Mawji *et al.*, 2011).

Table 11: The enriched seawater sample treatments used during this study. All treatments were done in duplicate and untreated seawater was used as control.

Date	Station	Treatments	Nutrients added
29/04/10	Inc. 1 58.34 °N, 21.51°W (3 m depth)	Control	-
		GNP	100µM glucose + 200 µM NH ₄ ⁺ + 20µM PO ₄ ³⁻
		GNP+Fe	100µM glucose + 200 µM NH ₄ ⁺ + 20µM PO ₄ ³⁻ + 9 nM Fe(III)
		GNP++Fe	100µM glucose + 200 µM NH ₄ ⁺ + 20µM PO ₄ ³⁻ + 90 nM Fe(III)
03/05/10	Inc. 2 59.59 °N, 37.55°W (27 m depth)	Control	-
		GNP	100µM glucose + 200 µM NH ₄ ⁺ + 20µM PO ₄ ³⁻
		GNP+Fe	100µM glucose + 200 µM NH ₄ ⁺ + 20µM PO ₄ ³⁻ + 9 nM Fe(III)
		GNP++Fe	100µM glucose + 200 µM NH ₄ ⁺ + 20µM PO ₄ ³⁻ + 90 nM Fe(III)
12/07/10	Inc. 3 60.02°N, 19.58°W (3 m depth)	Control	-
		GNP	100µM glucose + 200 µM NH ₄ ⁺ + 20µM PO ₄ ³⁻
		GNO ₃ P	100µM glucose + 200 µM NO ₃ ⁻ + 20µM PO ₄ ³⁻
		G	100 µM glucose
15/07/10	Inc. 4 60.02°N, 23.37°W (20 m depth)	Control	-
		GNP	100µM glucose + 200 µM NH ₄ ⁺ + 20µM PO ₄ ³⁻
		GNO ₃ P	100µM glucose + 200 µM NO ₃ ⁻ + 20µM PO ₄ ³⁻
		G	100 µM glucose
18/07/10	Inc. 5 60.02°N, 35.00 °W (3 m depth)	Control	-
		GNP	100µM glucose + 200 µM NH ₄ ⁺ + 20µM PO ₄ ³⁻
		GNO ₃ P	100µM glucose + 200 µM NO ₃ ⁻ + 20µM PO ₄ ³⁻
		G	100 µM glucose
19/07/10	Inc. 6 59.59 °N, 41.35°W (3 m depth)	Control	-
		GNP	100µM glucose + 200 µM NH ₄ ⁺ + 20µM PO ₄ ³⁻
		GNO ₃ P	100µM glucose + 200 µM NO ₃ ⁻ + 20µM PO ₄ ³⁻
		G	100 µM glucose
26/07/10	Inc. 7 58.13°N, 35.02 °W (40 m depth)	Control	-
		GNP	100µM glucose + 200 µM NH ₄ ⁺ + 20µM PO ₄ ³⁻
		GNO ₃ P	100µM glucose + 200 µM NO ₃ ⁻ + 20µM PO ₄ ³⁻
		G	100 µM glucose

5.3 Results and discussion

5.3.1 Bacterial growth in the nutrient enrichment samples

On day 1, the bacterial abundances in each seawater enrichment varied between 0.9- 1.1×10^6 cells mL⁻¹ and 0.9-2.0 $\times 10^6$ cells mL⁻¹ for Inc. 1 (Iceland Basin) and Inc. 2 (Irminger Basin) (Fig. 34), respectively, during the cruise in April-May 2010. An initial bacterial abundance in the control was 0.9×10^6 cells mL⁻¹ in both incubation experiments (Inc. 1 and Inc. 2).

In Inc. 1, the final bacterial abundance at day 5 varied with the type of nutrient enrichment. The highest bacterial abundance was 5.5×10^6 cells mL⁻¹ in the GNP+Fe treatment (Table 12, Fig. 33) of Inc. 1, which is nearly three times higher than the bacterial abundance in the control (1.9×10^6 cells mL⁻¹). While, there were 2.4×10^6 cells mL⁻¹ and 2.8×10^6 cells mL⁻¹ in the GNP and GNP++Fe treatment (Table 12), respectively, at the end of the incubation period in the Inc. 1.

Table 12: Concentrations and diversity of siderophore type chelates determined in nutrient enriched seawater in the high latitude North Atlantic Ocean.

Station	Incubation period (days)	Nutrient enrichment	Final bacteria ($\times 10^6$ cells mL^{-1})	Siderophores determined	
				Type chelates	Conc. (pM)
Inc. 1	5	Control	1.9	-	-
		GNP	2.4	-	-
		GNP+Fe	5.5	-	-
		GNP++Fe	2.8	-	-
Inc. 2	3	Control	1.6	-	-
		GNP	2.0	FOB	-
		GNP+Fe	1.6	FOB	-
		GNP++Fe	1.5	FOB	-
Inc. 2	5	Control	3.0	-	-
		GNP	4.3	FOB	2.039
		GNP+Fe	3.9	FOB	-
		GNP++Fe	3.3	FOB	-
Inc. 3	4	Control	2.9	-	-
		GNP	14.8	FOB	0.024
				FOG	-
				Amph. (883)	-
Inc. 4	4			Amph. D (885)	-
		Control	4.7	-	-
		GNP	13.7	FOG	0.849
				Amph. E (911)	-
Inc. 5	4			FOG	-
		GNP	13.8	Amph. E (911)	-
				FOG	-
				Amph. E (911)	-
Inc. 6	5	Control	1.7	-	-
		GNP	13.8	FOB	-
				FOG	0.072
				Amph. E (911)	-
Inc. 7	5			FOB	-
		Control	3.6	Amph. (883)	-
		GNP	14.0	Amph. D (885)	-
				Amph. E (911)	-
Inc. 7	5			FOB	-
		GNP	17.6	FOG	3.814
				FOB	0.133
				FOB	-
Inc. 7	5			FOB	-
		GNP	8.0	FOB	-
				FOB	-
		G	5.5	FOB	-

On the other hand, there was no significant difference in the bacterial abundances in the treatments of Inc. 2 (Fig. 33). At the end of the incubation period (day 5), the bacterial abundance varied between 3.0×10^6 cells mL^{-1} (in the control) and 4.3×10^6 cells mL^{-1} (in the GNP treatment) in Inc. 2 (Table 12). This indicated that the addition of extra Fe likely did not increase the abundance of bacterial in the high latitude North Atlantic seawater sample. The bacterial growth in these incubations is thus likely to be

more strongly influenced by other factors, e.g. temperature (Wiebe *et al.*, 1993; Kirchman *et al.*, 2005; Zhao *et al.*, 2010).

An addition of 100 μM glucose (G) to the samples was sufficient to result in a significant increase in the bacterial abundance ($3.5\text{-}7.5 \times 10^6 \text{ cells mL}^{-1}$, Table 12) at the end of the incubation for the cruise in July-August 2010 relative to the control ($1.7\text{-}4.7 \times 10^6 \text{ cells mL}^{-1}$, Table 12, Fig. 34). The addition of other nutrients NH_4^+ and PO_4^{3-} or NO_3^- and PO_4^{3-} along with glucose further increased the bacterial abundance in the GNP and GNO_3P treatment (Fig. 34). The final bacterial abundance in the GNP and GNO_3P treatments ranged between $13.8\text{-}17.6 \times 10^6 \text{ cells mL}^{-1}$ and $7.7\text{-}10.2 \times 10^6 \text{ cells mL}^{-1}$ (Table 12), respectively. This suggests that the combination of nitrogen, phosphate and glucose (GNP or GNO_3P) resulted in the greatest enhancement of bacterial abundance. These results imply that bacterial growth on glucose alone may have been less efficient than growth on the addition nitrogen source. Carbon-rich substrates such as glucose provide energy for cellular maintenance but do not provide all the essential nutrients needed to facilitate growth for the bacteria (Payne & Wiebe, 1978; Cherrier *et al.*, 1996).

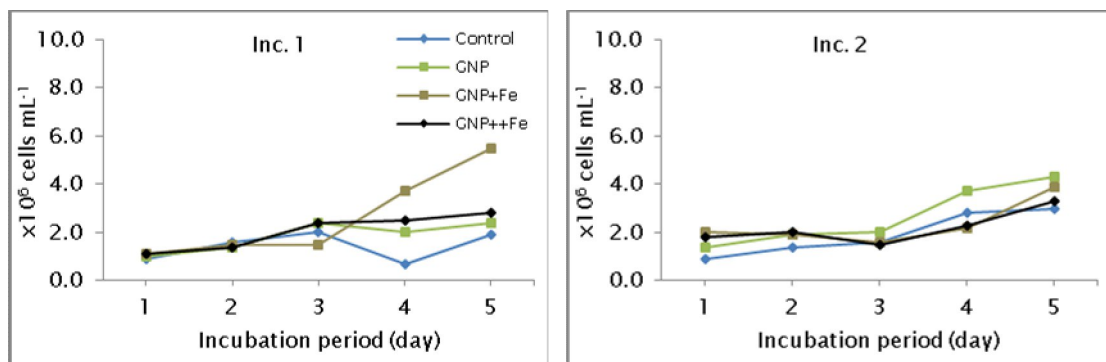


Figure 33: Bacterial abundance in the nutrient enriched samples during RRS *Discovery* cruise D350 in the Iceland Basin (Inc. 1) and Irminger Basin (Inc. 2). GNP represents the addition to the samples of glucose (100 μM), NH_4^+ (200 μM) and PO_4^{3-} (20 μM) to the samples. GNP+Fe and GNP++Fe represent addition of Fe at concentration 9 nM and 90 nM, respectively, along with GNP.

However, the GNP treatment produced higher bacterial abundance compared to the GNO_3P treatment (Fig. 35). It indicated a high uptake of NH_4^+ compared to the NO_3^- form for the bacterial growth. In fact, NH_4^+ is invariably the preferred nitrogen source for bacterial growth, although its concentration is less than NO_3^- concentration in the oceans (Wheeler & Kokkinakis, 1990). Kirchman & Wheeler (1998) have reported that the nitrogen uptake by heterotrophic marine bacterial was 78% and 32% of the total NH_4^+ and NO_3^- uptake, respectively. The uptake of NO_3^- is unusual because assimilatory

NO_3^- reduction is thought to be too energetically expensive to be carried out by heterotrophic bacteria that are carbon and energy limited (Kirchman et al., 1994).

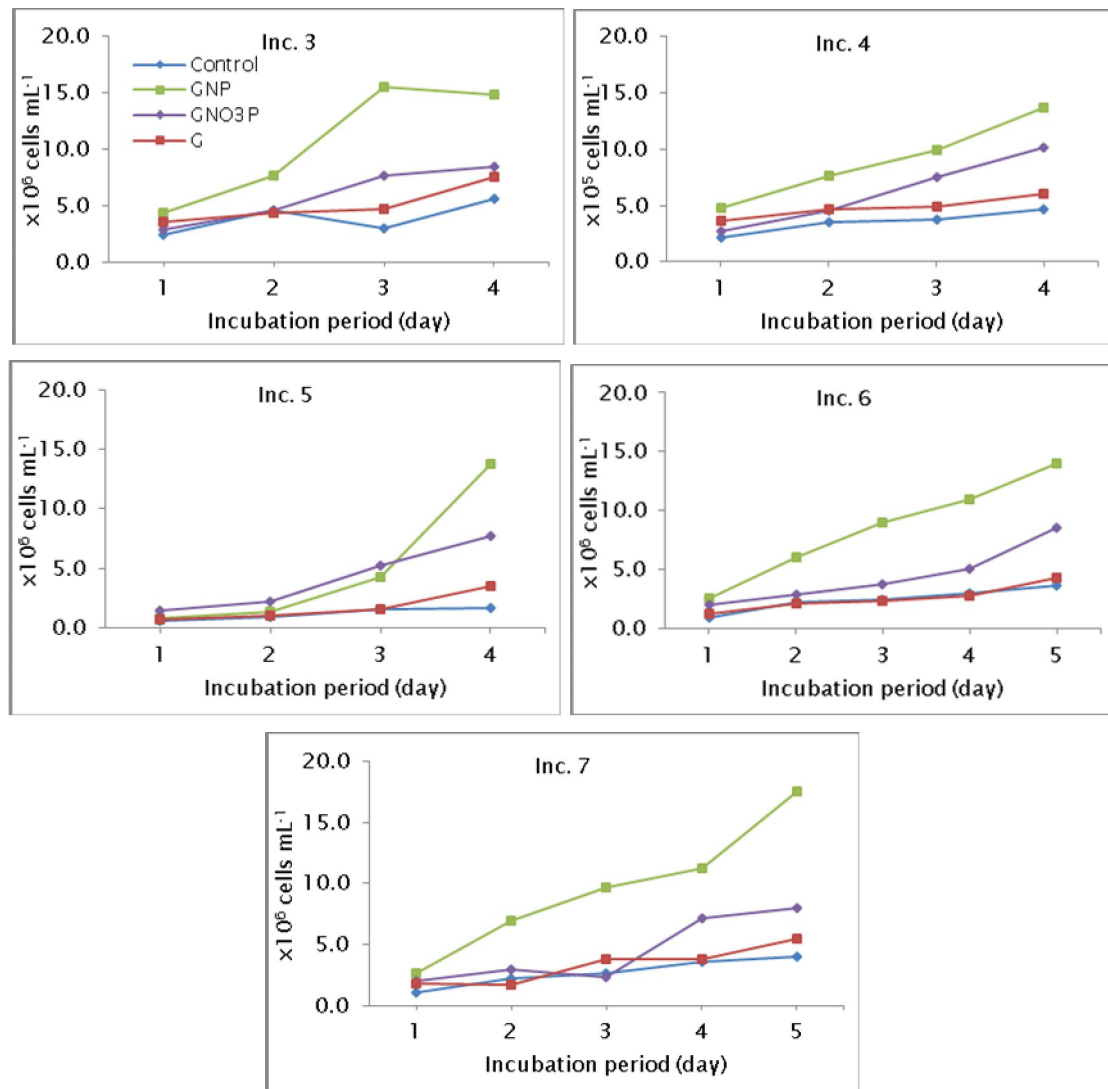


Figure 34: Bacterial abundance in the nutrient enriched incubations during RRS *Discovery* cruise D354 in the high-latitude North Atlantic Ocean. Two different sources of nitrogen (GNP and GNO₃P) were added to the sample along with glucose and phosphate. G represents the addition of glucose (100 μM) alone to the samples.

During this study, a higher bacterial abundance was observed in the GNP treatment during July-August 2010 compared to April-May 2010. In July-August 2010, the highest final bacterial abundance in the GNP treatment ranged between $13.7 \times 10^6 \text{ cells mL}^{-1}$ and $17.6 \times 10^6 \text{ cells mL}^{-1}$ with an average $14.8 \times 10^6 \text{ cells mL}^{-1}$ ($n=5$), while in April-May 2010, the highest final bacterial abundance was $4.3 \times 10^6 \text{ cells mL}^{-1}$ in the Inc. 2 (Table 12). The different seawater temperature during both cruises D350 (7-10°C) and D354 (8-13°C) in the high latitude North Atlantic Ocean may have contributed to the different of bacterial abundances in the nutrients enrichment samples. In addition, the bacterial

abundances in the nutrient enrichment samples in this region (ranged between $2.4\text{--}17.6 \times 10^6 \text{ cells mL}^{-1}$, with an average $11.5 \times 10^6 \text{ cells mL}^{-1}$, $n=7$) were lower than reported for nutrient enrichment samples carried out in the low latitude North Atlantic Ocean (ranged between $8.4\text{--}18.0 \times 10^6 \text{ cells mL}^{-1}$, with an average $13.4 \times 10^6 \text{ cells mL}^{-1}$, $n=6$) (Mawji *et al.*, 2011).

5.3.2 Diversity and concentration of siderophore type chelates

Siderophore type chelates were isolated from nutrient enriched seawaters collected in the high latitude North Atlantic Ocean. Five different siderophore type chelates were detected during this study (Table 12). The compounds comprised two groups, the ferrioxamines (ferrioxamine B (FOB) and ferrioxamine G (FOG)) and the amphibactins (amphibactin D, E and an unknown amphibactin). The two ferrioxamine siderophores have been detected in the seawater in this region (Chapter 4). On the other hand, the amphibactins D and E (Fig. 36) and the unknown amphibactin were not detected. However, these amphibactin siderophores have been observed in nutrient enriched incubations which were conducted in the open ocean (Mawji *et al.*, 2011) and in near-shore waters (Gledhill *et al.*, 2004). Amphibactins and FOG have previously been reported to be produced by gram-negative bacteria such as *Vibrio* species (Martinez *et al.*, 2001; Martinez *et al.*, 2003). On the other hand, desferrioxamines B and G are produced by gram-positive *Actinomycetes* species (Mucha *et al.*, 1999; Ghanem *et al.*, 2000). However, the distribution of the specific bacterial species was not been determined during this study.

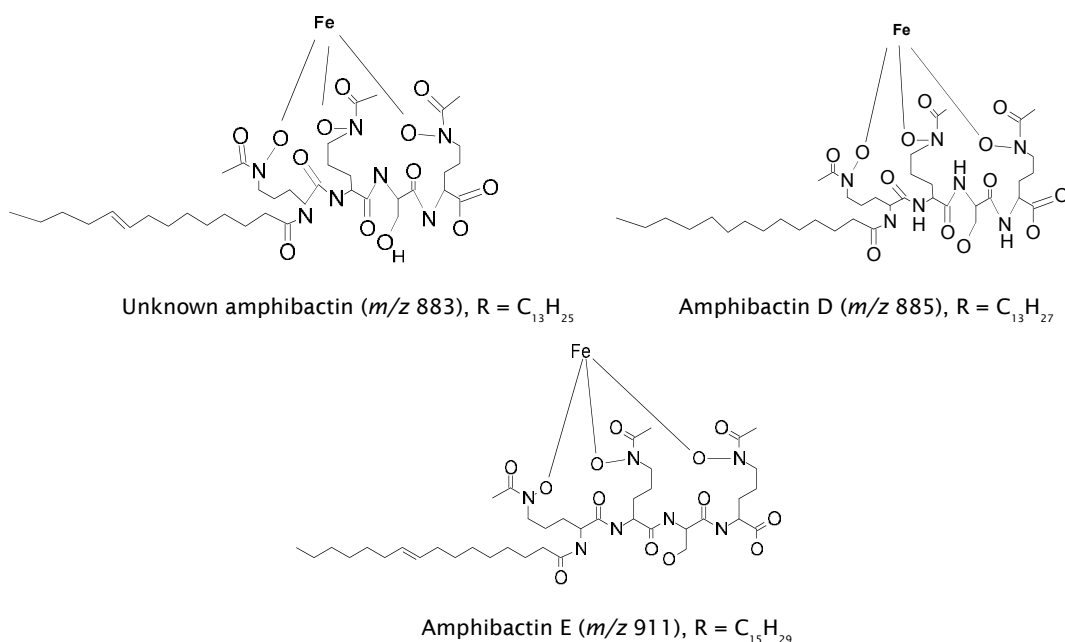


Figure 35: Structure of amphibactin in the high latitude North Atlantic Ocean during this study. For the FOB and FOG structure, please refer to Chapter 4.

The siderophore type chelates were identified by reanalysis of the samples using LC-ESI-MS analysis after overnight equilibration with excess (14 mM) Ga. A peak for Ga complexed with FOB (GaFOB) was observed at Rt = 7.35 minute in the chromatogram (Fig. 36). The mass to charge ratios (*m/z*) of 627 and 629, which indicate protonated complexes of $^{69}\text{GaFOB}$ and $^{71}\text{GaFOB}$, respectively, were observed at the retention time of 7.35 min. Mass chromatograms for other Ga-siderophore complexes present in the samples are shown in Figure 37 for Ga-ferrioxamine G (GaFOG) and Figure 38-39 for Ga-amphibactin complexes.

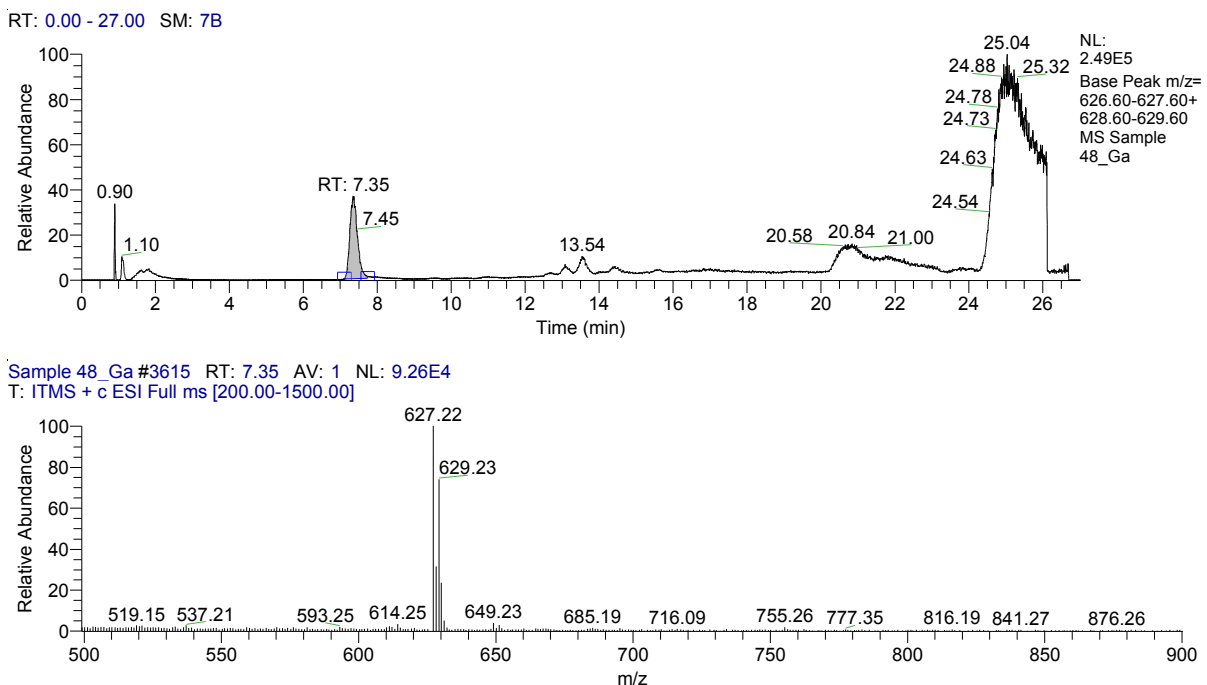


Figure 36: Extracted mass spectra for Ga complexed siderophore type compound (Ga-ferrioxamine B (GaFOB⁺), *m/z* 627/629). This siderophore was identified in the high latitude North Atlantic Ocean in Inc. 3 which was amended with glucose (100 μM), NH_4^+ (200 μM) and PO_4^{3-} (20 μM) (GNP).

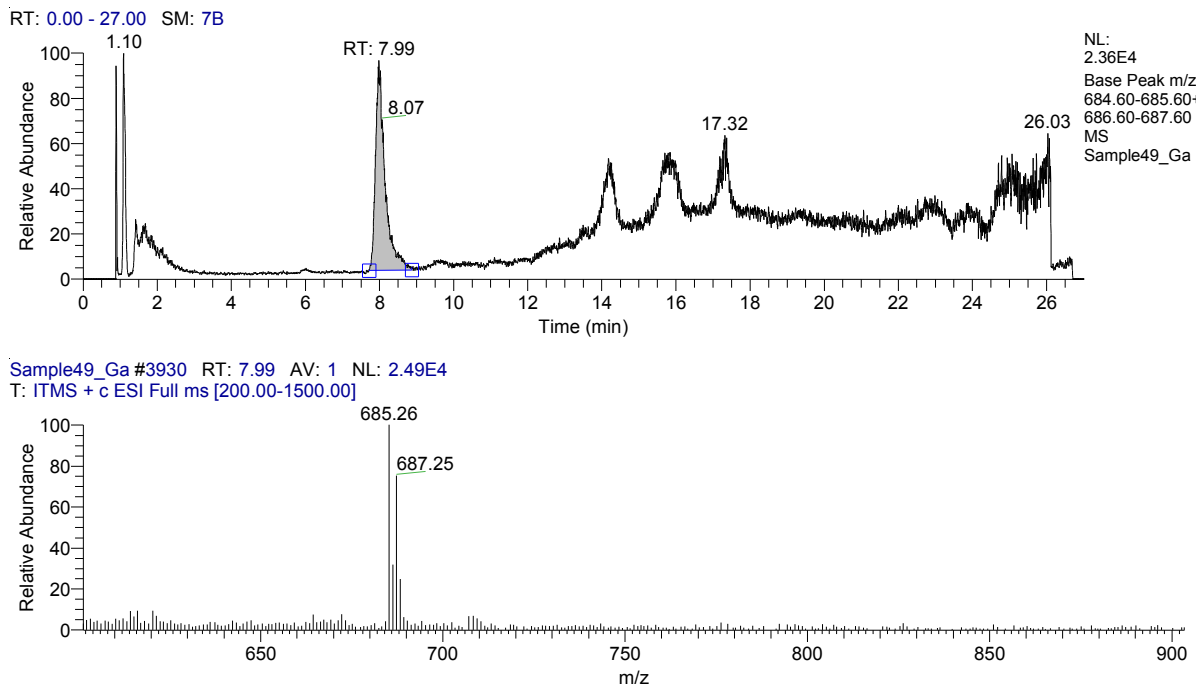


Figure 37: Extracted mass chromatograms for Ga-ferrioxamine G complexed (GaFOGH^+) identified in at $\text{Rt} = 7.99$ (m/z 685/687) obtained from Inc. 3 which was amended with glucose (100 μM), NH_4^+ (200 μM) and PO_4^{3-} (20 μM) (GNP).

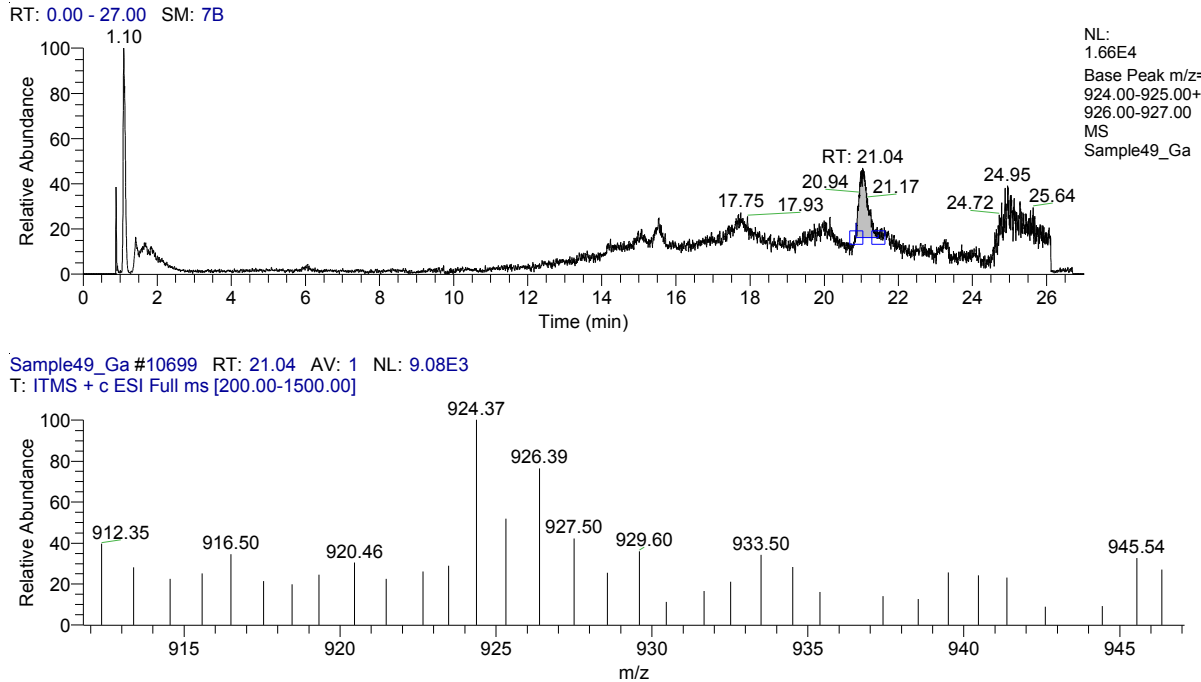


Figure 38: Extracted mass chromatograms for the protonated Ga-amphibactin E complex in the Inc. 3 which was amended with glucose (100 μM) plus PO_4^{3-} (20 μM) plus NH_4^+ (200 μM), at $\text{Rt}=21.04$ min (m/z 924/926).

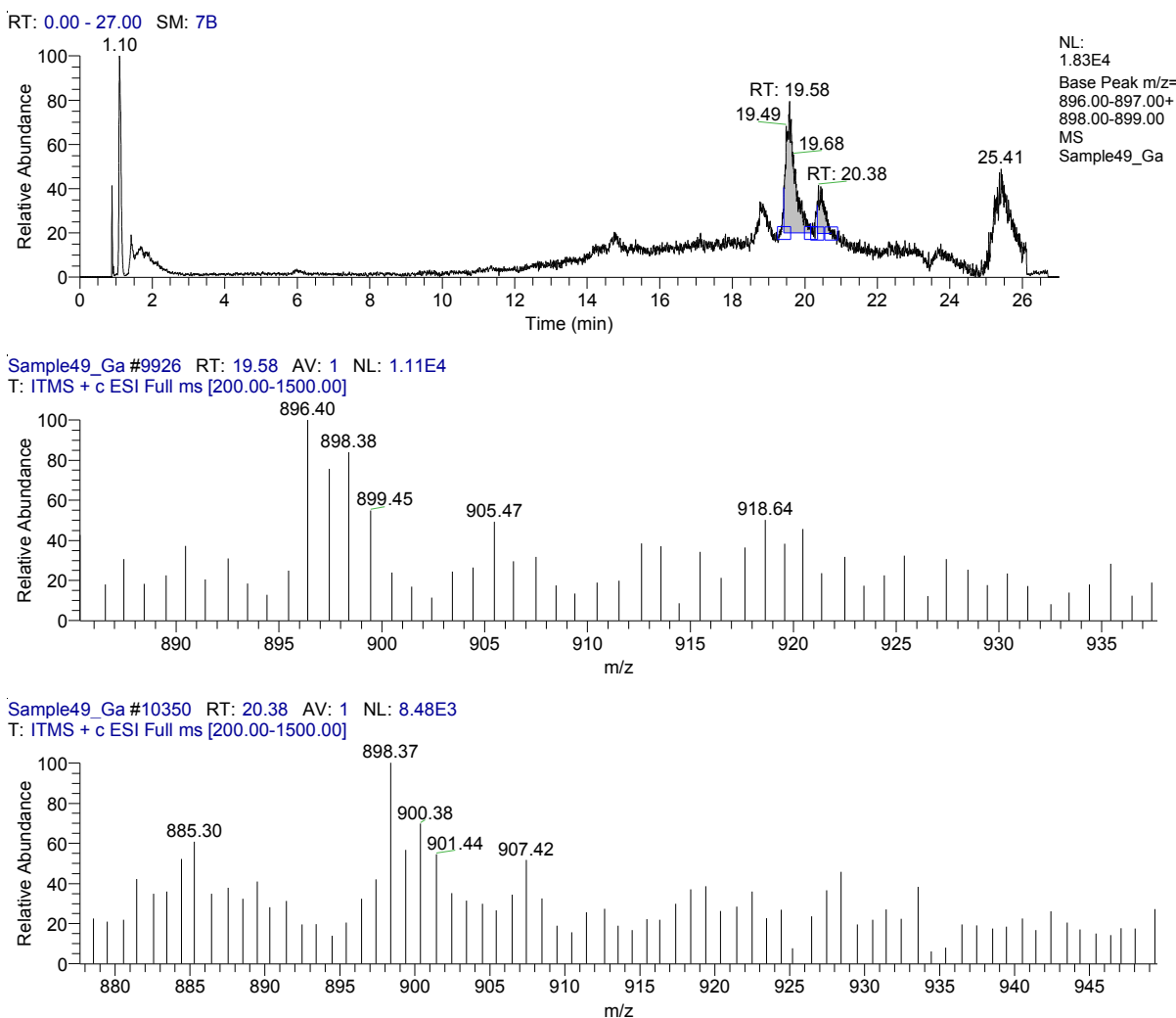
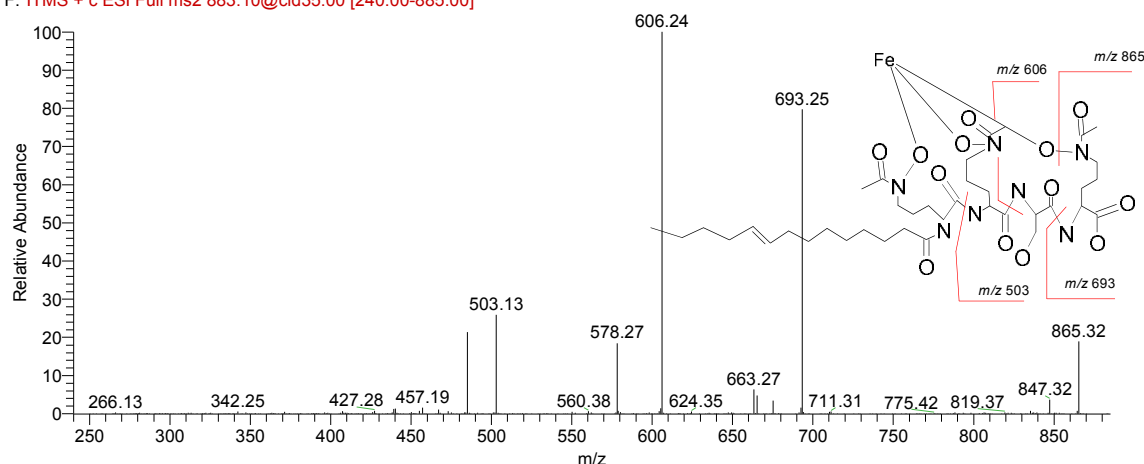


Figure 39: Extracted mass chromatograms for a Ga complexed siderophores identified in an extract from Incubation 3 which was amended with glucose (100 μ M), NH_4^+ (200 μ M) and PO_4^{3-} (20 μ M) (GNP). Peak at $\text{Rt} = 19.58$ min (m/z 896/898) was identified as the protonated Ga complex of the unknown amphibactin, and peak at $\text{Rt}=20.38$ min (m/z 898/900) was identified as the protonated Ga complex of amphibactin D.

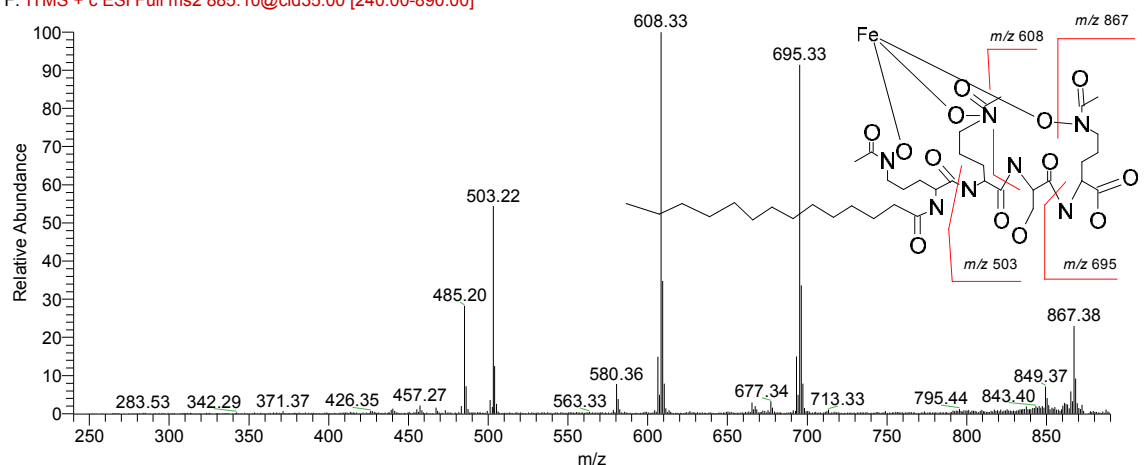
The collision induced dissociation (CID) analysis of the selected ions confirmed the presence of ferrioxamine (m/z 614, 672) and amphibactin (m/z 885, 911, 883) siderophores in the nutrient enrichment incubation samples (Fig. 40). The amphibactin siderophores were characterised by a peptide head group containing the amino acids (L-serine, D ornithine and L-ornithine) (Martinez *et al.*, 2003). Each amphibactin initially fragments through the loss of water (m/z 18), followed by fragmentation of m/z 190 (terminal hydroxamate chelating group) and m/z 277 (Fig. 40). An identical ion of m/z 503 in all spectra indicated a second fragmentation pathway, involving the loss of the third hydroxamic acid group together with the fatty acid tail. For the FOB and FOG fragmentation, please refer to Chapter 4.

a) Unknown amphibactin (m/z 883)

Sample125 MS2 #6911 RT: 19.49 AV: 1 NL: 7.39E3
 F: ITMS + c ESI Full ms2 883.10@cid35.00 [240.00-885.00]

b) Amphibactin D (m/z 885)

Sample125 MS2 #7102 RT: 20.37 AV: 1 NL: 1.06E4
 F: ITMS + c ESI Full ms2 885.10@cid35.00 [240.00-890.00]

c) Amphibactin E (m/z 911)

Sample125_MS2 #7233 RT: 20.97 AV: 1 NL: 8.46E3
 F: ITMS + c ESI Full ms2 911.10@cid35.00 [250.00-915.00]

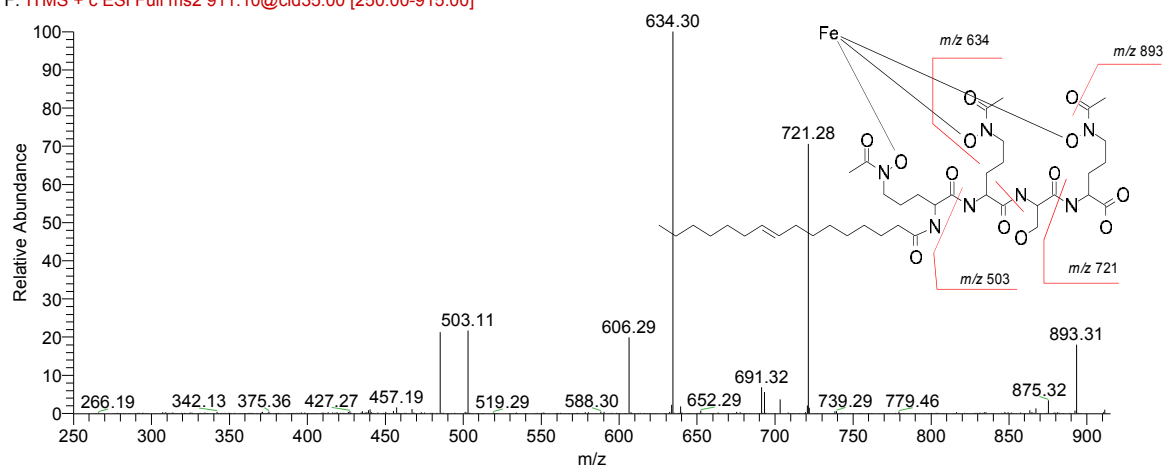


Figure 40: Mass spectra obtained on CID analysis of amphibactin D (m/z 885), E (m/z 911) and unknown amphibactin (m/z 883) in Inc. 6 which was amended with glucose (100 μ M), NH_4^+ (200 μ M) and PO_4^{3-} (20 μ M) (GNP).

Since, most of the amphibactin siderophore complexes eluted between Rt ~20-21 min in 100% organic solvent, this suggests that this group of siderophores is hydrophobic in nature. The masses of each amphibactin differed by an extension of saturated or unsaturated carbon chains, which ranges from C-14 to C-18 (Martinez *et al.*, 2003). Thus, two peaks of amphibactin were obtained in the mass chromatogram shown in Figure 39. The first peak (Rt = 19.58 min) was identified as an unknown amphibactin (m/z 883) and second peak (Rt = 20.38 minute) was identified as amphibactin D (m/z 885).

During this study, the number of siderophore type chelates detected by LC-ICP-MS was lower than that determined by LC-ESI-MS analysis due to the very low siderophore concentrations. Only ferrioxamine siderophores (FOB and FOG) (Fig. 41) were determined by LC-ICP-MS (Table 12, Fig. 41). Furthermore, FOB and FOG were only determined in the nutrient enriched incubations with GNP treatment. The concentrations for both FOB and FOG varied between 0.024–3.814 pM and 0.072–0.849 pM (Table 12), respectively.

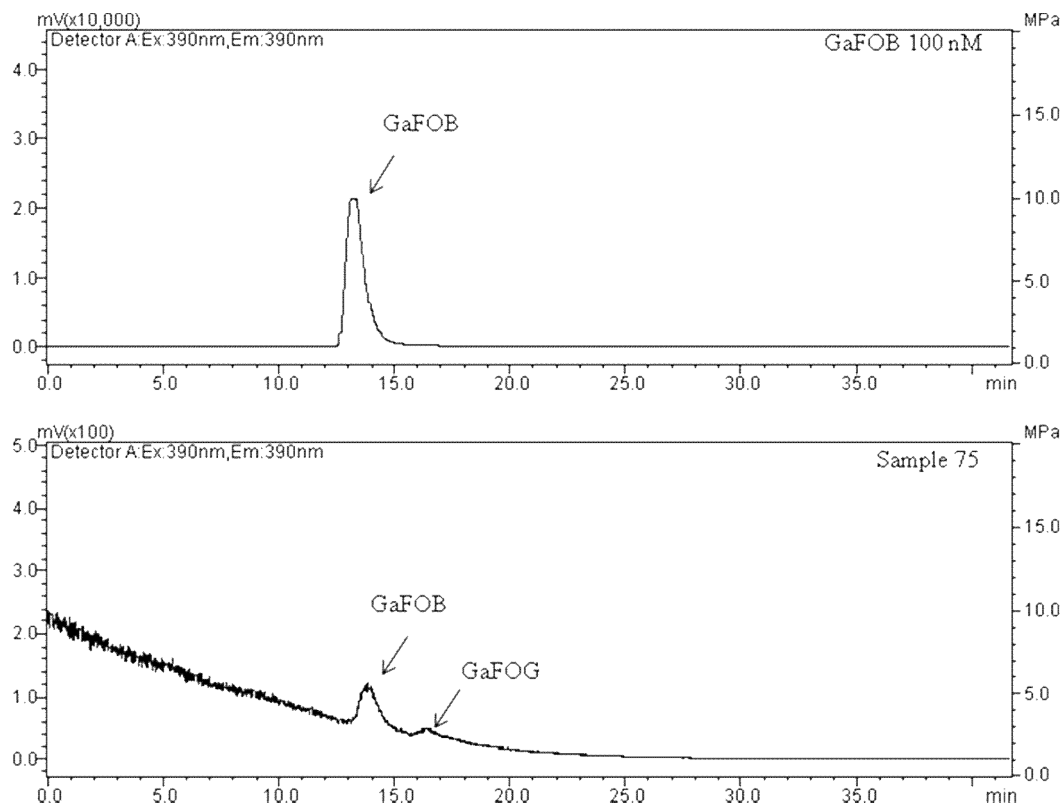


Figure 41: An example of a ^{69}Ga chromatogram from the HPLC-ICP-MS analysis. This chromatogram shows the peaks for the Ga-siderophore complexes in the working standard solution (GaFOB 100 nM) and nutrient enriched seawater sample for the GNP treatment (Sample 75, Inc. 7).

The diversity and concentrations of siderophore type chelates determined during this study was less than reported for the low latitude of Atlantic Ocean (43.74°N – 31.83°S) (Mawji *et al.*, 2011) and in coastal waters (Gledhill *et al.*, 2004). Both of these studies have determined more than 7 different siderophore type chelates (Gledhill *et al.*, 2004; Mawji *et al.*, 2011). Furthermore, Mawji *et al.* (2011) found a higher diversity of siderophore type chelates in the Western Tropical Atlantic (12-14 siderophore type chelates). Although the concentrations (0.024-3.814 pM) and diversity (5 siderophore type chelates) of siderophore produced by bacteria during this study are much lower than previously reported (0.1- 69.0 nM) (Mawji *et al.*, 2011), siderophores were nevertheless detected in the incubations carried out in the high latitude North Atlantic Ocean. This indicated that the bacteria capable of producing these siderophores are present in this region but that either they are naturally less abundant, or the production of siderophore type chelates was limited by a so far unidentified factor such as low seawater temperatures (Garibald.Ja, 1972; Worsham & Konisky, 1984; Colquhoun & Sorum, 2001).

5.3.3 Effect of iron and nitrogen on siderophores production in the high latitude North Atlantic

The effect of enhanced Fe concentrations on siderophores production was investigated in Inc. 1 (Iceland Basin) and Inc. 2 (Irminger Basin) (Fig. 32). There were no siderophore type chelates detected in any treatment conditions in Inc. 1 after 5 days (Table 11) and only FOB was identified in the Inc. 2 (Table 12) in all treatments after 3 days and 5 days, except in the control (Table 12). Thus it appears that addition of extra Fe does not necessarily alter siderophore production in seawaters of high latitude North Atlantic.

Seawater enriched with only glucose (G) produced a low diversity of siderophore type chelates compared to samples which were amended with GNP or GNO_3P (Table 12). This is consistent with the observed lower heterotrophic bacterial abundance in the glucose treatment when compared with treatments that include added nitrogen and phosphate (Fig. 34).

Samples amended with GNO_3P produced a lower diversity of siderophore type chelates when compared to GNP treatments (Fig. 34, Table 11). This indicates that siderophore diversity is also affected by nitrogen source, with NH_4^+ being more optimal for the production of siderophores. It is interesting to note that uptake of NH_4^+ is reported to be less temperature dependent than NO_3^- uptake (Reay *et al.*, 1999). Thus, it is

possible that NH_4^+ is more important as a nitrogen source for bacterial growth and siderophore production in the high latitude region.

During this study, the addition of GNP to the sample produced the highest diversity and concentrations of siderophores type chelates, and hence is the best condition for siderophore type chelates production by bacteria in the marine environment. However, in this study region, the siderophore production may be strongly affected by the low temperature which reduces the production by the heterotrophic bacteria.

5.4 Conclusion

Two types of ferrioxamine siderophores and amphibactin siderophores, produced by heterotrophic bacteria, were determined by HPLC-ESI-MS analysis in nutrient enriched seawater experiments in the high latitude North Atlantic Ocean. The siderophore type chelates detected in these experiments all belong to the tris-hydroxamate family and may reflect the selectivity of the chromatographic method used. It is thus possible that other siderophore type chelators may be present in the samples which were not detected due to methodological constraints. Since the Ga exchange analysis depends strongly on complexation of siderophore with Ga at low pH (~2), siderophore complexes that are unstable or insoluble at low pH (e.g. catecholate siderophores (Loomis & Raymond, 1991)) will not be detected using the conditions applied in this study. In addition to the pH effect, further method selectivity will be introduced by the preconcentration process, as a result of a loss of some hydrophilic siderophores.

The presented data showed that addition of iron did not result in a change in siderophore production in the high latitude North Atlantic Ocean. Furthermore, addition of ammonium (NH_4^+) as nitrogen source along with glucose and phosphate (PO_4^{3-}) produced highest higher diversity of siderophore type chelates compared to nitrate (NO_3^-). This finding shows the importance of nutrient type to the production of siderophores in nutrient enrichment experiments.

The diversity and concentration of siderophore type chelates detected during this study was low compared to previous studies in the low latitude Atlantic Ocean (Mawji *et al.*, 2011). Further studies are necessary in order to examine the relationship between siderophore production and geographical location. However it is possible that the low production of the siderophores detected in this study is related to the lower seawater temperatures in this region compared to the low latitude Atlantic Ocean.

References

Boyd, P. W. & Ellwood, M. J. (2010) The biogeochemical cycle of iron in the ocean. *Nature Geoscience*, 3, 675-682.

Butler, A. (2004) Amphiphilic and alpha-hydroxy acid-containing siderophores from marine bacteria. *Abstracts of Papers of the American Chemical Society*, 227, U1106-U1106.

Butler, A. (2005) Marine microbial iron mobilization: New marine siderophores. *Abstracts of Papers of the American Chemical Society*, 229, U893-U893.

Butler, A. & Martinez, J. S. (2007) Marine amphiphilic siderophores: Marinobactin structure, uptake, and microbial partitioning. *Journal of Inorganic Biochemistry*, 101, 1692-1698.

Butler, A. & Theisen, R. M. (2010) Iron(III)-siderophore coordination chemistry: Reactivity of marine siderophores. *Coordination Chemistry Reviews*, 254, 288-296.

Cherrier, J., Bauer, J. E. & Druffel, E. R. M. (1996) Utilization and turnover of labile dissolved organic matter by bacterial heterotrophs in eastern north Pacific surface waters. *Marine Ecology-Progress Series*, 139, 267-279.

Colquhoun, D. J. & Sorum, H. (2001) Temperature dependent siderophore production in *Vibrio salmonicida*. *Microbial Pathogenesis*, 31, 213-219.

Garibaldi (1972) Influence of Temperature on Biosynthesis of Iron Transport Compounds by *Salmonella-Typhimurium*. *Journal of Bacteriology*, 110, 262-&

Ghanem, N. B., Sabry, S. A., El-Sherif, Z. M. & Abu El-Ela, G. A. (2000) Isolation and enumeration of marine actinomycetes from seawater and sediments in Alexandria. *Journal of General and Applied Microbiology*, 46, 105-111.

Gledhill, M., McCormack, P., Ussher, S., Achterberg, E. P., Mantoura, R. F. C. & Worsfold, P. J. (2004) Production of siderophore type chelates by mixed bacterioplankton populations in nutrient enriched seawater incubations. *Marine Chemistry*, 88, 75-83.

Hopkinson, B. M. & Morel, F. M. M. (2009) The role of siderophores in iron acquisition by photosynthetic marine microorganisms. *Biometals*, 22, 659-669.

Ito, Y. & Butler, A. (2005) Structure of synechobactins, new siderophores of the marine cyanobacterium *Synechococcus* sp PCC 7002. *Limnology and Oceanography*, 50, 1918-1923.

Kirchman, D. L., Ducklow, H. W., McCarthy, J. J. & Garside, C. (1994) Biomass and Nitrogen Uptake by Heterotrophic Bacteria during the Spring Phytoplankton Bloom in the North-Atlantic Ocean. *Deep-Sea Research Part I-Oceanographic Research Papers*, 41, 879-895.

Kirchman, D. L., Malmstrom, R. R. & Cottrell, M. T. (2005) Control of bacterial growth by temperature and organic matter in the Western Arctic. *Deep-Sea Research Part II-Topical Studies in Oceanography*, 52, 3386-3395.

Kirchman, D. L. & Wheeler, P. A. (1998) Uptake of ammonium and nitrate by heterotrophic bacteria and phytoplankton in the sub-Arctic Pacific. *Deep-Sea Research Part I-Oceanographic Research Papers*, 45, 347-365.

Loomis, L. D. & Raymond, K. N. (1991) Solution Equilibria of Enterobactin and Metal Enterobactin Complexes. *Inorganic Chemistry*, 30, 906-911.

Maldonado, M. T. & Price, N. M. (1999) Utilization of iron bound to strong organic ligands by plankton communities in the subarctic Pacific Ocean. *Deep-Sea Research Part II-Topical Studies in Oceanography*, 46, 2447-2473.

Martinez, J. S. & Butler, A. (2007) Marine amphiphilic siderophores: Marinobactin structure, uptake, and microbial partitioning. *Journal of Inorganic Biochemistry*, 101, 1692-1698.

Martinez, J. S., Carter-Franklin, J. N., Mann, E. L., Martin, J. D., Haygood, M. G. & Butler, A. (2003) Structure and membrane affinity of a suite of amphiphilic siderophores produced by a marine bacterium. *Proceedings of the National Academy of Sciences of the United States of America*, 100, 3754-3759.

Martinez, J. S., Haygood, M. G. & Butler, A. (2001) Identification of a natural desferrioxamine siderophore produced by a marine bacterium. *Limnology and Oceanography*, 46, 420-424.

Mawji, E., Gledhill, M., Milton, J. A., Tarran, G. A., Ussher, S., Thompson, A., Wolff, G. A., Worsfold, P. J. & Achterberg, E. P. (2008) Hydroxamate Siderophores: Occurrence and Importance in the Atlantic Ocean. *Environmental Science & Technology*, 42, 8675-8680.

Mawji, E., Gledhill, M., Milton, J. A., Zubkov, M. V., Thompson, A., Wolff, G. A. & Achterberg, E. P. (2011) Production of siderophore type chelates in Atlantic Ocean waters enriched with different carbon and nitrogen sources. *Marine Chemistry*, 124, 90-99.

Mc Cormack, P., Worsfold, P. J. & Gledhill, M. (2003) Separation and detection of siderophores produced by marine bacterioplankton using high-performance liquid chromatography with electrospray ionization mass spectrometry. *Analytical Chemistry*, 75, 2647-2652.

Mucha, P., Rekowski, P., Kosakowska, A. & Kupryszeowski, G. (1999) Separation of siderophores by capillary electrophoresis. *Journal of Chromatography A*, 830, 183-189.

Nielsdottir, M. C., Moore, C. M., Sanders, R., Hinz, D. J. & Achterberg, E. P. (2009) Iron limitation of the postbloom phytoplankton communities in the Iceland Basin. *Global Biogeochemical Cycles*, 23, 1-13.

Payne, W. J. & Wiebe, W. J. (1978) Growth Yield and Efficiency in Chemosynthetic Microorganisms. *Annual Review of Microbiology*, 32, 155-183.

Reay, D. S., Nedwell, D. B., Priddle, J. & Ellis-Evans, J. C. (1999) Temperature dependence of inorganic nitrogen uptake: Reduced affinity for nitrate at suboptimal temperatures in both algae and bacteria. *Applied and Environmental Microbiology*, 65, 2577-2584.

Tortell, P. D., Maldonado, M. T., Granger, J. & Price, N. M. (1999) Marine bacteria and biogeochemical cycling of iron in the oceans. *Fems Microbiology Ecology*, 29, 1-11.

Tortell, P. D., Maldonado, M. T. & Price, N. M. (1996) The role of heterotrophic bacteria in iron-limited ocean ecosystems. *Nature*, 383, 330-332.

Vraspir, J. M. & Butler, A. (2009) Chemistry of Marine Ligands and Siderophores. *Annual Review of Marine Science*, 1, 43-63.

Wheeler, P. A. & Kokkinakis, S. A. (1990) Ammonium Recycling Limits Nitrate Use in the Oceanic Sub-Arctic Pacific. *Limnology and Oceanography*, 35, 1267-1278.

Wiebe, W. J., Sheldon, W. M. & Pomeroy, L. R. (1993) Evidence for an Enhanced Substrate Requirement by Marine Mesophilic Bacterial Isolates at Minimal Growth Temperatures. *Microbial Ecology*, 25, 151-159.

Wilhelm, S. W. & Trick, C. G. (1994) Iron-Limited Growth of Cyanobacteria - Multiple Siderophore Production Is a Common Response. *Limnology and Oceanography*, 39, 1979-1984.

Worsham, P. L. & Konisky, J. (1984) Effect of Growth Temperature on the Acquisition of Iron by *Salmonella-Typhimurium* and *Escherichia-Coli*. *Journal of Bacteriology*, 158, 163-168.

Zhao, S. J., Xiao, T. A., Lu, R. H. & Lin, Y. A. (2010) Spatial variability in biomass and production of heterotrophic bacteria in the East China Sea and the Yellow Sea. *Deep-Sea Research Part II-Topical Studies in Oceanography*, 57, 1071-1078.

Conclusion and future works

The high latitude North Atlantic Ocean is seasonally iron limited (Nielsdottir *et al.*, 2009). In this study an investigation into the dissolved speciation of iron was undertaken in this study region. The low total dissolved iron concentration (dFe < 0.1 nM) in the surface waters of the high latitude North Atlantic Ocean coincided with excess organic Fe(III) binding ligands (0.4-0.5 nM, $\log K'_{FeL} = 22-23$) (Chapter 3) (Mohamed *et al.*, 2011). Between 99.5-99.9% of dFe was organically complexed due to the presence of the excess ligands and the high stability of the organic Fe(III) binding ligands complexes (Chapter 3). The presence of organic Fe(III) binding ligands in this Fe limited region will work towards prevention of pronounced Fe stress in a microbial surface water community by maintaining Fe in the soluble phase and thereby enhancing the residence time of Fe in the oceanic water column (Chapter 3). The availability of the ligand bound Fe to the phytoplankton community is however still largely unclear. The low [dFe] and microbial ligand production responsible for the high and variable $[L_r]/[dFe]$ ratios in the surface waters in this region. However, in the deeper water (300-1000 m), the constant $[L_r]/[dFe]$ ratios was observed reflecting to the steady state between dissolved Fe and organic ligands.

Further investigations of the dissolved Fe-ligand pool were undertaken by characterisation of dissolved hydroxamate siderophores (Chapter 4). Very low concentrations of dissolved siderophores ($0-135 \times 10^{-18}$ M) and a relatively low diversity of siderophore type chelates was observed, compared to a previous study carried out at lower latitudes in the Atlantic Ocean (Mawji *et al.*, 2008). The iron limiting conditions in this region did not therefore appear to strongly influence to the production of the hydroxamate siderophores. The production of siderophore type chelates is may thus be affected by a combination of factors, including carbon and nitrogen availability, rather than a single factor. Moreover, a low seawater temperature also potentially plays an important role in influencing siderophores production and growth of a potential heterotrophic bacterial producing siderophores in the high latitude North Atlantic Ocean.

The Fe(III) binding ligand strength determined during this study (Chapter 3) was similar to that measured previously (Rue & Bruland, 1997) and similar to the condition stability constant for marine siderophore complexes. However the extremely low concentration of total dissolved siderophores detected during this study, showed that they was no relationship between both total dissolved hydroxamate siderophore concentrations and natural organic Fe(III) binding ligand concentrations. Although it has been speculated that some or all of the Fe(III) ligands may be siderophores, the finding from

this study suggested that the hydroxamate siderophores determined here are not an important fraction (< 0.1%) of this natural organic Fe(III) binding ligand pool in the high latitude North Atlantic Ocean. The ligand pool in this region may therefore originate from other ligand sources. Such other sources may include humic substances (humic acid and fulvic acid) (Laglera & Van Den Berg, 2009) and exopolysaccharides and phytoplankton exudates and breakdown products (Hassler *et al.*, 2011).

Characterisation of the ligands in seawater thus requires further work.

The restriction of siderophores production to the heterotrophic bacteria and the amphiphilic character of many marine siderophores (Martinez *et al.*, 2000; Martinez *et al.*, 2003; Butler, 2005) suggests that a portion of the siderophores in this region could be present in the colloidal or particulate phase (> 0.02 μm). In this phase, bacteria may be producing siderophores when attached to particles such as phytoplankton or zooplankton (Shaked *et al.*, 2005; Amin *et al.*, 2009). Although, only a few studies have been carried out on the distribution of organic ligands in the colloidal pool (Wu *et al.*, 2001; Cullen *et al.*, 2006; Thuroczy *et al.*, 2010), it is probable that colloidal organic ligands play an important role in Fe biogeochemistry.

This study has highlighted the importance of organic Fe(III) binding ligands for keeping Fe in solution in the water column of the seasonally Fe limited region of high latitude North Atlantic Ocean. This work also has provided valuable outcomes on the composition of these ligands in this region. Suggestions for future work on Fe speciation include:

1. This study has highlighted the need for further work on the distribution of organic Fe(III) binding ligands in the colloidal fraction. This work is challenging as it is difficult to separate the colloidal fraction without perturbing it, however it will provide a valuable insight into oceanic Fe chemistry.
2. This study has shown that it is important to determine the distribution of other than hydroxamate siderophores and other ligand types that have been proposed for Fe binding. These proposed ligands could include humic substance and exopolysaccharides. Further work is also required in order to assess whether these types of ligand are biologically available and how they react in the presence of competing ligands, like siderophores.
3. This study has also highlighted the need to investigate the distribution of potential heterotrophic bacteria producing siderophores in this high latitude region and the possible factors that might be influence the growth of these types of bacteria.

4. The utilisation a combination of on LC-ESI-MS and LC-ICP-MS forms a powerful tool for quantification and identification of very low hydroxamate siderophore concentrations in the seawater. However, further study is needed to improve the determination of other types of siderophores (catecholate or α -hydroxy carboxylic) which possibly exist in the seawater. In fact, pH is an important factor that influences the types of siderophore which can be detected using the current method. The using of Ga to replace an Fe(III) in the Fe(III)-siderophore complex at low pH (~2) could be replaced with isotope labelled Fe (^{54}Fe) in order to avoid loss of unstable or insoluble siderophore type chelates at low pH.

References

Amin, S. A., Green, D. H., Kupper, F. C. & Carrano, C. J. (2009) Vibrioferin, an Unusual Marine Siderophore: Iron Binding, Photochemistry, and Biological Implications. *Inorganic Chemistry*, 48, 11451-11458.

Butler, A. (2005) Marine microbial iron mobilization: New marine siderophores. *Abstracts of Papers of the American Chemical Society*, 229, U893-U893.

Cullen, J. T., Bergquist, B. A. & Moffett, J. W. (2006) Thermodynamic characterization of the partitioning of iron between soluble and colloidal species in the Atlantic Ocean. *Marine Chemistry*, 98, 295-303.

Hassler, C. S., Alasonati, E., Nichols, C. a. M. & Slaveykova, V. I. (2011) Exopolysaccharides produced by bacteria isolated from the pelagic Southern Ocean - Role in Fe binding, chemical reactivity, and bioavailability. *Marine Chemistry*, 123, 88-98.

Laglera, L. M. & Van Den Berg, C. M. G. (2009) Evidence for geochemical control of iron by humic substances in seawater. *Limnology and Oceanography*, 54, 610-619.

Martinez, J. S., Barbeau, K. & Butler, A. (2000) Marine bacterial siderophores. *Abstracts of Papers of the American Chemical Society*, 219, U850-U850.

Martinez, J. S., Carter-Franklin, J. N., Mann, E. L., Martin, J. D., Haygood, M. G. & Butler, A. (2003) Structure and membrane affinity of a suite of amphiphilic siderophores produced by a marine bacterium. *Proceedings of the National Academy of Sciences of the United States of America*, 100, 3754-3759.

Mawji, E., Gledhill, M., Milton, J. A., Tarran, G. A., Ussher, S., Thompson, A., Wolff, G. A., Worsfold, P. J. & Achterberg, E. P. (2008) Hydroxamate Siderophores: Occurrence and Importance in the Atlantic Ocean. *Environmental Science & Technology*, 42, 8675-8680.

Mohamed, K. N., Steigenberger, S., Nielsdottir, M. C., Gledhill, M. & Achterberg, E. P. (2011) Dissolved iron(III) speciation in the high latitude North Atlantic Ocean. *Deep-Sea Research I*, 58, 1049-1059.

Nielsdottir, M. C., Moore, C. M., Sanders, R., Hinz, D. J. & Achterberg, E. P. (2009) Iron limitation of the postbloom phytoplankton communities in the Iceland Basin. *Global Biogeochemical Cycles*, 23, 1-13.

Rue, E. L. & Bruland, K. W. (1997) The role of organic complexation on ambient iron chemistry in the equatorial Pacific Ocean and the response of a mesoscale iron addition experiment. *Limnology and Oceanography*, 42, 901-910.

Shaked, Y., Kustka, A. B. & Morel, F. M. M. (2005) A general kinetic model for iron acquisition by eukaryotic phytoplankton. *Limnology and Oceanography*, 50, 872-882.

Thuroczy, C. E., Gerringa, L. J. A., Klunder, M. B., Middag, R., Laan, P., Timmermans, K. R. & De Baar, H. J. W. (2010) Speciation of Fe in the Eastern North Atlantic Ocean. *Deep-Sea Research Part I-Oceanographic Research Papers*, 57, 1444-1453.

Wu, J. F., Boyle, E., Sunda, W. & Wen, L. S. (2001) Soluble and colloidal iron in the oligotrophic North Atlantic and North Pacific. *Science*, 293, 847-849.

Appendix

Cruises

1. RRS *Discovery* D328 (April 2008)
2. RRS *Discovery* D340 (Jun 2009)
3. RRS *Discovery* D354 (August-September 2010)

Conferences/ meeting attended

1. "Iron biogeochemistry across marine systems at changing times" in Göteborg, Sweden, 14-16 May 2008.
2. "Ocean challenges in the 21st century" The 14th Biennial Challenger Conference for Marine Science, National Oceanography Centre, Southampton, 6 - 9 September 2010.
3. "Marine Biogeochemistry: Observations from near and far" Marine Biogeochemistry Forum and Marine Optics Group, Challenger Society for Marine Science, Portsmouth, 7 - Friday 9 September 2011.

Distributions

1. GEOTRACES intercalibration cruise data (Fe speciation) 2008 and 2009.
2. The speciation intercomparison data for the ASLO meeting, February 2010.
3. Iron speciation data for BODC, 2009-2010.

Publications

1. Dissolved iron(III) speciation in the high latitude North Atlantic Ocean (2011) Khairul N. Mohamed, Sebastian Steigenberger, Maria C. Nielsdottir, Martha Gledhill, Eric P. Achterberg, *Deep-Sea Research I* 58, 1049-1059.
2. Influence of Ocean Acidification on trace metal speciation. Eric P. Achterberg, Keqiang Li, Martha Gledhill, Khairul N Mohamed & Micha Rijkenber (*in preparation*).
3. Determination and identification of siderophore type chelates. Khairul N. Mohamed, Martha Gledhill, Eric P. Achterberg in "Ocean challenges in the 21st century" meeting 2010. National Oceanography Centre, Southampton, 6 - 9 September 2010.
4. Determination of dissolved siderophores in the high latitude North Atlantic Ocean (2011). Khairul N. Mohamed, Martha Gledhill*, Eric P. Achterberg in "Marine Biogeochemistry: Observations from near and far" Marine Biogeochemistry Forum and Marine Optics Group, Challenger Society for Marine Science. University of Portsmouth, 7-9 September 2011.

